

**MAGMATIC AND TECTONIC EVOLUTION OF
THE YUNTDAĞ VOLCANIC COMPLEX
(WESTERN ANATOLIA)**

**A Thesis Submitted to the
Graduate School of Natural and Applied Science of Dokuz Eylül University
in Partial Fullfilment of the Requirements for
the Doctor of Philosophy Degree
in Geology Engineering, General Geology Programme**

**by
Erhan Akay**

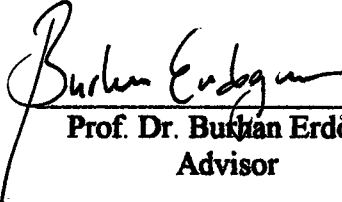
98308

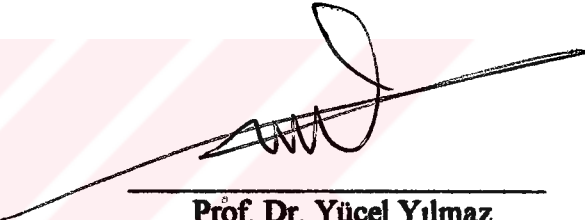
**July, 2000
İzmir**


**T.C. YÜKSEKÖĞRETİM KURULU
DOKUZ EYLÜL ÜNİVERSİTESİ
İZMİR MERKEZİ**

PHD THESIS EXAMINATION RESULT FORM

We certify that we have read this thesis and that in our opinion it is fully adequate, in scope and in quality, as thesis for the degree of Doctor of Philosophy.


Prof. Dr. Burhan Erdoğan
Advisor


Prof. Dr. Yücel Yılmaz
Committee member


Prof. Dr. Cahit Helvacı
Committee member

Approved for the Graduate School of Natural and Applied Sciences


Prof. Dr. Cahit Helvacı
Director

Graduate School of Natural and Applied Sciences

ACKNOWLEDGEMENT

The author wishes to express his gratitude to Prof. Dr. Burhan ERDOĞAN for his guidance and continuous encouragement throughout the work, especially with regard to field work and constructive discussions during the preparation of this thesis.

Special thanks must go to Prof. Dr. Alastair H. F. ROBERTSON for his collaboration, kind helps and vital discussions throughout the studies in Department of Geology and Geophysics of the University of Edinburgh. I am grateful to Prof. Dr. John DIXON for his critical comments on the results of the chemical analyses. The chemical analyses, carried out in the University of Edinburgh, were done by Dr. Doddie JAMES who is geochemist in the University of Edinburgh. I would also like to express my special thanks to her for her kind helps. Yılmaz GÜLTEKİN and Nedim TATARİ are thanked for their assistance in the geochemical studies in the Dokuz Eylül University.

This study was financially supported by projects of Scientific and Technical Research Council of Turkey (TUBITAK) (project no: YDABCAG-399), and the Graduate School and Applied Science of Dokuz Eylül University (project no: 0908. 95. 06. 02). Author specially thanks to the managers of the mentioned companies for their appreciations to this study and supports.

The author also wishes to express his thanks to Municipality of Aliğa for their supports on accomodation during field studies around Aliğa.

Gülesin SOYDAŞ, Hüseyin YILDIZ, Günay BOYACIOĞLU, Fatih ÖZÇOLAK and Altuğ HASÖZBEK who are/were BSc students in Department of Geology, in Dokuz Eylül University, are thanked for their assistance throughout the field studies.

Erhan AKAY

ABSTRACT

In the Aliğa-Foça region, three main rock associations crop out. These are, 1. The Yuntdağ volcanics, 2. The Foça volcanic complex and 3. Aliğa limestone. The Yuntdağ volcanics form the oldest unit in the area and consist of a thick and widespread andesitic-trachyandesitic lava sequence and accompanying coarse grained volcanoclastic rocks. In the Yuntdağ volcanics four main rock units are distinguished which are 1. The Helvacı andesites consisting of pink to gray, coherent lava flows of andesite composition, 2. The Çaltılı andesites which are formed by the black, aphanitic andesite lava flows, 3. The Haykıran blocky pyroclastics which are made up of the blocky andesites in fine grained tuffaceous matrix and 4. The Dumanlıtepe dykes consisting of dykes and subvolcanic stocks of these coherent lavas in central parts of the main vents. In the Yuntdağ volcanic complex, 6 different volcanic facies are distinguished which are 1. Flow banded lavas, 2. Subvolcanic andesites, 3. Columnar jointed andesite, 4. Flow breccias, 5. Block and ash flow deposits and 6. Grain supported, andesite lava-scoria facies .

Geochemically, the coherent facies of the Yuntdağ volcanics are andesite to dacite in composition and calc-alkaline in nature. The chemical composition of various rocks in the succession indicate that the Yuntdağ volcanic association is made up of genetically related units and has evolved in continental margin.

The Yuntdağ volcanics are overlain by the rhyolitic Foça volcanic complex. In this sequence, three different subunits are distinguished which are 1. The Foça rhyolites, 2. The Foça volcanoclastics and 3. Foça alkaline volcanics. The Foça rhyolites are made up of massive rhyolite lava flows and domes. The Foça rhyolites are surrounded by the Foça volcanoclastic sequence in which three different subunits are distinguished which are 1.

Pyroclastic flows, 2. Hyaloclastic breccias, 3. Perlites. Close to the domes, coarse grained hyaloclastites and perlites cover the massive rhyolites and succeeded laterally by fine grained, intensely to slightly welded ignimbrites. The lithological and sedimentological features of this unit show that the rhyolite domes intruded phreatically into a shallow lacustrine environment and the accompanying pyroclastic sequence formed as blankets surrounding the domes. Since the shallow lakes filled by the rapid deposition, in upper parts of the hyaloclastites subaerial pyroclastic rocks were formed characterized by channel-fill deposits. In the upper parts of the rhyolitic volcanoclastic sequence, there are alkaline lava flows interdigitating with the volcanoclastics and lacustrine sedimentary rocks. In the Foça volcanic complex 13 different facies are distinguished depending on their conditions of formation. These are 1. Massive rhyolite, 2. Massive perlites, 3. In-situ hyaloclastic breccias, 4. Reassembled hyaloclastic breccias, 5. Laminated mudstone, 6. Fine grained rhyolite pumice-lithic fragment facies, 7. Coarse grained rhyolite pumice-lithic fragment facies, 8. Lithic fragment-rich channel-fill facies, 9. Subaqueous welded ignimbrite facies, 10. Brecciated perlite, 11. Subaqueous ash fallout deposits, 12. Coherent alkaline lavas and 13. Alkaline dykes.

Geochemically, the Foça rhyolites are calc-alkaline in nature. They resemble to a volcanic association of a post orogenic tectonic setting. The alkaline lava flows show chemical characteristics of within plate basalts or rift-related volcanics.

The Foça volcanic complex laterally and vertically passes into the Neogene Aliğa limestone consisting of white to yellow, gastropoda-bearing limestones and clayey limestones.

The stratigraphic relations and geochemical affinities of the Yuntdağ volcanics, the Foça volcanic complex and the Foça alkaline volcanics indicate that they were formed progressively under a single and genetically interrelated tectonic regime.

ÖZET

Aliğa-Foça çevresinde başlıca üç farklı kaya grubu yüzlek verir. 1. Yuntdağ volkanikleri, 2. Foça volkanik kompleksi ve 3. Aliğa kireçtaşı birimi. Yuntdağ volkanikleri alandaki en yaşlı kaya birimini oluşturur ve yaygın olarak yüzlek veren, kalın andezitik, trakiandezitik lavlar ve lavlarla birlikte bulunan kaba dokulu piroklastik kayalardan yapılıdır. Yuntdağ volkanikleri içinde 4 farklı kaya birimi ayırtlanmıştır. Bunlar: 1. Pembe-gri renkli masif andezitik lavlardan yapılı Helvacı andezitleri, 2. Siyah renkli, afanitik dokulu andezit lavları, 3. İnce taneli beyaz-gri renkli tuf matris içinde yer alan andezit blok ve lapillilerinden yapılı Haykıran bloklu piroklastikleri ve 4. Yuntdağ volkanizmasının merkezi çıkış alanlarında yüzlekler veren dayk ve subvolkanik stoklardan yapılı Dumanlıtepe daykları. Yuntdağ volkanitleri içinde başlıca 6 farklı volkanik fasiyes tanımlanmıştır. 1. Akma liminalanmalı andezit lavı fasiyesi, 2. Subvolkanik andesitler, 3. Sütun eklemli andezit lavı fasiyesi, 4. Akma breşi fasiyesi, 5. Blok ve kül akma birikintileri fasiyesi ve 6. Tane destekli, andezitik lav-cüruf fasiyesi.

Yuntdağ volkanikleri jeokimyasal olarak andezit-dasit bileşimlidir ve kalk-alkali karakterlidir. Jeokimyasal analiz sonuçları Yuntdağ volkanizması içinde ayırtlanan farklı kaya birimlerinin kökensel olarak birbirleriyle ilişkili olduklarını ve kıtasak kabuk kenarı andezitik kuşaklarına benzerlik gösterdiklerini işaret eder.

Yuntdağ volkanikleri, riyolitik bileşimli Foça volkanik kompleksi tarafından üzerlenir. Foça volkanik kompleksi içinde üç farklı kaya birimi yüzlek verir. Bunlar: 1. Foça riyolitleri, 2. Foça volkaniklastikleri ve 3. Foça alkali volkanitleri. Foça riyolitleri masif riyolit lav akmaları ve domlarından yapılıdır. Riyolit domları Foça volkaniklastik istifi tarafından sarılırlar. Foça volkaniklastik istifi içinde üç farklı birim ayırtlanabilir. Bunlar: 1. Piroklastik akmalar, 2. Hyaloklastik breşler ve 3. Perlitlerdir. Masif riyolit domları,

merkeze yakın kesimlerde kaba kırıntılı piroklastikler ve perlitler tarafından çevrenir ve domlardan uzaklaştıkça ince taneli piroklastikler ve kaynaklı tüflere geçilir. Foça volkaniklastiklerinin litolojik ve sedimentolojik özellikleri ve domlarla ilişkileri riyolitik volkanizmanın sıg su ortamına sokulduğunu ve piroklastik istifin aynı ortamda domların sokulumuyla beraber gelişerek domları sardığını gösteren veriler taşır. Üst kesimlere doğru volkanik malzemenin sıg su ortamını doldurması nedeniyle yersel karasal alanlar gelişmiş ve buralarda kaya kırıntılarınca zengin kanal dolgusu fasiyesleri gelişmiştir. Foça volkaniklastikleri üst seviyelerde Foça alkali lavlarına ait ara düzeyler içerirler. Foça volkanik kompleksi içinde oluşum koşullarına göre 13 farklı fasiyes ayırtlanmıştır: 1. Masif riyolit fasiyesi, 2. Masif perlit fasiyesi, 3. Yerinde breşleşmiş hyaloklastit fasiyesi, 4. Yeniden işlenmiş hyaloklastit fasiyesi, 5. Laminalı çamurtaşı fasiyesi, 6. İnce taneli riyolit pumis-kaya kırıntısı fasiyesi, Sualtı kaynaklı ignimbirit fasiyesi, 7. Kaba taneli riyolit pumis-kaya kırıntısı fasiyesi, 8. Kaya kırıntısınca zengin kanal dolgu fasiyesi, 9. Sualtı kaynaklı ignimbirit fasiyesi, 10. Breşik perlit fasiyesi, 11. Sualtı kül yağntı fasiyesi, 12. Alkali lav akma fasiyesi ve 13. Alkali dayklar.

Foça riyolitleri kalk-alkali karakterlidir ve kimyasal özellikleri orojenez sonrası granitoidik kayalarla benzerlikler sunar. Diğer yandan alkali lav akmaları riftleşmeyle ilişkili veya kıta içi bazaltlara ait kimyasal özelliklere sahiptir.

Foça volkanik kompleksi yanal ve düşey yönde sarı-beyaz renkli gastrapod fosilleri içeren kireçtaşları ve killi kireçtaşlarına geçer ve bu birim çalışma alanında gözlenen en genç kaya birimidir.

Yuntdağ volkanitleri, Foça volkanik kompleksi ve Foça alkali volkanitleri arasındaki geçişli stratigrafi ilişkileri ve bu kayaların jeokimyasal özellikleri Batı Anadolu' da Aliğa-Foça çevresindeki volkanizmanın birbirini izleyen ve birbirleriyle ilişkili bir tektonik rejim altında oluştuğunu gösterir.

CONTENTS

	Page
Acknowledgements	iii
Abstract	iv
Özet	vi
List of Figures	xii
List of Tables	xxiv

Chapter one INTRODUCTION

1. 1. Study area	1
1. 2. Review the previous studies	4
1. 3. Objectives	5
1. 4. Methods used	7

Chapter two STRATIGRAPHY

2. 1. YUNTDAĞ VOLCANICS	9
2. 1. 1. Helvacı andesites	11
2. 1. 2. Haykıran blocky pyroclastics	13
2. 1. 3. Çaltılı andesites	14
2. 1. 4. Dumanlıtepe dykes	17
2. 1. 5. Age of the Yuntdağ volcanics	19

2. 2. FOÇA VOLCANIC COMPLEX.....	19
2. 2. 1. Foça rhyolites.....	21
2. 2. 2. Foça volcanics.....	27
2. 2. 2. 1. Pyroclastic flows.....	28
2. 2. 2. 2. Hyaloclastic breccias.....	31
2. 2. 2. 3. Perlites.....	35
2. 2. 3. Foça alkaline volcanics.....	39
2. 2. 4. Age of the Foça volcanic complex.....	43
2. 3. ALIĞA LİMESTONE.....	45

Chapter three
GEOCHEMISTRY

3. 1. YUNTDAĞ VOLCANICS.....	49
3. 1. 1. Helvacı andesites.....	49
3. 1. 2. Çaltılı andesites.....	55
3. 1. 3. Dumanlıtepe dykes.....	59
3. 2. FOÇA VOLCANIC COMPLEX.....	65
3. 2. 1. Foça rhyolites.....	65
3. 2. 2. Foça alkaline volcanics.....	72

Chapter four
VOLCANIC FACIES AND STRUCTURES

.....	77
4. 1. FACIES OF YUNTDAĞ VOLCANICS.....	79
4. 1. 1. Flow banded lavas(Facies 1).....	79
4. 1. 2. Subvolcanic andesites (Facies 2).....	79
4. 1. 3. Columnar jointed andesite(Facies 3).....	80
4. 1. 4. Flow breccias (Facies 4).....	81
4. 1. 5. Block and Ash flow deposits (Facies 5).....	82
4. 1. 6. Grain supported, andesite lava-scoria facies (Facies 6).....	85

4. 2. MORPHOLOGY AND VOLCANIC STRUCTURES IN YUNTDAG	
VOLCANISM	86
4. 2. 1. Dumanlıdağ Caldera	87
4. 2. 2. Yuntdağ Caldera	89
4. 3. FACIES OF FOÇA VOLCANIC COMPLEX	90
4. 3. 1. Eski Foça Area	92
4. 3. 1. 1. Massive rhyolite (Facies 7)	92
4. 3. 1. 2. Massive perlites (Facies 8)	95
4. 3. 1. 3. Reassembled hyaloclastic breccias (Facies 9)	95
4. 3. 2. Eski Foça-Bağarası Area	98
4. 3. 2. 1. Massive rhyolite (Facies 7)	98
4. 3. 2. 2. In-situ hyaloclastic breccias (Facies 10)	98
4. 3. 2. 3. Massive perlites (Facies 8)	99
4. 3. 2. 4. Reassembled hyaloclastic breccias (Facies 9)	100
4. 3. 2. 5. Laminated mudstone (Facies 11)	101
4. 3. 2. 6. Fine grained rhyolite pumice-lithic fragment facies (Facies 12)	102
4. 3. 2. 7. Coarse grained rhyolite pumice-lithic fragment facies (Facies 13)	103
4. 3. 2. 8. Lithic fragment-rich channel-fill facies (Facies 14)	104
4. 3. 3. Eski Foça-Yeni Foça Area	105
4. 3. 3. 1. Subaqueous welded ignimbrite facies (Facies 15)	106
4. 3. 3. 2. Brecciated perlite (Facies 16)	112
4. 3. 3. 3. Reassembled hyaloclastic breccias (Facies 8)	113
4. 3. 3. 4. Subaqueous ash fallout deposits (Facies 17)	113
4. 3. 3. 5. Coherent alkaline lavas (Facies 18)	114
4. 3. 3. 6. Alkaline dykes (Facies 19)	115

4. 4. MORPHOLOGY AND ERUPTION HISTORY OF FOÇA VOLCANIC COMPLEX.....	116
--	------------

Chapter five	
TECTONIC CONTROLS in the NEOGENE	
FOÇA VOLCANISM	
.....	121

Chapter six	
CONCLUSIONS	
.....	125

REFERENCES.....	128
------------------------	------------

APPENDICES.....	
------------------------	--

PLATE 1. Geological Map of the Foça Peninsula	
PLATE 2. Geological Map of the Geren Village-Yeni Foça Area	
PLATE 3. Geological Map of the Aliğa Region	
PLATE 4. Geological Map of the Çaltıldere-Yenişakran Area	
PLATE 5. Geological Map of the Dumanlıtepe Area	
PLATE 6. Geological Map of the Yuntdağ Area	
PLATE 7. Explanations	

LIST OF FIGURES

	Page
Figure 1. 1 Location Map of the Study Area.....	2
Figure 1. 2 Map Showing Distribution of the Neogene Volcanic Rocks in the Aliğa-Foça region and Surroundings.....	3
Figure 2. 1 Generalized Stratigraphical Column Section of the Aliğa-Foça Region.....	10
Figure 2. 2 Mesozopic Scale Flow Foliations in the Helvacı Andesite Unit.....	12
Figure 2. 3 Photomicrograph showing the glassy matrix in Helvacı andesites.....	12
Figure 2. 4 Photomicrograph showing the typical microlitic matrix and trachytic texture, observed in Helvacı andesites.....	13
Figure 2. 5 Photomicrograph showing the euhedral clinopyroxene phenocrysts in Helvacı andesites.....	13
Figure 2. 6 Haykıran blocky pyroclastic subunit underlying the Helvacı andesites.....	14

Figure 2. 7 Haykırın blocky pyroclastics interdigitating the massive lavas of the Helvacı andesites.....	14
Figure 2. 8 Photomicrograph showing the serpentinized olivine phenocrysts in Çaltılı andesites.....	15
Figure 2. 9 Çaltılı andesites overlying the Haykırın blocky pyroclastics subunit.....	16
Figure 2. 10 Massive lava flows of the Çaltılı trachyandesite subunit intercalating with the Haykırın blocky pyroclastics.....	16
Figure 2. 11 Andesitic dykes cutting the massive lava flows of the Helvacı andesite unit.....	17
Figure 2. 12 Massive andesitic lava enclaves of the Helvacı andesite unit observed in dykes and the subvolcanic stocks of the Dumanlıtepe dykes subunit.....	18
Figure 2. 13 High-angle, planar cross-cutting contact between the Dumanlıtepe dykes and the Helvacı andesite unit.....	18
Figure 2. 14 Age and the geochemical affinities of the volcanic areas in western Anatolia and adjacent islands.....	20
Figure 2. 15 Detailed geological map of the Foça Peninsula.....	22
Figure 2. 16 Massive rhyolite lava flows with significant flow foliation in the Bağarası rhyolite lava subunit.....	23
Figure 2. 17 Rhyolitic stocks emplaced in the Foça volcanics.....	23

Figure 2. 18 Well-developed flow foliations in the Bağarası rhyolite lava.....	23
Figure 2. 19 Calsedony nodules in Bağarası rhyolite lava elongated along the flow laminae.....	23
Figure 2. 20 Photomicrograph showing the embayed quartz phenocrysts in Foça Rhyolites.....	24
Figure 2. 21 Recrystallized glassy matrix in the Foça massive rhyolites growing onto the euhedral quartz phenocrysts.....	25
Figure 2. 22 Devitrification in the glassy matrix in the Foça rhyolites.....	25
Figure 2. 23 Stratigraphic section measured around Bağarası village showing the stratigraphic relation between the Bağarası rhyolite lava and Foça alkaline lava subunits.....	26
Figure 2. 24 The cross-cutting contact relation between the Foça rhyolites and the Foça volcanoclastics.....	27
Figure 2. 25 High-angle flow foliations at the periphery of the rhyolitic stocks in the Eski Foça composite dome.....	27
Figure 2. 26 Massive perlites covering the massive rhyolite dome around Eski Foça town.....	27
Figure 2. 27 Photomicrograph Showing the Carbonate Cement	

Bounding the pyroclastic Material in Foça Volcaniclastics Unit.....	29
Figure 2. 28 Stratigraphic section measured around Güzelhisar village.....	30
Figure 2. 29 Field photographs showing the gradational contact between the Çaltılı andesites and the Foça volcaniclastics. 10-20 cm-thick mafic lava lenses in the Foça pyroclastics in this area is significant.....	31
Figure 2. 30 Photograph showing the massive andesite lavas of the Helvacı andesite unit overlying the pyroclastic flows of the Foça volcaniclastics.....	31
Figure 2. 31 Cross section from Eski Foça-Bağarası road showing the stratigraphic relation between the Foça massive rhyolites, Foça pyroclastic sequence and perlites.....	32
Figure 2. 32 Thin, green-colored mudstone intervals within the pyroclastic flows subunit.....	34
Figure 2. 33 In situ hyaloclastic breccias surrounding the massive rhyolite domes. Note the typical angular form of grains, jig-saw fit texture and coherent nature of the matrix.....	34
Figure 2. 34 Reassembled hyaloclastic breccias.....	34
Figure 2. 35 Field photograph showing the contact zone between the reassembled hyaloclastic breccias and the massive perlites around Eski Foça town.....	35
Figure 2. 36 Reassembled hyaloclastic breccias with irregular	

lower contact of the individual flow unit.....	35
Figure 2. 37 Small mud dykes intruded in to the overlying hyaloclastic breccia flow unit.....	35
Figure 2. 38 Photomicrograph showing the perlitic texture in massive perlites subunit of the Foça volcanoclastics.....	36
Figure 2. 39 Measured stratigraphic sections for the pyroclastic sequence in Eski Foça-Yeni Foça area.....	37
Figure 2. 40 In the Foça pyroclastic flows, the laterally discontinues brecciated perlite lenses containing massive rhyolite and massive perlite breccias in a glassy, perlitic matrix are also found.....	38
Figure 2. 41 Brecciated rhyolitic dykes cutting the overlying brecciated perlite lense.....	38
Figure 2. 42 Photomicrograph showing the grain supported brecciated texture of the rhyolite dyke in the brecciated perlite lense.....	38
Figure 2. 43 Around Eski Foça town, surrounding the massive rhyolite dome massive perlites laterally pinge out in the reassembled hyaloclastic breccias.....	38
Figure 2. 44 Massive perlites laterally and vertically intercalate with the resedimented hyaloclastites in different levels and overlie them.....	38
Figure 2. 45 Massive perlites intercalate the Foça pyroclastic flows in different straigraphic levels.....	39

Figure 2. 46 Photomicrograph showing the characteristic porphyritic texture in Foça alkaline lavas.....	40
Figure 2. 47 Photomicrograph showing the typical trachytic texture in Foça alkaline lavas.....	41
Figure 2. 48 In the Foça alkaline lavas, the high-Ca plagioclase phenocrysts are commonly found as partly or completely converted into calcite.....	41
Figure 2. 49 The dominant mafic mineral, observed in Foça alkaline lavas, is the aegyrine-augite-type clinopyroxenes with significant low extinction angle and light to dark green pleochroism.....	42
Figure 2. 50 Photomicrograph showing the augite-type clinopyroxene phenocrysts with high-calcium content, converted into the calcite.....	42
Figure 2. 51 Field photograph showing the coherent lava flows of the Foça alkaline volcanics, overlain by the Aliğa limestone unit.....	43
Figure 2. 52 Cross section from the Bozköy village showing the gradational contact between the Foça volcanoclastics and the Aliğa limestone units.....	44
Figure 2. 53 Mafic alkaline dykes with high-angle cross cutting contact in the Foça pyroclastic flows subunit.....	45
Figure 2. 54 Cross section from the Samurlu village showing the gradational contact between the Foça volcanoclastics and the Aliğa limestone units.....	47

Figure 2. 55 Cross section from the southern flank of the Bozdivlit Mt. showing the lacustrine limestone lenses in the Foça volcanoclastics.....	48
Figure 3. 1 (Na ₂ O + K ₂ O) vs SiO ₂ variation of the Helvacı andesites.....	52
Figure 3. 2 Frequency of the samples from the Helvacı andesites in nomenclature diagrams of Winchester and Floyd (1977).....	52
Figure 3. 3 The chemical affinity of the Helvacı andesites.....	53
Figure 3. 4 Frequency of the Helvacı andesites in a. FeO / (Na ₂ O + K ₂ O) / MgO and b. SiO ₂ / MgO diagrams of Irvine and Baragar (1971).....	53
Figure 3. 5 The frequency of the Helvacı andesites in K ₂ O vs SiO ₂ diagram of Gill (1981).....	54
Figure 3. 6 (Na ₂ O + K ₂ O) vs SiO ₂ variation of the Çaltılı andesites.....	57
Figure 3. 7 Frequency of the samples from the Çaltılı andesites in nomenclature diagrams of Winchester and Floyd (1977).....	57
Figure 3. 8 The chemical affinity of the Çaltılı andesites.....	58
Figure 3. 9 Frequency of the Çaltılı andesites in a. SiO ₂ / (Na ₂ O + K ₂ O) / MgO triangle of Irvine and Baragar (1971) and b. SiO ₂ / MgO diagrams of Miashiro (1974).....	58
Figure 3. 10 The frequency of the Çaltılı andesites in K ₂ O vs SiO ₂ diagram of Gill (1981).....	59
Figure 3. 11 (Na ₂ O + K ₂ O) vs SiO ₂ variation of the Dumanlıtepe dykes.....	61

Figure 3. 12 Frequency of the samples from the Dumanlítepe dykes in nomenclature diagrams of Winchester and Floyd (1977).....	61
Figure 3. 13 The chemical affinity of the Dumanlítepe dykes.....	62
Figure 3. 14 Frequency of the Dumanlítepe dykes in a. FeO / (Na ₂ O + K ₂ O) / MgO triangle of Irvine and Baragar (1971) and b. SiO ₂ / MgO diagram of Miashiro (1974).....	62
Figure 3. 15 The Harker-type variation diagrams of the Helvacı and Çaltılı Andesites and the Hatundere dykes.....	63
Figure 3. 16 a. Chondrite and b. MORB-normalized spider diagrams of the Helvacı and Çaltılı andesites and the Hatundere dykes.....	66
Figure 3. 17 (Na ₂ O + K ₂ O) vs SiO ₂ variation of the Foça rhyolites.....	69
Figure 3. 18 Frequency of the samples from the Foça rhyolites in nomenclature diagrams of a. Si ₃ -(K+Na+2Ca/3) vs K-(Na+Ca) diagram of debon and lefort (1983) and b. Zr/TiO ₂ *0.0001 vs Nb ₇ Y diagram of Winchester and Floyd (1977).....	69
Figure 3. 19 The chemical affinity of the Foça rhyolites.....	70
Figure 3. 20 Frequency of the Dumanlítepe dykes in FeO / (Na ₂ O + K ₂ O) / MgO triangle of Irvine and Baragar (1971).....	70
Figure 3. 21 a. Nb vs Y and b. Rb vs Y+Nb (Pearce et al., 1984) variations of the Foça rhyolites.....	71
Figure 3. 22 (Na ₂ O+K ₂ O) vs SiO ₂ variation of the Foça alkaline volcanics.....	75
Figure 3. 23 Frequency of the samples from the Foça alkaline volcanics in	

nomenclature diagrams of Winchester and Flyd (1977).....	75
Figure 3. 24 The chemical affinity of the Foça alkaline volcanics.....	76
Figure 4. 1 The Typical Porphyritic Texture in the Çaltılı Andesites with Abundant Plagioclase and Pyroxene Phenocrysts in Microlitic Matrix.....	81
Figure 4. 2 Trachytic Texture in Columnar Jointed Andesites Characterized by the Elongated Microlites in Matrix.....	81
Figure 4. 3 Brecciated Texture, Observed in Flow Breccia Facies Typified by the Angular Clasts Set in a Coherent Lava Matrix.....	82
Figure 4. 4 The Block and Ash Flow facies is characterized by the Poorly Sorted Pebble to Boulder Size Lava Clasts Set in Ash-Size Matrix.....	83
Figure 4. 5 The coherent Andesite Lavas Along an Irregular Contact.....	83
Figure 4. 6 Poorly Developed Bedding is the Unique Sedimentary Structure, Observed in the Block and Ash Flow Facies.....	84
Figure 4. 7 Coherent Lava Flows Interlayering with the Thick Block and Ash Flow Deposits.....	84
Figure 4. 8 Field Photograph Showing the Grain Flow Deposits with Poorly Developed Bedding of 20-30°	86
Figure 4. 9 Detailed Geological Map of the Dumanlıdağ Caldera.....	88
Figure 4. 10 The Central Parts of the Yuntdağ Caldera.....	90

Figure 4. 11 Detailed Geological Map a Rhyolite Dome Cropping Out around eski Foça.....	91
Figure 4. 12 The Steeply Dipped Periphery of the Dome-Shape Rhyolite Intrusion.....	93
Figure 4. 13 In the Central Parts of Domes, Porphyritic Texture with Quartz and Feldspar Phenocrysts, Set in a Recrystallized and Partly Devitrified Matrix, is Characteristic.....	93
Figure 4. 14 Photomicrograph Showing the Porphyritic Texture in Massive Rhyolite Facies with Recrystallized Glassy Matrix.....	93
Figure 4. 15 Well-Developed Flow Lamination at the Periphery of Rhyolite Dome.....	94
Figure 4. 16 During the Intrusion, Due to the Progressive Updoming, the Hosting Massive Perlites and Hyaloclastic Breccias Displays Inward Dips.....	94
Figure 4. 17 Plastically Deformed Flow Lamination in Massive Perlite Facies.....	96
Figure 4. 18 Photomicrograph Showing the Perlitic Texture in Massive Perlites... 	96
Figure 4. 19 Field Photographs Showing the Reassembled Hyaloclastic Breccias... 	97
Figure 4. 20 a. Massive perlites Interlayering with the reassembled Hyaloclastic Breccias, b. At the Contact Between Massive Perlites and the Reassembled Hyaloclastic Breccias, the Latter Becomes Richer in Perlitic Breccias.....	97
Figure 4. 21 The Massive Rhyolite Bodies Around Eski Foça.....	99

Figure 4. 22 In Situ Brecciated Hyaloclastites.....	100
Figure 4. 23 Lacustrine Volcanic Mudstone Interlayers Observed in Reassembled Hyaloclastic Breccias.....	102
Figure 4. 24 Normal Grading in Fine Grained Rhyolite Pumice-Lithic Fragment Facies.....	102
Figure 4. 25 The Irregular, Scoured Lower Contact of the Coarse Grained Rhyolite Pumice-Lithic Fragment Facies.....	103
Figure 4. 26 The Lithic Fragment-Rich Channel-Fill Facies Scouring the Underlying Fine Ash Horizons.....	105
Figure 4. 27 Subaqueous Welded Ignimbrites.....	107
Figure 4. 28 Photomicrographs Showing the texture and Components of the Subaqueous welded Ignimbrite Facies.....	107
Figure 4. 29 Photomicrographs Showing the Flattened Pumice Fragments, Filled by Recrystallized Granoblastic Quartz.....	108
Figure 4. 30 The Pore Spaces of the Pumice Fragments are Filled by Recrystallized Granoblastic Quartz or Feldspar in Whole Sequence.....	108
Figure 4. 31 Photomicrographs Showing the Siliceous Nodules, Observed in Subaqueous Welded Ignimbrites.....	109
Figure 4. 32 Poorly developed Columnar Joints in Slightly Welded Upper Parts of the Subaqueous Ignimbrites.....	109
Figure 4. 33 Flowing-Related Sedimentary Structures in Subaqueous Ignimbrites.....	110

Figure 4. 34 Field Photograph Showing the Coarse Grained Rhyolite Pumice-Lithic Fragment Facies.....	111
Figure 4. 35 Field photographs Showing the Subaqueous Ash Fallout Deposits.....	114
Figure 4. 36 A model for the formation of subaqueous pyroclastic sequences in Foca region.....	117



LIST OF TABLES

	Page
Table 3. 1 The Major and Trace Element Composition of the Helvacı Andesites.....	51
Table 3. 2 The Average Major and Trace Element Composition of the Helvacı Andesites and Some Other Typical Andesite Types.....	54
Table 3. 3 Major and Trace Element Composition of the Çaltılı Andesites. Samples, Signed by (*), are After Altuntaş (1997).....	56
Table 3. 4 The Average Chemical Composition of the Çaltılı Andesites and Some Typical Andesite Types.....	60
Table 3. 5 Major and Trace Element Composition of the Dumanlıtepe Dykes.....	64
Table 3. 6 Average Major and Trace Element Composition of the Dumanlıtepe Dykes, Helvacı and Çaltılı Andesites.....	67
Table 3. 7 Major and Trace Element Composition of the Foça Rhyolites.....	68
Table 3. 8 Major and Trace Element Composition of the Foça Alkaline Volcanics.....	74

**Table 3. 9 Average Major and Trace Elemet Composition of the
Foça Alkaline Volcanics and Some Typical Within
Plate Alkaline Rocks..... 76**



CHAPTER ONE

INTRODUCTION

In Western Anatolia, the Neogene volcanic rocks with various facies are exposed in extensive areas. To the north of İzmir, in the Aliğa-Foça area (Figures. 1.1,2), this volcanic succession is made up of thick andesitic to latit-andesitic lava succession, rhyolitic lavas, pyroclastics and subvolcanic stocks. Lacustrine sedimentary successions accompany the volcanic sequences in many outcrops indicating the close relationship between the volcanism and lacustrine deposition in time and space. In this study, the stratigraphy, petrological features, facies characteristics, eruption mechanisms and the environments of formation of the volcanic sequences are examined and the stratigraphy of the Neogene sequences are redefined.

1. 1. Study Area

The study area is located about 50 km to the north of İzmir, and include Menemen, Aliğa and Foça towns (Figure 1.1). In this study, an area of 10 topographic sheets of 1/25 000 scale (İzmir K 18 a1, a2, a3, a4, d1, Urla K 17 b3, b4, c1, c2, and d2) was mapped. The İzmir-Çanakkale highway passes through the study area in the north-south direction which also roughly divides the study area into two parts. On the east side of this highway, the andesitic lava flows have extensive outcrops and on the west side the rhyolitic volcanoclastic sequence is dominant. Menemen and Aliğa towns are located on this highway. Minor roads to Foça and the other villages also provide the access to the area. The study area is bounded by the Pleistocene-Quaternary Gediz Plain to the south and Bakırçay Plain to the north.



Fig. 1. 1. Location Map of The Study Area

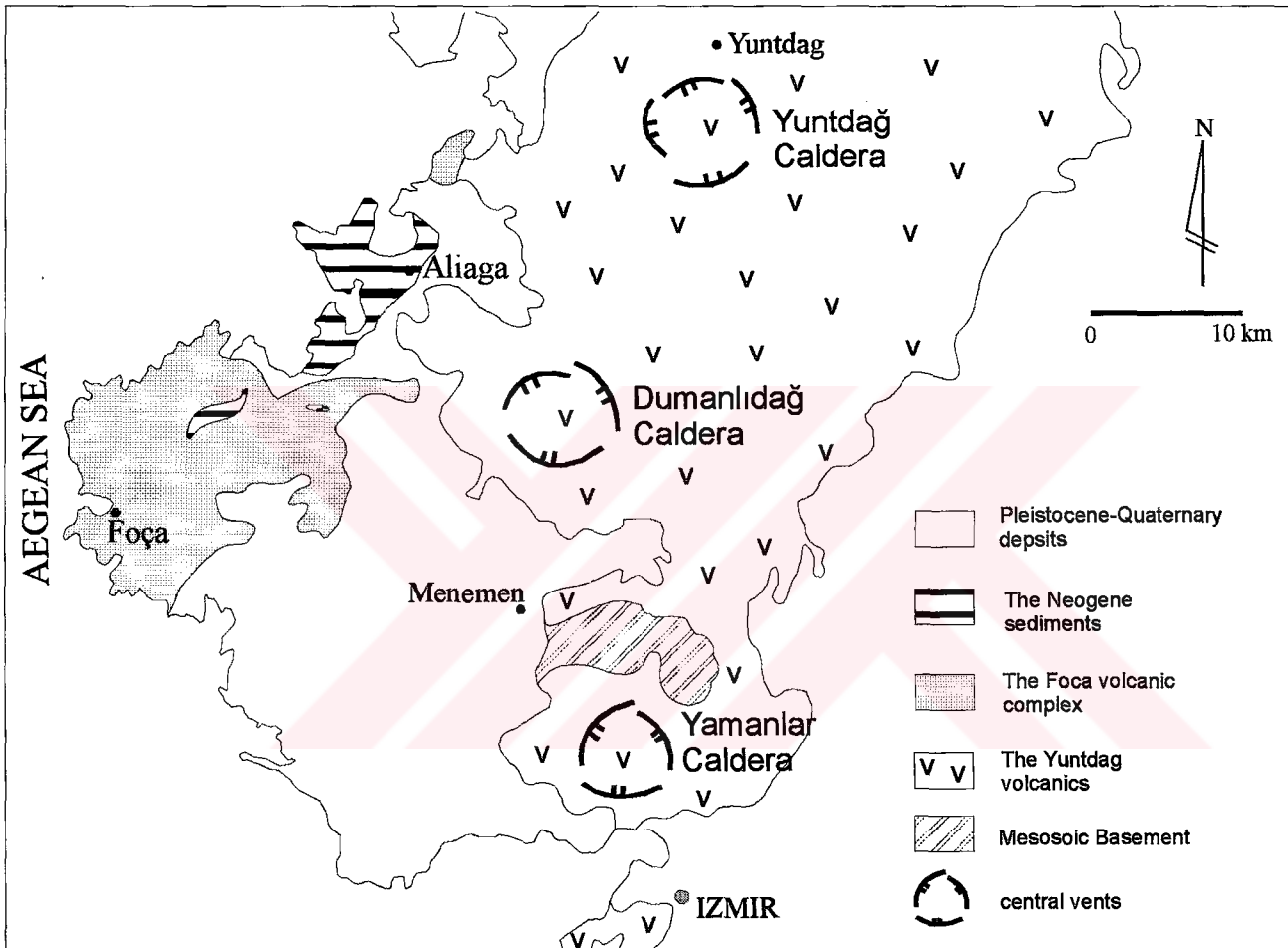


Fig. 1. 2. Map Showing Distribution of the Volcanic Rocks and the Main Central Vents in the Aliaga-Foça Region and the Surroundings

1. 2. Review of the Previous Studies

Neotectonic evolution of the Western Anatolia has been subjected to many studies since 1960's (Arpat & Bingöl, 1969; Ketin, 1970; Şengör & Dewey, 1980; Şengör & Yılmaz, 1981; Şengör, 1982; Şengör, Satır & Akkök, 1984). The main aim of these studies was understanding the tectonic regimes controlling the tectonic evolution of the Western Anatolia in Neotectonic period. To achieve this goal, graben systems which are the main structures in the region, and sedimentary sequences of these grabens have been subjected to detailed geological studies and the works on the stratigraphic and sedimentologic features of these basins were done as well as the crustal scale tectonic interpretations (Kaya, 1981; Seyitoğlu & Scott, 1990; Seyitoğlu & Scott, 1992; Seyitoğlu, Scott & Rundle, 1992; Seyitoğlu & Scott, 1994; Seyitoğlu, Benda and Scott, 1994; Emre, 1996). Since the magmatic activity and the tectonic setting have close relationship in time and space, the Neotectonic magmatic activity in Western Anatolia has been studied in recent years and numerous works have been carried out on the magmatic associations of the region (Savaşçın, 1978; Ercan, 1979; Kaya & Savaşçın, 1981; Ercan, Satır, Kreuzer, Türkecan, Günay, Çevikbaş, Ateş, and Can, 1985; Innocenti, Manetti, Mazzuoli, Peccerillo and Poli, 1985; Ercan, 1987; Yılmaz, 1989; Yılmaz, 1990; Mc Kenzie and Yılmaz, 1991; Güleç, 1991; Seyitoğlu & Scott, 1991; Altunkaynak & Yılmaz, 1998; Genç, 1998; Karacık & Yılmaz, 1998). In addition to these geochemical, petrological and geodynamic interpretations, some radiometric age determinations of the same volcanic associations have also been done (Borsi, Ferrara, Innocenti, and Mazzuoli, 1972; Fytikas, Giuliani, Innocenti, Marinelli and Mazzuoli, 1976; Fytikas, Innocenti, Manetti, Mazzuoli, Peccerillo and Villari, 1979; Ercan et al., 1985) which indicate an 21.5 to 7 my age for different stratigraphic levels of this sequence. Savaşçın (1978) and Kaya & Savaşçın (1981) noted that the volcanic succession cropping out in the area, were formed in both a progressive activities and independently developed stages during the period of 11-21 my.

In the light of these observations, the models, suggested for the magmatic activity and the tectonic evolution in the region, may be outlined under the following three major headings (Altunkaynak & Yılmaz, 1998):

1. The magmatic activity has been developed under a N-S directed extensional tectonic regime starting from the Late Oligocene and being continuous since then (Seyitoğlu & Scott, 1991; Seyitoğlu & Scott, 1992),

2. The magmatism was generated in relation with the north-dipping subduction of the east Mediterranean ocean floor along the Hellenic trench (Fyticas et al., 1984; Pe-Piper & Piper, 1989; Gülen, 1990) and

3. There are different episodes of magma generations, occurred in different tectonic settings (Şengör & Yılmaz, 1981; Ercan et al., 1984, Ercan et al., 1995; Yılmaz, 1989; Yılmaz et al., 1994; Savaşçın & Gülen, 1990; Güleç, 1991).

In recent years this third view has been noted in many studies and it was stated that during the first episode, the magma was generated under a N-S compressional regime during the Late Oligocene-Middle Miocene time, and during the following stages, the magma was formed under the younger N-S extensional regime (Şengör & Yılmaz, 1981; Ercan et al., 1984, 1985, 1995; Yılmaz, 1990; Altunkaynak & Yılmaz, 1998; Genç, 1998). Yılmaz, (1990) also noted that the compressional episode generated the calc-alkaline magmatism and the extensional regime gave way to the alkaline magmatism.

1. 3. Objectives

In the area, most of the previous works were based on the petrographic and geochemical analyses or radiometric age determinations of the randomly collected samples from the different stratigraphic levels, or they include global tectonic interpretations without detailed and unequivocal field data. So that, although there are plenty of documents on the volcanism of the Western Anatolia, scientists are still far from to be agree on the volcanic history of the region as well as tectonic setting which had controlled the volcanism.

In the Foça Region, presence of an alkaline volcanism which is so-called as the Foça-Urla alkaline volcanism (Savaşçın, 1978, Savaşçın, 1990), has been mentioned for a long time. However, this term has generally been considered as representative for the whole Foça Region (Savaşçın & Erler, 1994). In the field, on the other hand, the alkaline

volcanic rocks have only limited outcrops and the area is dominantly characterized by a calc-alkaline rhyolitic magmatic association. Stratigraphic and tectonic relations of the alkaline suit with the accompanying calc-alkaline volcanism are need to be documented in detail which forms another major objective of this study. These felsic components of the volcanic succession dominate the Foça Region where rhyolitic pyroclastics and lavas are common rock types, and they have only been briefly mentioned in the earlier studies, under a general term of “Foça tuffs” and were just included in the West Anatolian volcanic association (Savaşçın, 1978; Akyürek & Soysal, 1978). Kaya & Savaşçın (1981) and Kaya (1981) carried out relatively detailed works on this succession but they mainly examined petrographic and chemical characteristics of these rocks. However detail mapping and facies analyses of these rocks have not been done yet. Particularly the subvolcanic facies of these successions and mode of their emplacement have not been discussed. The petrography and the field properties of these pyroclastics and subvolcanic facies have important clues to approach the eruption mechanism and environment of emplacement of this volcanism.

In this work, the stratigraphic relations between the different volcanic and volcanoclastic facies and the Neogene sedimentary units are studied. Typical sections representing the stratigraphy and relations between the different volcanic facies were measured and different volcanoclastic facies were determined to describe the physical conditions and types of the volcanism. Where the rhyolitic subvolcanic stocks or dykes are observed, some detailed geological maps were done to approach the mode of emplacement of rhyolitic subvolcanic stocks and their geometry. Petrographic investigations of about 250 samples from the different rock units and geochemical analyses of about 100 samples from the massive volcanic facies were done in order to define the petrological features and the tectonic regimes which controlled the magmatism in the area.

In the organization of this thesis, first the stratigraphy of the area will be given and the lithological and petrographical features of the units will be described. In this section the stratigraphical relations of the different units and subunits will be outlined. In the second section, the results of the major and trace element analyses, carried out on the samples collected from the massive lava facies of different units will be given. The geochemical affinities of the various units and their probable tectonic setting of formation will also be

discussed. In the section of “Volcanic facies and structures”, different volcanic and volcanoclastic facies will be defined and their interrelationships are outlined. In the same section, the volcanic centres from which the volcanic activity occurred, will be defined and some typical features of them will be described. In the fifth section which is named as the “Structural controls on volcanism”, the tectonic regime which controlled the volcanism will be discussed in the light of the field and geochemical data.

1. 4. Methods used

This study which was supported by The Scientific and Technical Research Council of Turkey (TUBITAK) project of YDABCAG-399 and the Research Fund of Dokuz Eylül University Project no: 0908. 95. 06. 02, was carried out as a PhD thesis in the the Graduate School and Applied Science, Dokuz Eylül University. The field studies were carried out in the 1/25 000-scale topographic maps. In naming the stratigraphic units previously given names were used as much as possible, and some of them were redefined.

The total geochemical analyses of 100 samples from different units were done and the results were interpreted by related graphs. In the geochemical studies major and trace element analyses were partly carried out in the geochemistry laboratory of the Geology Department of Dokuz Eylül University and partly in the Department of Geology and Geophysics of the University of Edinburgh, Scotland. The studies, carried out in the University of Edinburgh were supported financially by the British Council, and Unesco. In the geochemistry laboratory of the Department of Geology of Dokuz Eylül University, major element analyses were completed by atomic absorption and trace elements by X-Ray Fluorescent methods. For the atomic absorption analyses, 0.25 gr sample was mixed with 2 gr lithium tetraborate and glassified at 1000 °C and dissolved with HCl and finally prepared solutions 1000 ppm. In the X-Ray fluorescent studies 7 gr sample was mixed with 2.8 gr starch and made into a tablet in 25 ton presses. Then, samples were examined with (LIF 220 crystal in 2θ between 29°-40° for Zr, Nb, Y, Rb, Sr under the conditions of 50 kV/30 mA; (LIF 200 crystal in 2θ between 38°-40°) for Ga under the conditions of 50 kV/50 mA; (LIF 220 crystal in 2θ between 86.5°-88.5°) for Ba under the conditions of 50 kV/50 mA; (Au crystal in 2θ between 68°-71°) for Cr under the conditions of 50 kV/45 mA; (LIF 200 crystal in 2θ between 47°-50°) for Cu, Ni and Zn under the conditions of 50

kV/50 mA; Peaks belonging to the elements were found and the amounts of these elements were obtained as ppm values by peak heights.

In the geochemistry laboratory of the Department of Geology and Geophysics of the University of Edinburgh samples were analysed for 10 major and 17 trace elements using the Philips PW 1480 wavelength-dispersive, automatic, sequential X-Ray fluorescent spectrometer fitted with Rh anode side-window X-Ray tube. To correct for instrument drift on the PW 1480 monitors were used to update the current calibration before each batch of samples was analysed. The samples were, routinely, measured only once. For major element analyses the rock powders were dried in an oven overnight at 110 °C. Approximately 1 gr of each powder was ignited for 20 minutes in a Pt-5%Au crucible at 1100 °C and a value for LOI (=H₂O loss+CO₂ loss-O₂ gain) was calculated from the weight change. The ignited powder was then fused for 20 minutes at 1100 °C using a lithium borate flux (Johnson Matthey Spectroflux 105) with a 5:1 (flux:sample) dilution. The molten material was poured from the crucible onto a graphite plate and pressed into a disc by lowering an aluminium plunger onto the globule. The casting operation was carried out on a hotplate at 220 °C and the glass disc allowed to anneal at this temperature for 10 minutes before cooling. For the trace element analyses approximately 6 gr of rock powder was mixed with 4 drops of binding agent (2% PVA in distilled water). The mixture was placed in a steel mol, surrounded and backed by boric acid powder, and compressed at 8 tons to form a 40 mm diameter pellet using a hydraulic press. The spectrometer was calibrated for major and trace element analyses using USGS and CRPG standard samples.

CHAPTER TWO

STRATIGRAPHY

In the study area, three main rock associations are distinguished in the Neogene succession. These are: **1.** The Yuntdağ volcanics, **2.** The Foça volcanic complex and **3.** The Aliğa limestone (Figures 1.2, 2.1). The Yuntdağ volcanics, observed in Aliğa, Foça and surroundings, form the lowest unit of the volcanic succession and crop widely on the east side of the İzmir-Çanakkale highway (Figure 1.2). The unit is mainly made up of andesitic to trachyandesitic lavas and accompanying coarse-grained volcanoclastic rocks. The andesitic suite changes upward into the typically columnar-jointed, dark coloured andesitic lava facies. Especially close to the central vents, the andesitic dykes which are compositionally and genetically subvolcanic equivalents of the lava facies, cut thick lava succession. The Foça volcanic complex, on the other hand, have extensive outcrops on the west side of the İzmir-Çanakkale highway and particularly around the Foça area (Figure 1.2). The Foça volcanic complex consists of massive rhyolitic lavas, rhyolitic pyroclastics and minor occurrences of mafic alkaline lavas. The Aliğa limestone unit consists dominantly of the lacustrine limestones and minor mudstone intervals, and this unit interdigitates and overlies the Foça volcanic complex around Aliğa and in the Foça Peninsula (Figures 1.2, 2.1).

In this chapter the main field characteristics of the rock units, above, will be described. The detailed facies features and hence the lithological properties is explained in chapter 4, so that the lithological features of the units are briefly presented here to avoid the repetitions in text.

2. 1. YUNTDAĞ VOLCANICS

The Yuntdağ volcanics crop out in a large area between Bergama and İzmir. The different facies of the unit were generally named by local names by Savaşçın & Kaya, (1981) and Kaya, (1981). Yılmaz (1989) named this thick succession cropping out nearly

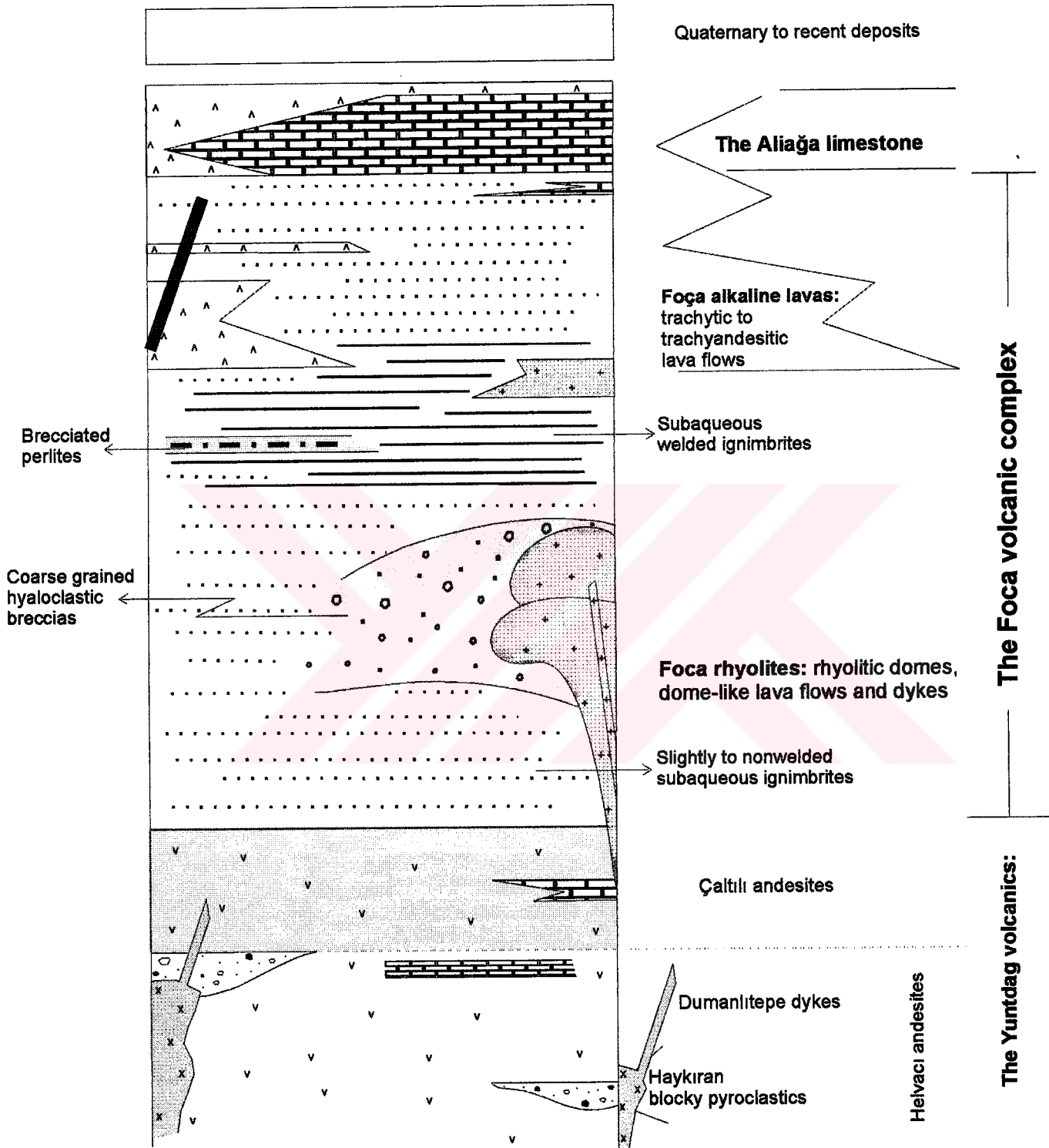


Figure 2. 1 Generalized Columnar Section of Aliğa-Foça Region

all around the western Anatolia as the “Andesitic suite”. Akyürek & Soysal (1978) named this unit as the Yuntdağ volcanics in their work, covering a large area between Ayvalık and Bergama, and this name is about the most common name used for this widespread volcanic sequence. The lateral equivalent of the unit is well-known as the Yamanlar Group around İzmir (Kaya, 1981). The Yuntdağ volcanics are dominated by the andesitic-trachyandesitic lavas of the Helvacı andesites. Upward these lava flows pass into the andesitic-trachyandesitic lavas with well-developed columnar joints which will be mentioned here as the Çaltılı andesites, Dumanlıtepe dykes and the Haykıran blocky pyroclastics form the other subunits of the Yuntdağ volcanics.

2. 1. 1. Helvacı andesites

Description: The thick and widespread, generally pink and gray-coloured andesitic lava flows showing well-developed flow foliations, are named in this study as the Helvacı andesites. The unit which is the most common volcanic rock type in the whole Western Anatolia, crops widely out around İzmir to the south, and Bergama to the north (Figure 1.2). In the study area, the unit is observed mainly on the east side of the İzmir-Çanakkale highway, around Buruncuk, Hatundere, Helvacı villages, and to the north of the Menemen-Emiralem-Manisa highway, and to the north along the entire Yuntdağ Region (Plates 4,5,6, Figure 1.2). In the previous studies, this unit has generally been mentioned by local names or just lithological names as “andesite unit” or “andesitic lavas”. The unit corresponds the lava flows of the Çukurköy Formation of Kaya (1981) and Kaya & Savaşçın (1981). However, the stratigraphical position of the unit in the study area, is different from that of Kaya (1981) and Kaya & Savaşçın (1981).

Lithology: The Helvacı andesites are composed of pink-gray, massive andesitic, trachyandesitic to rhyodacitic lavas with well-observed porphyritic texture. The lavas show successive flow units with a thickness of 10 cm to 1 m. Flow foliation and mineral lineation defined by the long axes of feldspar phenocrysts are common in the lava sequence. In some places, transported lapilli and block size accessory rock fragments are significantly aligned in the matrix, indicating flow process, and direction of linear flow alignment is even noticed in hand specimens (Figure 2.2). Locally, the length of the plagioclase phenocrysts reach up to 4-5 mm in pinky glassy matrix. The phenocrysts constitute 20 to 50 percent of andesites. The main felsic minerals are plagioclase, and rare

sanidine. The mafic minerals are amphibole, biotite and pyroxenes. Matrix is generally microlitic and in places glassy (Figure 2.3a,b). Where microlitic matrix is observed, trachytic flow texture which is characterized by clearly elongated microlites (Figure 2.4) and pilotaxitic texture in which matrix is made up of randomly oriented microlites, are common. The plagioclase phenocrysts showing polysynthetic twinning with 22 to 28° extinction angle which corresponds the Andesine composition of Plagioclases (An_{40-50}), dominate the whole mineral association in the unit. The biotites and hornblends are the dominant mafic minerals. The euhedral to subhedral pyroxenes are 2 to 5 percent in average abundance. Clinopyroxenes are dominant and orthopyroxenes (Figure 2.5) are relatively minor in abundance. Chloritization of the mafic minerals, and conversion of the feldspars into the clay minerals are the main alteration types. In the biotites and hornblends iron-oxidised rims surrounding the phenocrysts are common. The average mineralogical composition of the andesites is as follows: Matrix 55 %, plagioclase 25 %, hornblend 5 %, biotite 5 %, klinopyroxene 2.5 %, orthopyroxene 1.5 %, sanidine 1 %, chlorite 2 %, opaque mineral 2%, clay minerals 1 %.

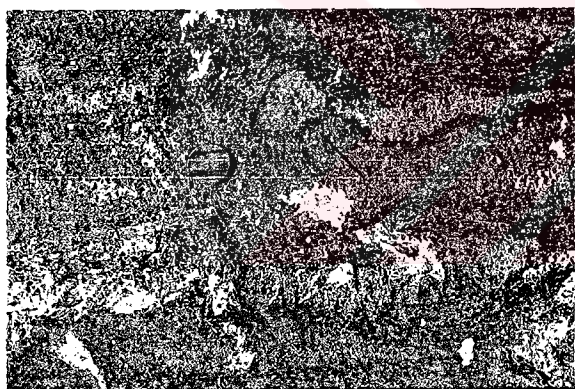


Figure 2. 2 Mesoscopic Scale Flow Foliations in the Helvacı Andesite Unit. Arrow Shows the Massive Andesite Rock Fragments Transported by Flowing.
İzmir K 18 a 4; 06 075 / 91 475

Boundary Relations: The Helvacı andesite unit forms the stratigraphically lowermost part of the whole volcanic succession in the study area and surroundings. The lower contact of the unit does not crop out in the area studied. Around İzmir, on the other hand, it

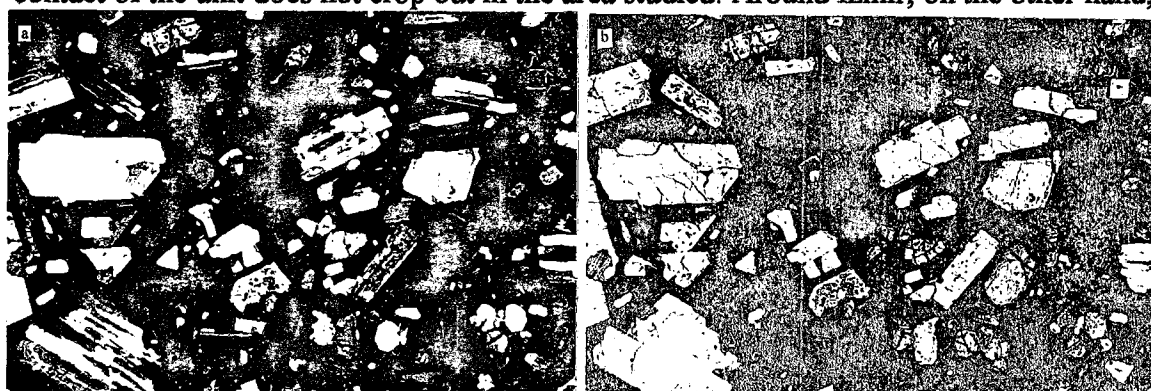


Figure 2. 3 Fotomicrograph Showing the Glassy Matrix in Helvacı Andesites. Porphyritic Texture with Polysynthetically Twinned Plagioclase, Biotite and Pyroxene Phenocrysts Set in Glassy Matrix, is Clear. **a.** Cross Polirized Light, **b.** Parallel Polirized Light. Note the Crude Flow Foliation in Glassy Matrix in Parallel Polirized Light. The Long Side of the Photographs are 4.6 mm in Length

is well-known that the Yamanlar Group of Kaya (1981) which is the lateral equivalent of the Yuntdağ volcanics of this study, clearly overlie the İzmir-Ankara Zone (Dora, 1964; Ünker, 1984). Upward, the Helvacı andesite subunit changes into the andesitic-trachyandesitic rocks of the Çaltılı andesites and around Helvacı and Hatundere villages they alternate each other in different stratigraphic levels (Plate 5). The boundary relations of these two unit will be discussed in detail in the following sections.

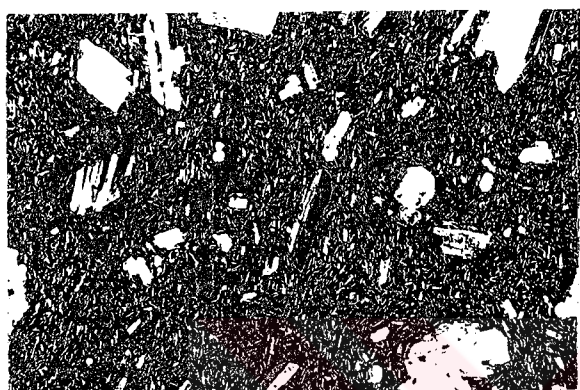


Figure 2. 4 Photomicrograph Showing the Typical Microlitic Matrix and Trachytic Texture, Observed in Helvacı Andesites. The Long Side of the Photograph is 4 mm in Length

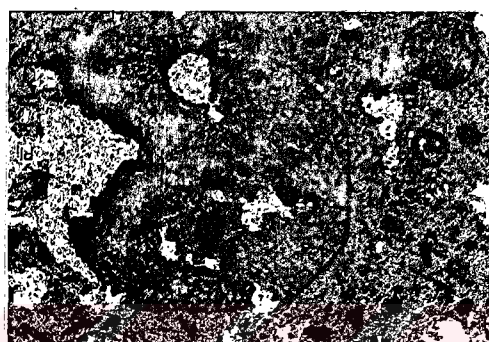


Figure 2. 5 Photomicrograph Showing Euhedral Cylindrical Pyroxene Phenocrysts in Helvacı Andesites. The Long Side of the Photograph is 7 mm in Length

2. 1. 2. Haykırın blocky pyroclastics

Description : In the study area, the massive lava flows of the Helvacı andesites and the Çaltılı trachyandesite units are intercalated, in different stratigraphic levels, with the coarse grained, lithic clast-rich volcanoclastic rocks, deposited in different volcanoclastic facies. Especially around Dumanlıdağ and Haykırın area (Plate 5) and to the north, around Güzelhisar, Uzunhasanlar and Çoraklar villages (Plate 4), the coarse grained pyroclastics of the Haykırın unit have open outcrops. In most of the previous studies these volcanoclastic rocks were described by a lithological terms as “agglomerates”. Kaya (1981) and Kaya & Savaşçın (1981), on the other hand, considered the equivalents of these widespread blocky pyroclastic rocks as the volcanoclastic subunits of the Yanık, Çukurköy and Belen Formations. The unit form typically the topographic levées, include steep flow fronts and have the large surface blocks.

Lithology: The Haykırın blocky pyroclastics are composed mainly of coarse grained monolithic blocky mass flow unit consisting of poorly-sorted and angular to subrounded

boulder and cobble-sized andesitic to trachyandesitic clasts in white ash or lava matrix. Type of the clasts generally represents the composition of the preceding lava eruption. Depending on the composition of the former eruption, the clasts are derived from the pinky and gray massive lavas of the Helvacı andesites or black massive lavas of the Çaltılı andesites. Clast size ranges from 5 to 60 cm in diameter. In the Haykıran unit three different volcanoclastic facies are distinguished. These are: 1. Flow breccias, 2. Block and ash flow deposits and 3. Grain supported, andesite scoria facies. These different facies and their detailed characteristics will be described in chapter 4.

Boundary relations: The Haykıran blocky pyroclastic unit forms laterally discontinuous flow units in the massive lava facies of the Helvacı andesite and the Çaltılı trachyandesite units. Around Çukurköy and Dumanlıdağ area (Plate 5) the Haykıran blocky unit have open outcrops where the pyroclastic flow units are found in the massive andesite lava suite as laterally discontinuous intervals (Figure 2.6) and lenses which laterally pinges out in the massive lava flows (Figure 2.7). Passing from the coarse grained blocky unit into the massive lavas are in places sharp or in some outcrops gradational zones characterized by 20 cm to 1 m-thick ash horizons, are observed.



Figure 2. 6 Haykıran Blocky Pyroclastic Subunit Underlying the Helvacı Andesites.
İzmir K 18 d 1; 04 175 / 83 425

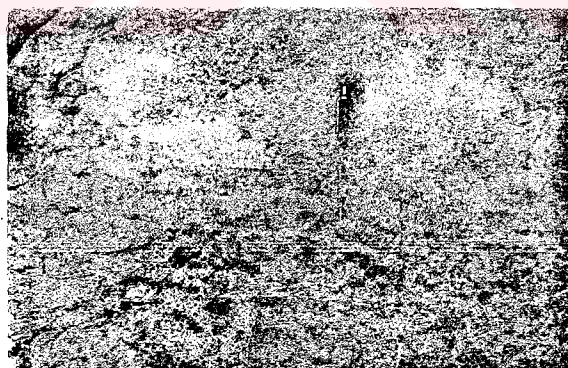


Figure 2. 7 Haykıran Blocky Pyroclastics Interdigitating the Massive Lavas of the Helvacı Andesites.
İzmir K 18 d 1; 06 175 / 86 400

2. 1. 3. Çaltılı andesites

Description: The unit is composed of typically dark-coloured, aphanitic trachyandesites and andesites and typically looks like basalts in field due to its dark colour. It forms an extensive outcrops around Yanık, Doğa and Haykıran villages, to the north of Aliğa,

around Çaltılıdere village and in the Foça peninsula (Plates 1 and 4). The unit significantly have well-developed columnar joints around Çaltılıdere village to the north of Aliğa (Plate 4). In most of the previous studies this unit is described as the calcalkaline earlier phase of the volcanism which grades into shosonitic rocks upward (Savaşçın, 1978; Yılmaz, 1989; Yılmaz, 1990; Fytikas et al., 1979). The Çaltılı trachyandesite unit corresponds this high-K shosonitic phase of the calcalkaline association

Lithology: The Çaltılı andesites are composed mainly of dark gray-black, aphanitic lava flows with 1 to 10 cm-thick well-developed flow banding and 15 cm to 2 m-thick individual flow units. To the north of Aliğa, around Çaltılıdere village (Figure 1.1, Plate 4), the lava flows are characterized by columnar joints. The rocks are composed of plagioclases as felsic mineral and pyroxene, amphibole and biotite as mafic mineral. Olivine, calcite, sanidine and some opaque minerals are found in minor amounts (Figure 2.8). The total phenocryst ratio reaches up to 40 %. The matrix is most commonly microlitic or glassy. In the samples with microlitic matrix, trachytic flow texture is common. In the glassy matrix, on the other hand, vitrophric texture is characteristic. The plagioclase phenocrysts are dominantly euhedral in form with polysynthetic twinning and show extinction angle of $28-36^{\circ}$ indicating An_{50-64} of labradorite composition. Sanidine is another plagioclase-group mineral which is rarely found in thin sections. The mafic mineral association, found in the Çaltılı unit, is dominated by euhedral to subhedral



Figure 2. 8 Photomicrograph
Showing the Serpentinized Olivine
Phenocrysts in Çaltılı Andesites.
The Long Side of the Photograph is
4.3 mm in Length.

clinopyroxene phenocrysts and rare olivines (Figure 2.10). Hornblend-type amphiboles and biotites are found in relatively minor amount. Olivine is present in some samples but relatively low in amount. The average mineral composition of the Çaltılı andesites is as follow: Matrix 60 %, plagioclase 21 %, pyroxene 10 %, hornblend 2 %, biotite 2 %, sanidine 1 %, calcite 0.5 %, olivine 2 %, opaque mineral 1.5 %. Alteration in this unit is not as intensive as the Helvacı andesites. Fe-oxidization, rare chloritization in mafic

minerals and conversion into clay minerals of the plagioclases are the main alteration types. As well as the outcrop appearance the mineralogical content and the textural features of the unit are very similar to basalts. However, the geochemical analyses which will be given in the next sections, show that they are trachyandesite and andesite in composition.

Boundary relations: The Çaltılı andesite unit alternates with the Helvacı andesites in the upper parts of the andesitic suite around Helvacı, Yanık and Belen villages. Around Çaltılıdere village it forms the uppermost part of the massive lava suite. About in all outcrops. Along the boundary between the Helvacı andesites and the Çaltılı andesites, laterally discontinuous, coarse grained volcanoclastic intervals of the Haykırın blocky pyroclastic flow deposits are observed which have more or less truncated lower boundaries and in the upper parts pass through the lavas along fine ash zones. Around Güzelhisar, Uzunhasanlar and Çoraklar villages (Plate 4) where the coarse grained block and ash flow deposits of Haykırın unit extensively crop out, the massive lava flows of the Çaltılı unit overlay and intercalate with the Haykırın blocky pyroclastics (Figures 2.9,10). In places where dark-coloured Çaltılı andesites overlie directly the pinky-red andesites of the Helvacı unit the boundary is generally sharp. In some locations, on the other hand, a gradational contact which is distinguished by the colour changes from the pinky-red to gray and black, is observed.



Figure 2. 9 Çaltılı andesites Overlying the Haykırın Blocky Pyroclastics Subunit.

İzmir K 18 a 1; 09 975 / 05 350



Figure 2. 10 Massive Lava Flows of the Çaltılı Trachyandesite Subunit Intercalating with the Haykırın Blocky Pyroclastics.

İzmir K 18 a 4; 06 425 / 93 300

2. 1. 4. Dumanlítepe dykes

Description: The massive andesitic lava flows of the Helvacı andesite unit are cut by the pink to gray andesitic dykes and subvolcanic stocks of 2 to 20 m-wide and 50 m to 1.5 km-length, which generally form significant morphology between Hatundere and Çukurköy villages (Figure 2.11, Plate 5). These subvolcanic equivalents of the Helvacı andesite unit are first named in this study as the Dumanlítepe dykes. The dykes are high-angle to vertical with planar lateral extend. Only in one area they form a stock in the east of Hatundere village (Plate 5).

Lithology: The Dumanlítepe dykes are pink to gray in colour and glassy to porphyritic in texture. At the periphery of the dykes and stock, the glassy to fine grained texture is typical, and toward the centre relatively coarse porphyritic texture is clearly observed (Figure 2.12). Euhedral plagioclase are the dominant component in the porphyritic parts, and less amount of amphibole and biotite crystals are also found. In handspecimens, matrix is glassy or rarely very fine grained. In the periphery of the dykes and stock, gray, massive andesitic inclusions of 2 to 15 cm in diameter, are sobserved (Figure 2.12). The inclusions are partly resorbed and surrounded by light gray auroles (Figure 2.12).

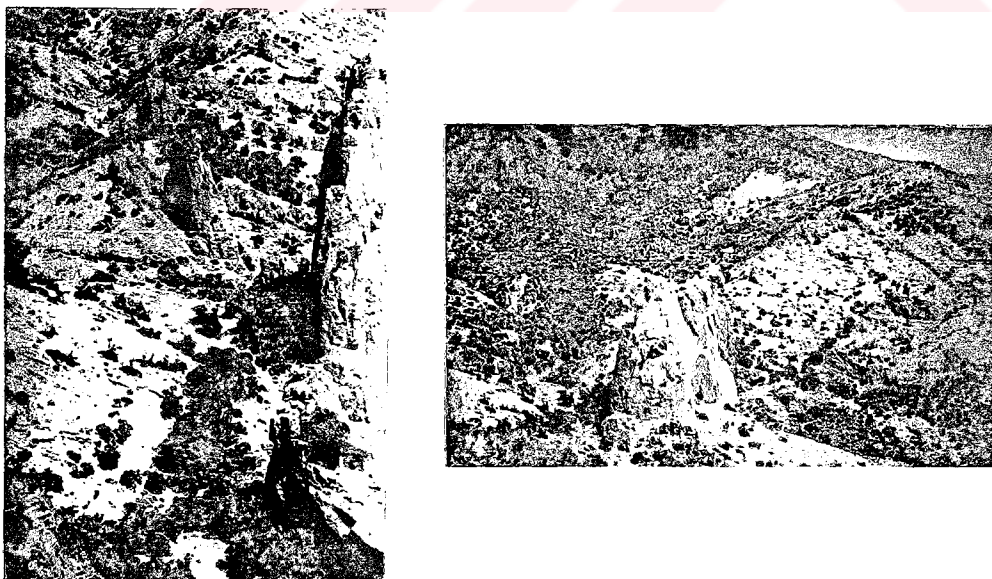


Figure 2. 11 Andesitic Dykes Cutting the Massive Lava Flows of the Helvacı Andesite Unit.

İzmir K 18 d 1; 07 050 / 85 150

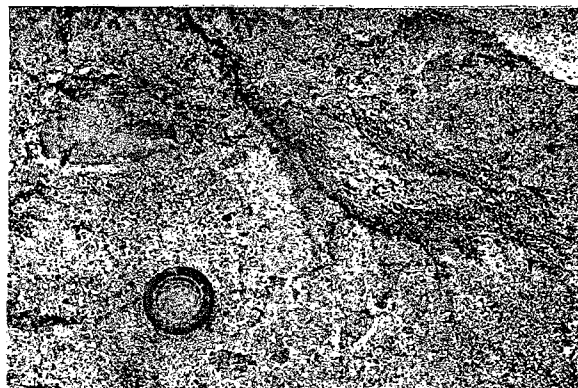


Figure 2. 12 Massive Andesitic Lava Inclusions of the Helvacı Andesite Unit Observed in Dykes and the Subvolcanic Stocks. The Inclusions are partly resorbed.
İzmir K 18 d 1; 07 050 / 85 150

Petrographically, the Dumanlıtepe dykes are andesite in composition and porphyritic in texture. The matrix is typically microlitic or in places glassy. Polysynthetically twinned and significantly zoned euhedral plagioclase crystals characterize the main felsic component. The extinction angle of the plagioclase twins range from 22° to 24° which indicates that, they are andesine (An_{40-44}) in composition. The dominant mafic minerals are amphiboles and biotites. Rare orthopyroxenes may also be observed in some thin sections. The average proportions of components are: matrix, 50 %; plagioclase, 30 %; biotite, 9 %; amphibole, 8 %; pyroxene, 2 % and opaque minerals, 1 %. Argilic alteration in plagioclases and oxidization in mafic minerals are the common alteration types.

Boundary relations: Around Helvacı, Hatundere and Çukurköy villages (Plate 5) the Dumanlıtepe dykes cut the massive andesite lavas and the coarse grained pyroclastics of the Yuntdağ volcanics (Figures 2.11,13). Along these sharp, high-angle to vertical contacts the glassy to fine grained massive andesitic inclusions are observed. Toward the center of the dykes, the texture characteristically becomes coarser grained where relatively larger phenocrysts, a few millimeters in size, are found (Figure 2.12). In Dumanlıdağ area, the dykes have maximum 1.5 km lateral extend and roughly form a radial field appearance (Plate 5, Figure 4.9) which will be detaily mentioned in ch. 4.2.1



Figure 2. 13 High-Angle, Planar Cross-Cutting Contact Between the Dumanlıtepe Dykes and the Helvacı Andesite Unit.

İzmir K 18 d 1; 06 350 / 86 475

2. 1. 5. Age of the Yuntdağ volcanics

Many studies have been carried out on the age of the volcanism of Western Anatolia (Figure 2.14). Besides paleontological ages of the accompanying sedimentary sequences, the radiometric age determinations also indicate the different, equivocal and large span of ages because of the widespread magmatic activity during the Tertiary time all around the Western Anatolia. In addition to that, the samples which have radiometrically examined, were generally collected randomly, without accompanying detailed field work. For that reason, the tectonic and volcanological interpretations, based on these age determinations, are so controversial. In this study no radiometric or paleontological age determination were done. However, in most of the previous studies, the Oligocene-Miocene to Pliocene ages are commonly proposed for the magmatic activity occurred in the western Anatolia (Akartuna, 1958; Borsi et al., 1972; Fyticas et al., 1976; Savaşçın, 1978; Şengör and Yılmaz, 1981; Ercan et al, 1985; Şengör et al., 1993). In these works, two main magmatic cycles are proposed, the first occurred from the Late Oligocene to Middle Miocene and the second from the Late Miocene-Pliocene to Prehistoric times. The previous works have suggested that during the first cycle, calc-alkaline lavas of andesitic to rhyodacitic in composition were extruded and rhyolitic and some alkaline components are also found accompanying this calc alkaline lava suit. In the second stage, on the other hand, alkaline trachytic and latite andesitic volcanism was predominant. The age determinations, given in the previous studies are summarized in the figure 2.14 in which the mainly calcalkaline affinity of the earlier stage is clear. The Yuntdağ volcanics of this study petrographically and chemically corresponds the rocks of the first stage of the previous study. The nearest locations where the age determinations were done previously, are Dikili, Bergama and Foça. In these areas an age of 21.5 to 16.5 Ma for the equivalents of the Yuntdağ volcanics have been measured (Borsi et al., 1972; Savaşçın, 1977). So that the Early to Middle Miocene age is accepted for the Yuntdağ volcanics of the study area.

2. 2. THE FOÇA VOLCANIC COMPLEX

The Yuntdağ volcanics are overlain by a thick rhyolitic-dacitic to trachytic rock association which is named for the first time in this study as the Foça volcanic complex. The unit crops out extensively around the Foça Peninsula and Aliğa (Plates 1,2,3). The lateral equivalents of this unit was named by Kaya (1981) and Kaya and Savaşçın (1981)

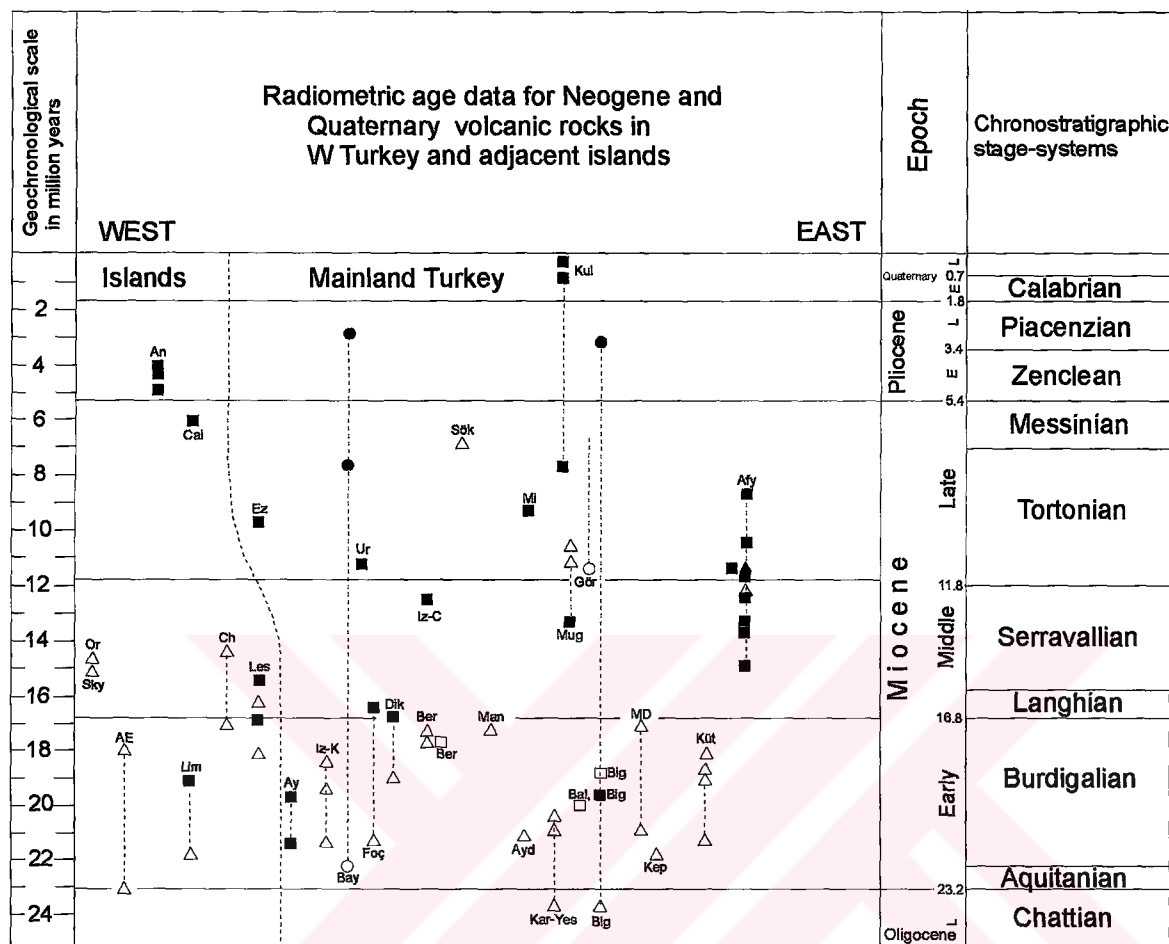


Figure 2.14 Age and Geochemical affinities of the volcanic areas in Western Anatolia and adjacent islands. (Δ) : calcalkaline affinity, radiometrically determined age; (\blacksquare) : alkaline affinity, radiometrically determined age; (\square) : nondetermined chemical affinity, radiometrically determined age; (\circ): calcalkaline affinity, paleontological or relative age; (\bullet): alkaline affinity, paleontological or relative age. Or: Orion; Sky: Skyros; AE: Ağios Efstratios; Lim: Limnos; An: Antiparos; Cal: Caloyeri; Foç: Foça; Ch: Chios; Les: Lesvos; Ez: Ezine; Ay: Ayvacık-Tuzla; İz-K: İzmir-Karaburun; Gör: Gördes; Ur: Urla; Dik: Dikili; Ber: Bergama; İz: İzmir-Cumaovası; Sök: Söke; Afy: Afyon; Man: Manisa-Saruhanlı; Ayd: Aydın-Çavdar; Mi: Milas; Mug: Muğla; Kar-Yes: Karalar-Yeşiller; Kul: Kula; Kep: Kepsut-Balıkesir; Big: Bigadiç; MD: Muratdağı; Küt: Kütahya-Sofça.

Ages are after Becker-Platen et al., 1971; Borsi et al., 1972; Benda et al., 1974; Besang et al., 1977; Ercan et al., 1985; Fytikas et al., 1979; Innocenti et al., 1982; Bellon et al., 1979; Krushensky, 1976; Bingöl, 1977).

Compiled after Yılmaz, 1989 and Seyitoğlu & Scot, 1990.

as the Foça Tuff Unit, and this name is generally the most well-known name for the unit. Savaşın and Güleç (1992) named the same volcanic and volcanoclastic sequence as the Volcanic and Volcano-Sedimentary Unit (VAVU). Yılmaz (1989) called the acidic suit of this complex as the granitic suite. In these previous studies, however, detailed mapping and definition of the different rocks in the unit are absent. So that, a new name is proposed in this study. In the Foça volcanic complex, depending on their lithological and chemical affinities, three different units are described which are 1. The Foça rhyolites, 2. The Foça volcanoclastics and 3. The Foça alkaline volcanics. In the Foça volcanoclastic unit, additionally, three different subunits are distinguished. These are: 1. Hyaloclastic breccias, 2. Pyroclastic flows, and 3. Perlites (Figure 2.15).

2. 2. 1. Foça rhyolites

Description: In the Foça Peninsula, around Eski and Yeni Foça towns and Bağarası village and to the north of Aliğa around Çaltıldere and Yenişakran villages (Plates 1,4), massive rhyolitic to dacitic rocks of the Foça massive rhyolite unit, crop out. The unit is generally found as the massive lava flows with well-developed flow foliations and subvolcanic stocks and dykes cutting the accompanying pyroclastic series. There are four different massive rhyolite bodies cropping out in the study area. Around the Bağarası village, the stubby coherent lava flows of the unit is observed which is named here as the Bağarası rhyolite (Figures 2.15,16; Plate 1). Rhyolitic to rhyodacitic domes and dykes of up to 1.5 km-long and 15 m-wide, of the same unit are found around Eski and Yeni Foça towns (Figures 2.15,17) and Çaltıldere and Yenişakran (Plate 4).

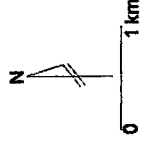
In the Foça rhyolites, four different rhyolitic bodies are distinguished in this study. The rhyolitic domes exposing around Çaltıldere and Yenişakran villages are named here as the Zeytindağ rhyolite and form the southwest edge of the rhyolitic bodies cropping out around Zeytindağ village (İzmir) (Plate 4) where the perlitic rocks have extensive outcrops and economical reserves. The Yeni Foça rhyolite is a dome-shaped body cropping out 1 km southwest to Yeni Foça town (Plate 1). The Eski Foça rhyolite, on the other hand, is a composite dome consisting of several local, relatively small-scale domes and dykes (Plate 1) cropping out around Eski Foça town and on the Eski Foça-Bağarası road (Figure 2.15).

Uria K 17 b4

Uria K 17 c1

Uria K 17 c1

Uria K 17 d2



AEGEAN SEA

T.C. YATIRIM VE EKONOMİK KALKINMA BAKANLIĞI

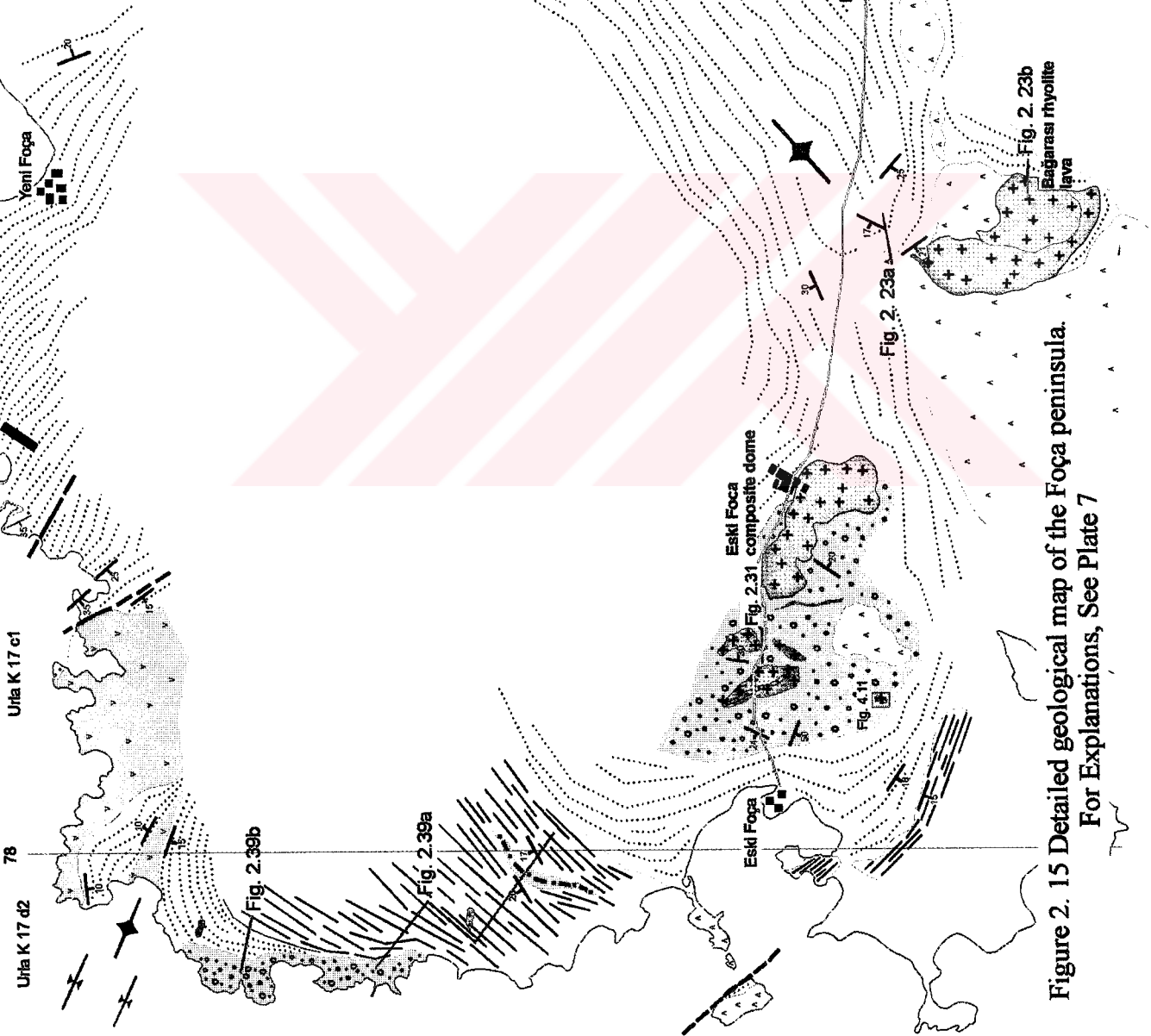


Figure 2. 15 Detailed geological map of the Foça peninsula.
For Explanations, See Plate 7

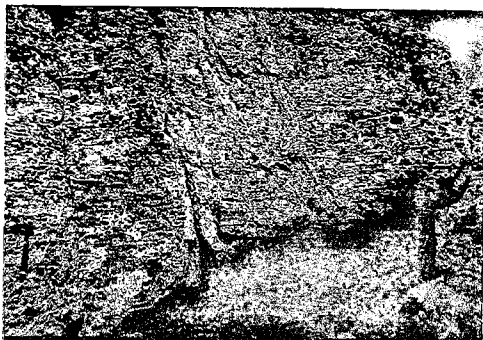


Figure 2. 16 Massive Rhyolite Lava Flows with Significant Flow Foliation in the Bağarası Rhyolite Lava Subunit.
 Urla K 17 c 1; 84 875 / 77 775



Figure 2. 17 Rhyolitic Stocks Emplaced in the Foça Volcaniclastics.
 Urla K 17 d 2; 76 975 / 86 800

Lithology: The Foça massive rhyolite unit is made up of the rhyolitic lava flows, domes and dykes. Around Bağarası villages rhyolites consist of lava flows with well-developed flow foliations (Figure 2.18). Silica and calcedony nodules, 0.3 to 2 cm in diameter and elongated along the flow foliation planes are observed in this location (Figure 2.19). Glassy to porphyritic texture with euhedral quartz and feldspar phenocrysts in a glassy matrix are clearly observed even in hand specimens. The Eski Foça and Yeni Foça domes, on the other hand, massive rhyolitic bodies are semicircular in form and they have a diameter of about 100 m to 1 km cutting the accompanying rhyolitic pyroclastic units of the Foça volcanic complex. In these areas glassy texture in the periphery of the domes and porphyritic texture in the central parts are significant.



Figure 2. 18 Well-Developed Flow Foliations in the Bağarası Rhyolite Lava.
 Urla K 17 c 1; 85 575 / 77 350

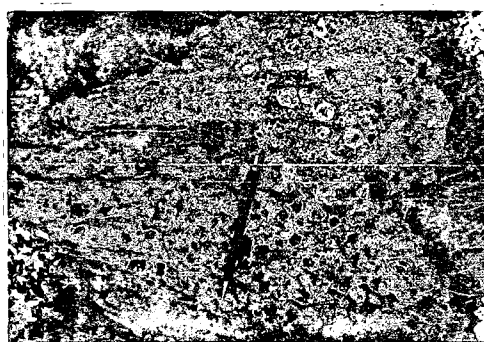


Figure 2. 19 Calcedony Nodules in Bağarası Rhyolite Lava Elongated Along the Flow Laminae.
 Urla K 17 c 1; 85 450 / 77 425

Petrographically, the porphyritic rhyolites are composed of about 20 % phenocrysts of euhedral and, in places, embayed quartz and K-feldspar (Figure 2.20). The maximum length of the phenocrysts is about 2 mm. The matrix is generally glassy with well-developed flow banding to fine grained granoblastic aggregates that are grown onto the phenocrysts in some places (Figure 2.21). Devitrification in the glassy matrix is the most common micro-textural features of the massive rhyolitic rocks of the Foça volcanic complex (Figure 2.22).

Boundary relations: The Foça rhyolites are found in the Foça volcanic complex as coherent lava flows and subvolcanic stocks (Figure 2.15, Plate 1). Around Bağarası village the rhyolites are observed as laterally-discontinues, stubby lava flows in the pyroclastic facies. The lavas overly in places the pyroclastic facies of the Foça volcanic complex and in other areas mafic lavas of the Foça alkaline volcanics. Thin and laterally discontinues perlitic zones are found at contact between the rhyolitic pyroclastics and the stubby rhyolitic lavas near Bağarası (Figure 2.23). At this location the rhyolitic lavas are directly overlain by the massive lava flows of the Foça alkaline suite. The Eski Foça, Yeni Foça and Zeytindağ rhyolites, on the other hand clearly cut the accompanying pyroclastic units along high-angle contacts (Figure 2.24) and show typical dome structures. The Yeni Foça dome is surrounded by the sea in its SW to NE side, and the full shape of the dome can not be observed.

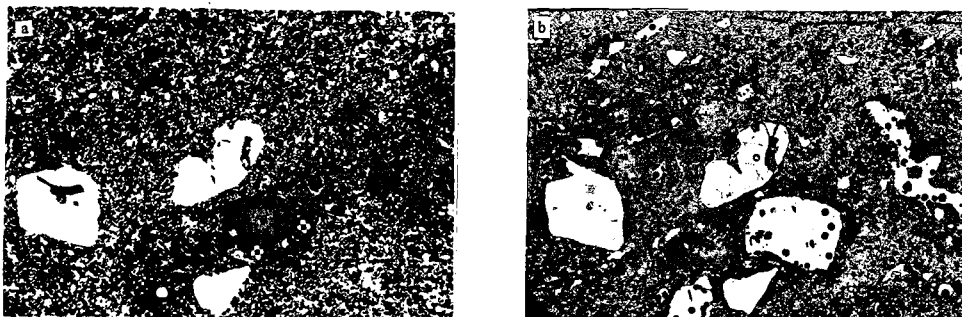


Figure 2. 20 Photomicrograph showing the embayed quartz phenocrysts in Foça rhyolites. a. Cross polirezed light, b. Parallel polirezed light. The long side of the photograph is 11 mm in length



Figure 2. 21 Recrystallized Glassy Matrix in the Foça Massive Rhyolites Growing onto the Euhedral Quartz Phenocrysts. The Long Side of the Photograph is 3.8 mm in Length.

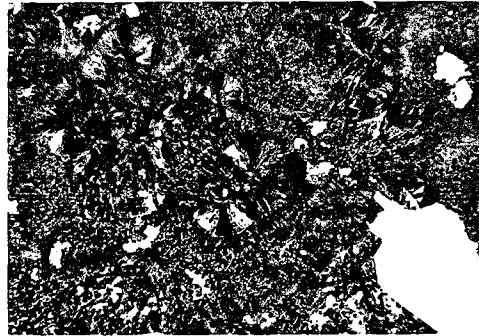


Figure 2. 22 Devitrification in the Glassy Matrix in the Foça Rhyolites. The Long Side of the Photograph is 4.1 mm in Length.

The Zeytindağ and the Eski Foça domes, however, have open outcrops on all sides to study the contact relations with the surrounding rock series. 2 km to the south of the Eski Foça town, a rhyolite dome of a radius of 100 m crops out (Figure 2.15). The central part of the dome is massive, and toward the boundary well developed flow foliations surround the periphery of the massive core and dip outward with 55 to 85 degrees (Figures 2.15,25). In some places the foliations are vertically inclined, and along the southwestern boundary of the dome they are overturned dipping with 50 degrees towards the center of the dome (Figure 2.15). At this place, bedding of the pyroclastic sequence is inclined vertically and overturned inwardly toward the centre of the dome suggesting continuous updoming of the core and overturning of one side of the dome during emplacement. At this location, the massive rhyolites are surrounded by the massive perlites and the resedimented hyaloclastic breccias along sharp contacts (Figures 2.15,26).

BAĞARASI SECTIONS

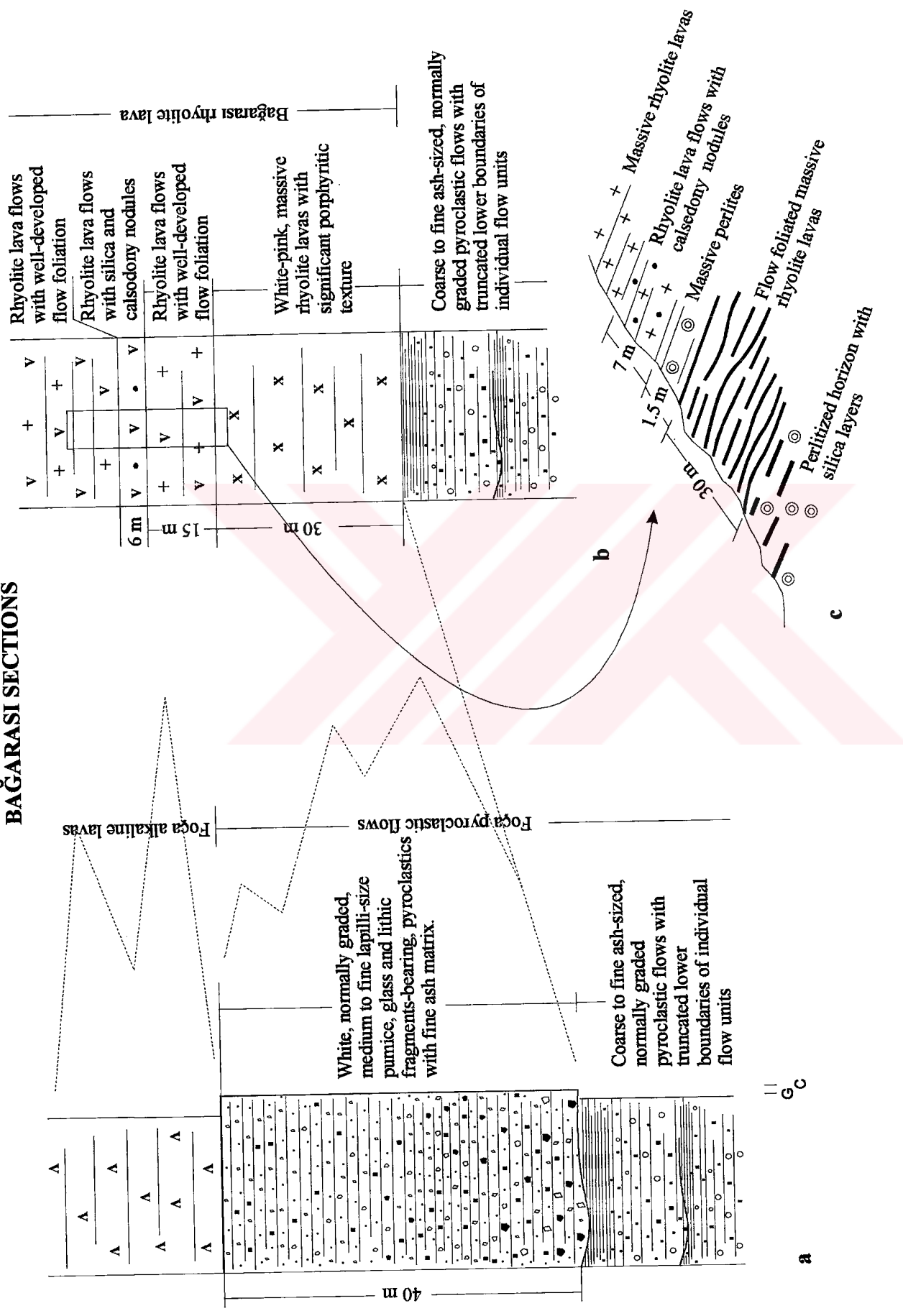


Figure 2. 23 Stratigraphic Section Measured Around Bağarası Village Showing the Stratigraphic Relation Between the Bağarası Rhyolite Lava and Foça Alkaline Lava Subunits. Section Line is Shown in Plate 1.



Figure 2. 24 The Cross-Cutting Contact Relation Between the Foça Rhyolites and the Foça Volcaniclastics.
 Urla K 17 c1; 79 750 / 79 100



Figure 2. 25 High-Angle Flow Foliations at the Periphery of the Rhyolitic Stocks in the Eski Foça Composite Dome.
 Urla K 17 c1; 79 750 / 79 050.

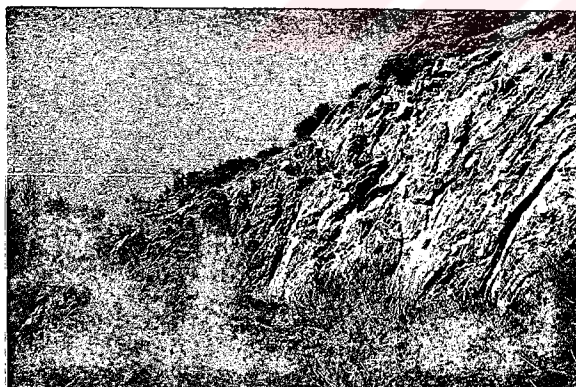


Figure 2. 26 Massive Perlites Covering the Massive Rhyolite Dome Around Eski Foça Town.
 Urla K 17 c1; 79 750 / 79 100

2. 2. 2. Foça volcaniclastics

In the Foça Peninsula and around Aliğa, widespread, white to pink, volcaniclastic sequence interlayered with the lacustrine sedimentary rocks, crops out. This volcaniclastic sequence is the equivalent of the Foça Tuff Unit of Kaya (1981) and Kaya and Savaşçın (1981). In their description, however, no subunits were differentiated and the detailed properties of various subunits were not described. In this study, three lithologically and

texturally different subunits are distinguished in the Foça volcanics. These are: **1. Pyroclastic flows, 2. Hyaloclastic breccias and 3. Perlites**

2. 2. 2. 1. Pyroclastic flows

Description: The Pyroclastic flows subunit of the Foça volcanic complex is equivalent to the widely-known Foça tuffs of Kaya & Savaşçın (1981) and Savaşçın & Erler (1994) cropping out in all around the Foça Peninsula and around Aliğa (Plates 1,3). This subunit is composed mainly of white, pink and yellow coloured and fine grained massive to well-bedded pyroclastic flow units which volumetrically and areally dominate the Foça volcanic complex.

Lithology: The Pyroclastic flows are made up of pyroclastic rocks, deposited in various volcanoclastic facies. The dominant clast association consists of medium to coarse ash and fine to medium lapilli-sized pumice, glass shards, crystal and lithic fragments and they are set in a fine ash matrix. A medium to well sorted, grain supported texture is typical for this unit. Wide-spread, 2 to 50 cm-thick, well-developed planar and, in places, cross stratification are characteristics. Normal and reverse grading, truncated lower boundaries of the individual flow units, crudely-developed Bauma sequences, flattening in pumice fragments, locally-developed welding and silica-filled gass bubbles are the volcanic and sedimentary structures, observed in the unit depending on the volcanoclastic facies in which the pyroclastic flows occurred. The matrix is commonly fine ash in which flow lamination and microgranular texture formed by recrystallization are found. In places, silica and carbonate cement are also found in the pyroclastic flow unit bounding the pyroclastic clasts (Figure 2.27). In the pyroclastic flows four distinct volcanoclastic facies are described as **1. Rhyolite pumice and lithic fragment bearing volcanoclastic facies, 2. Subaqueous welded ignimbrite facies, 3. Subaqueous pyroclastic fall deposits and 4. Channel-fill facies.** The detailed microscopic and field characteristics of these different facies will be described in chapter 4

Boundary relations: The Pyroclastic flows overly the different subunits of the Yuntdağ volcanics generally along a sharp lower boundary. 1 km south to the Güzelhisar village, 1.5 km northeast to the Samurlu village and 1 km south to the Çaltılıdere village (Plate 4), it overlies massive lava flows of both the Çaltılı andesites and Helvacı andesites (Figure

2.28). . On the Eski-Yeni Foça road, where the uppermost parts of the Çaltılı andesites, underlying the Foça volcanics, are observed at the central parts of the antiform structures (Figure 2.15), the lower boundary of the unit is clearly observed and the mafic lava flows pass into the pyroclastic sequence along a gradational contact (Figure 2.29).

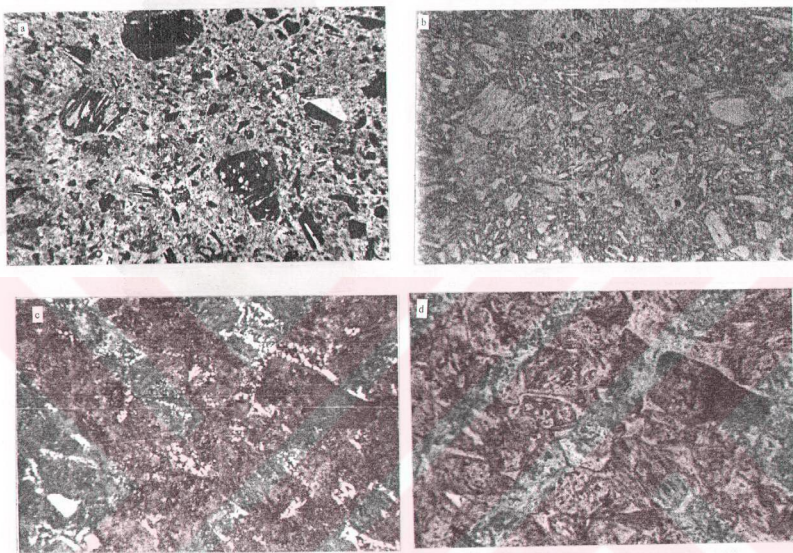


Figure 27. Photomicrograph Showing the Carbonate Cement Bounding the pyroclastic Material in Foça Volcanic Unit. **a** and **b** The Pores in the Pumice Fragments are Filled and All Components are Bounded Completely by the Carbonate Cement (Cross Polarized Light and Parallel Polarized Light), **c** and **d**. Silica Cement is Typically Observed in the Pores Between the Volcanic Clasts (Cross Polarized Light and Parallel Polarized Light). The Long Axis of the Photographs are 1.9 mm in Length

Along this contact, in the pyroclastic sequence, three different and laterally discontinuous mafic lava intervals are observed in different stratigraphic levels. Around Güzelhisar and Samurlu villages thin coherent lava interlayers of the Helvacı and Çaltılı andesite subunits are observed in the pyroclastic flows (Figures 2.28, 29, 30). Around Bozköy and Samurlu villages (Plates 2,4), this unit is overlain and pass gradually to lacustrine limestones which are widely exposed in the Western Anatolia. The pyroclastic flows graditionally passes into the lacustrine limestones along thin mudstone and muddy limestone intervals of the Neogene sedimentary units (Figure 2.28a).

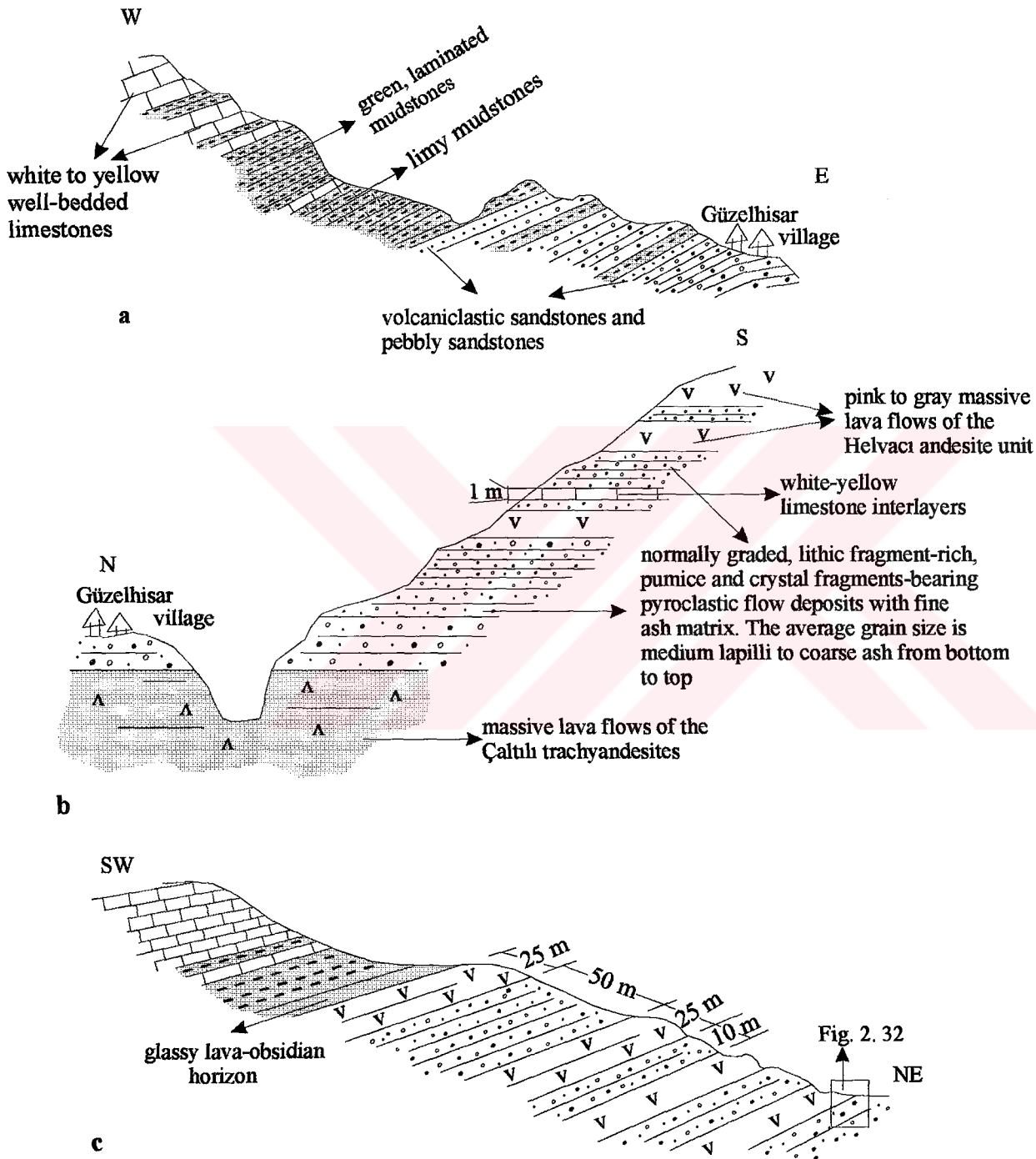


Figure 2. 28 Stratigraphic Section Measured Around Güzelhisar Village. Section line is shown in Plate 4.



Figure 2. 29 Field Photographs Showing the Graditional Contact Between the Çaltılı Andesites and the Foça Volcaniclastics. 10-20 cm-Thick Mafic Lava Lenses in the Foça Pyroclastics in This Area is Significant.
Urla K 17 c 1; 81 750 / 88 800.

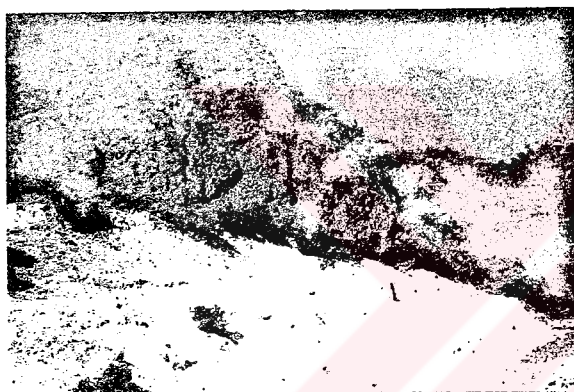


Figure 2. 30 Photograph Showing the Massive Andesite Lavas of the Helvacı Andesite Unit Overlying the Pyroclastic Flows of the Foça Volcaniclastics.
İzmir K 18 a4; 01 600 / 91 400

In the Pyroclastic flows, different volcaniclastic facies are observed gradationally passing into each other laterally and vertically (Figure 2.31). Formation of these different facies is dominantly controlled by the emplacement and updoming of the massive rhyolite domes. In this unit, the pyroclastic flow deposits form the dominant rock type in the unit and Perlites and Hyaloclastic breccias are found as laterally discontinued lenses in varying thickness. Thin lacustrine mudstone intervals, found in various parts of the pyroclastic sequence, indicate the contemporaneous occurrence of volcanism and lacustrine deposition (Figure 2.32).

2. 2. 2. 2. Hyaloclastic breccias

Description: In the Foça volcanic complex, crudely surrounding the massive rhyolitic domes and in different stratigraphic levels within the whole pyroclastic sequence, white to green, coarse grained breccia unit with fine ash matrix, is observed. The most extensive exposures of the unit crop out around Eski Foça town, and on the Eski Foça-Bağarası road (Plate 1).

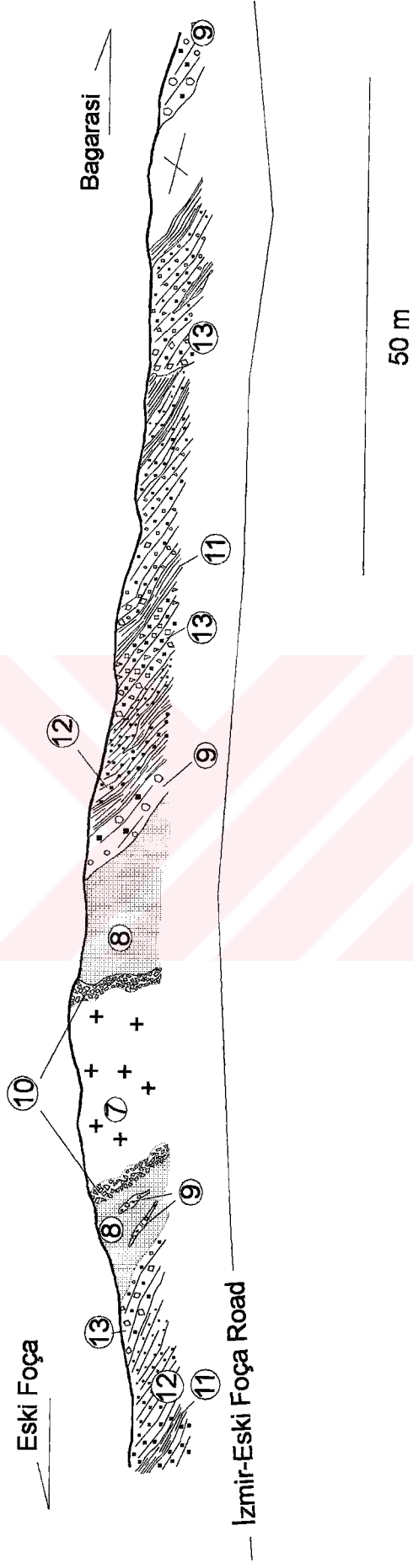


Figure 2. 31 Cross Section From Eski Foça-Bağarası Road Showing the Stratigraphic Relation Between the Foça Massive Rhyolites, Foça Pyroclastic Sequence and Perlitites.

Facies Numbers are Used as They are in Text. Section Line is Shown in Plate 1.

Lithology: The Hyaloclastic breccias are composed of white, gray, green, massive to crudely-bedded coarse-grained volcanoclastic rocks with a glassy or fine ash matrix. Two main volcanoclastic facies are distinguished in the Hyaloclastic breccia subunit: 1. the in-situ hyaloclastic breccia facies and 2. the resedimented hyaloclastic breccia facies (see chapter 4 for details). The thickness of the hyaloclastic breccias varies laterally and thins out in short distances. Around the Eski Foça dome, the in-situ hyaloclastic breccias surround the periphery and outward pass into the resedimented hyaloclastics, perlites and pyroclastic flows (Figure 2.31). Close to the contacts of the massive rhyolite domes and lava flows, the in-situ hyaloclastic breccias are dominated only by massive to foliated rhyolitic lava breccias, set in a massive rhyolitic matrix (Figure 2.33). The maximum thickness of these parts are up to 4 m surrounding the rhyolitic domes. Outward the massive domes and within the volcanoclastic sequence, the second type of the hyaloclastic breccia becomes dominant which is characterized by the angular to subrounded, relatively well-sorted medium to coarse lapilli-sized rhyolite, rhyodacite, pumice, perlite and rare mafic lava breccias in descending order (Figure 2.34a,b). Grains are set in glassy or fine ash matrix. The thickness of this type of the hyaloclastic breccias ranges from 10 to 50 m.

Boundary relations: The Hyaloclastic breccia subunit is dominantly observed surrounding the massive rhyolite domes and within the different stratigraphic levels of the Foça volcanic complex (Figure 2.15) and outward, they pass into the different facies of the pyroclastic flows subunit (Figure 2.31). The in-situ hyaloclastic breccias typically surrounds the massive rhyolites and are found at the periphery of the massive rhyolite domes along a diffuse contact. Outward they are overlain by resedimented hyaloclastics or massive perlitic rocks along a gradational contact as well. Where the resedimented hyaloclastics directly cover the massive rhyolites, they are rich in massive rhyolite lava clasts and toward the contact between the perlitic rocks, become rich in perlitic clasts (Figure 2.35). The gradual intergradation from the rhyolite dome to the in-situ breccias and finally to resedimented breccias are important clues for their cogenetic evolution that will be described in the model of the domes in Chapter 4. Resedimented hyaloclastic breccias are also observed within the pyroclastic flows of the Foça volcanic complex as laterally discontinuous lenses which have generally gradational and, in places, sharp, truncated lower contact (Figure 2.36). Where the resedimented hyaloclastic breccias overlie the fine grained mud intervals, thin mud dykes, intruded into the hyaloclastites are found (Figure 2.37).



**Figure 2. 32 Thin, Green-Colored
Mudstone Intervals within the
Pyroclastic Flows Subunit.
Urla K 17 c 1; 80 275 / 80 325**

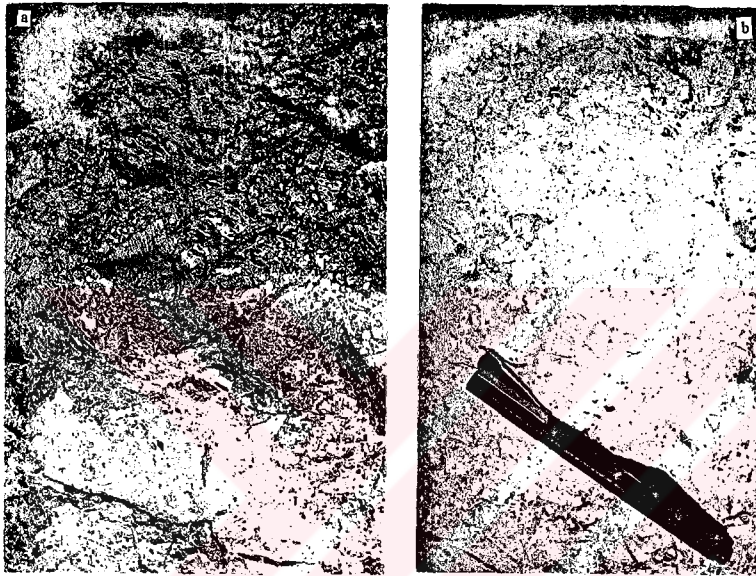


**Figure 2. 33 In Situ Hyaloclastic Breccias Surrounding the Massive Rhyolite
Domes. Note the Typical Angular Form of Grains, Jig-Saw Fit Texture and
Coherent Nature of the Matrix.
Urla K 17 c 1; 80 250 / 80 325**

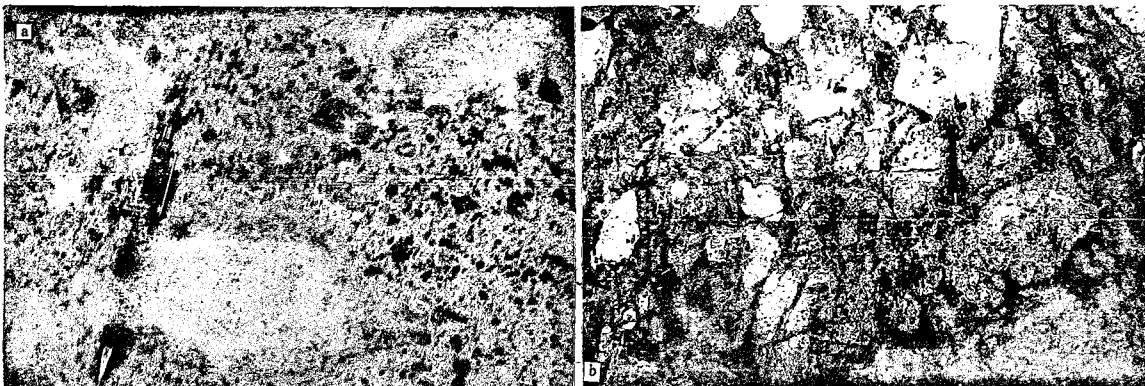


**Figure 2. 34 Reassembled Hyaloclastic Breccias. a. Massive Rhyolite and Perlite Breccias
Set in Altered Glassy Matrix, b. Rhyolitic Breccias in Perlitized Glassy Matrix.
Urla K 17 d 2; 76 775 / 85 200**

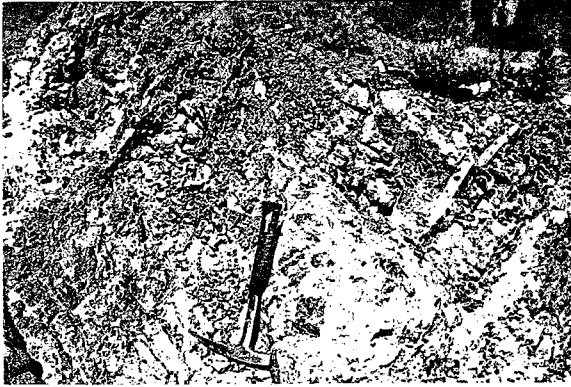


Figure 2. 35 Field Photograph Showing the Contact Zone Between the Reassembled Hyaloclastic Breccias and the Massive Perlites Around Eski Foça Town. From the Internal Parts of the Resedimented Hyaloclastic Breccias, to the Massive Perlites the Perlitic Breccias Become Dominant in the Hyaloclastites.

Urla K 17 c 1; 79 675 / 79 050.

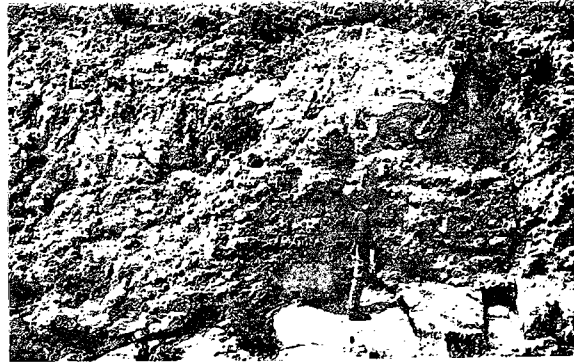


Figure 2. 36 Reassembled Hyaloclastic Breccias with Irregular Lower Contact of the Individual Flow Unit.

Urla K 17 c 1; 86 350 / 80 325

Figure 2. 37 Small Mud Dykes Intruded in to the Overlying Hyaloclastic Breccia Flow Unit.

Urla K 17 c 1; 86 350 / 80 325



2. 2. 2. 3. Perlites

Description and lithology: Gray to dark green massive perlitic rocks generally surrounding the massive rhyolite domes in circular to semicircular form. The laterally discontinuous, brecciated perlite horizons are called in this study as the Perlites subunit. The perlites are extensive around Bağarası, Çaltıldere and Yeni Şakran villages and Eski Foça town (Plates 1,4).

Around the Eski Foça and the Zeytindağ domes and the Bağarası rhyolite, the central massive rhyolites pass into the massive perlites. These are gray-white to dark green in colour and glassy and conchoidally fractured textures are clearly observed in hand specimens. The perlitic texture with the conchoidally fractured glassy matrix is easily recognized in thin sections (Figure 2.38). Rare biotite and feldspar phenocrysts of 3-5 % are observed in this matrix.

Between Eski and Yeni Foça towns, 4 km north to Eski Foça, light to dark gray brecciated perlitic rocks intercalate with the pyroclastic flows (Figures 2.39,40). The poorly sorted, laterally discontinuous perlitic lenses are formed mainly by rhyolite lava, perlite and rare pumice breccias in a partly to completely perlitized matrix. The total thickness of the subunit is up to 15 m. Rare dykes, up to 75 cm-thick, of the underlying pyroclastic unit cut this perlitic zone in which rhyolitic lava breccias and perlitic fragments are the dominant components (Figure 2.41). Grain supported texture is significant for these dykes (Figure 2.42).

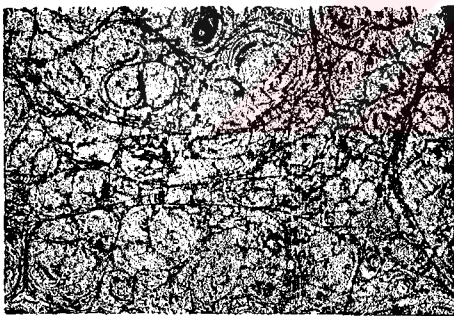


Figure 2. 38 Photomicrograph Showing the Perlitic Texture in Massive Perlites Subunit of the Foça Volcaniclastics. The Long Side of the Photograph is 6.1 mm in Length.

Boundary relations: The boundary between the massive rhyolite and massive perlite facies are typically gradational, but in some areas relatively sharp boundaries are observed (Figure 2.26). The massive perlites laterally thins out in the hyaloclastic breccias surrounding the Eski Foça dome (Figures 2.15,43) and, in places it overlies them along a gradational contact (Figure 2.44). Along the eski Foça-Bağarası road massive perlite intervals are found successively in the Pyroclastic flows (Figures 2.30,45). From the internal parts of the hyaloclastic breccias toward the massive perlites the perlitic grains become dominant component in the hyaloclastic breccias (Figure 2.35).

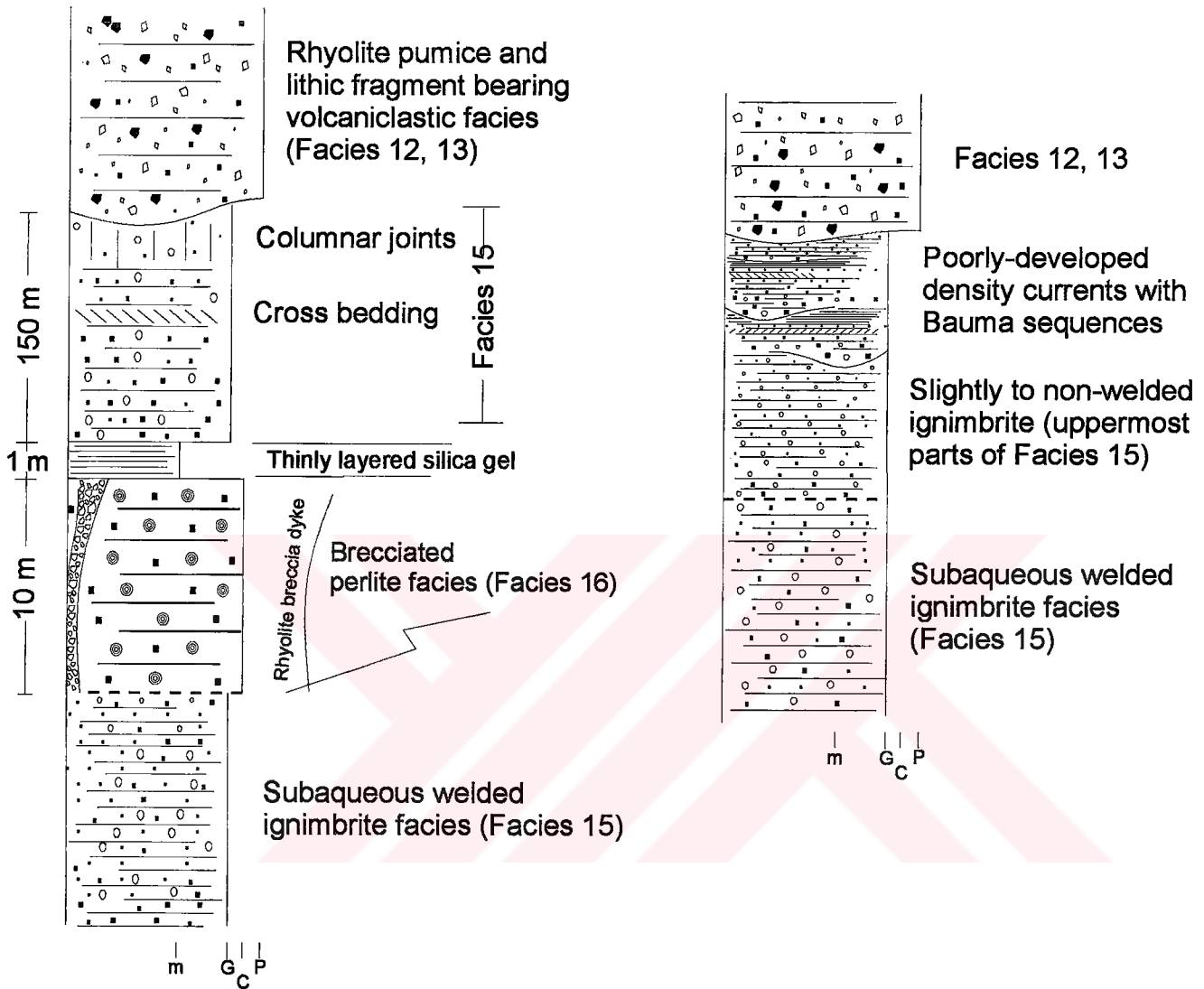


Figure 2. 39 Measured Stratigraphic Sections for the Pyroclastic Sequence in Eski Foca-Yeni Foca Area. Numbers Used for Each Facies Correspond with the Numbered Facies Descriptions in the Text. See Figure 2. 15 and Plate 1 for Locations.

The Horizontal Scale at the Bottom of Each Column is Grainsize.

m, Mud, G, Granule Size, P, Pebble, C, Cobble. .



Figure 2. 40 In the Foça Pyroclastic Flows, the Laterally Discontinues Brecciated Perlite Lenses Containing Massive Rhyolite and Massive Perlite Breccias in a Glassy, Perlitic Matrix are also Found.

Urla K 17 d 2; 77 550 / 82 725

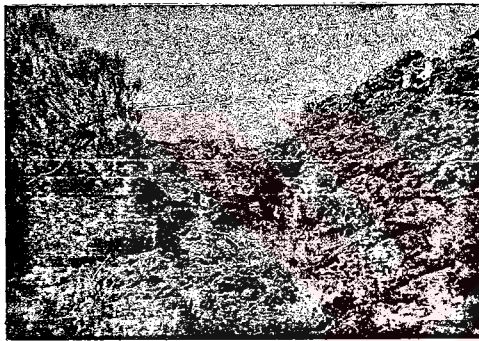


Figure 2. 41 Brecciated Rhyolitic Dykes Cutting the Overlying Brecciated Perlite Lens.

Urla k 17 d 2; 77 550 / 82 725

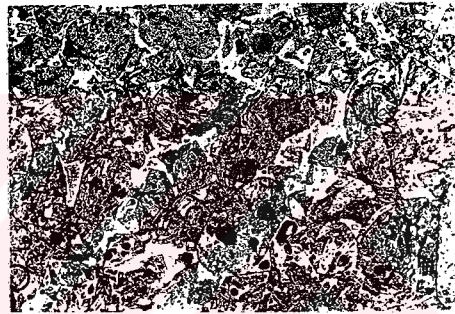


Figure 2. 42 Photomicrograph Showing the Grain Supported Brecciated Texture of the Rhyolite Dyke in the Brecciated Perlite Lens. The Long Side of the Photograph is 4.1 mm in Length.



Figure 2. 43 Around Eski Foça Town, Surrounding the Massive Rhyolite Dome Massive Perlites Laterally Pinch Out in the Resedimented Hyaloclastic Breccias.

Urla K 17 c 1; 79 750 / 79 000



Figure 2. 44 Massive Perlites Laterally and Vertically Intercalate with the Resedimented Hyaloclastites in Different Levels and Overlie Them.

Urla K 17 c 1; 79 750 / 79 000

On the Eski-Yeni Foça road the brecciated perlite lense intercalate with the pyroclastic flows subunit. Upward they are overlain by the thin layered silica gel interval and slightly to non welded subaqueous pyroclastics (Figure 2.38).



Figure 2. 45 Massive Perlites Intercalate the Foça Pyroclastic Flows in Different Straigraphic Levels. Urla K 17 c 1; 79 750 / 79 100

2. 2. 3. Foça alkaline volcanics

Description: Around Bağarası village, between Bağarası and Eski Foça and on the Eski-Yeni Foça road (Plate 1), massive lava flows of the trachyandesite to phonolite in composition, and dykes of the same volcanism are observed intercalating and cutting the pyroclastic rocks of the Foça volcanic complex. These mafic volcanic suite can be correlated with the basaltic suite of Yılmaz (1989) and the Foça alkaline volcanics (Savaşçın, 1978; Kaya, 1981; Kaya & Savaşçın, 1981; Savaşçın & Güleç, 1992; Savaşçın & Erler, 1994). The stratigraphic definitions and relations of the unit with the accompanying units have not been clarified in the previous studies. In this study, the detailed mapping and stratigraphic definition of the unit will be outlined.

Lithology: The Foça alkaline volcanics are composed of dark gray to black lava flows and dykes associated with the acid pyroclastics of the Foça volcanic complex. In the lava facies, well-developed, 10 to 30 cm-thick flow foliation is observed. The rocks are porphyritic in texture with phenocrysts of 2 mm length, and black, aphanitic matrix. The dykes are 1-10 m-thick and laterally 0.5 to 1 km in length. Petrographically both, the lava flows and the dykes, are basaltic in composition and the dominant mafic mineral is clinopyroxene with low extinction angle. In thin sections the porphyritic texture is dominant (Figure 2.46) and in places trachytic flow laminae are common in the matrix.

The matrix is glassy or micrystalline. In the microlitic parts, elongation of microlites is characteristic (Figure 2.47). In the glassy parts, on the other hand, recrystallization is common and the plagioclase phenocrysts are engulfed (Figure 2.47b). The main felsic mineral is euhedral, partly zoned plagioclase with typical polysynthetic twinning. Argillation and sossuritization are the common alteration types in plagioclases (Figure 2.48).

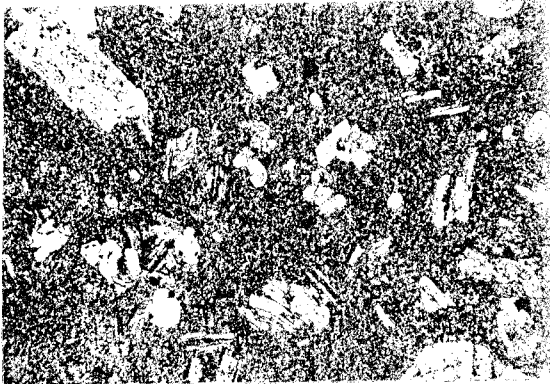


Figure 2. 46 Photomicrograph Showing the Characteristic Porphyritic Texture in Foça Alkaline Lavas. The Long Side of the Photograph is 4.5 mm in Length.

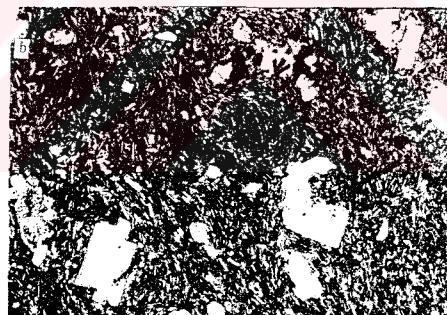


Figure 2. 47 Photomicrograph Showing the Typical Trachytic Texture in Foça Alkaline Lavas. Note the Typically Elongated Microlitic Matrix **(a)**, Microlitic Matrix Wrapping the Phenocrysts **(b, shown by dashed arrow)**. The Solid Arrow Shows the Microcrystalline Matrix Grown Over the Feldspar Phenocryst. The Long Side of the Photograph is 6 mm in Length.

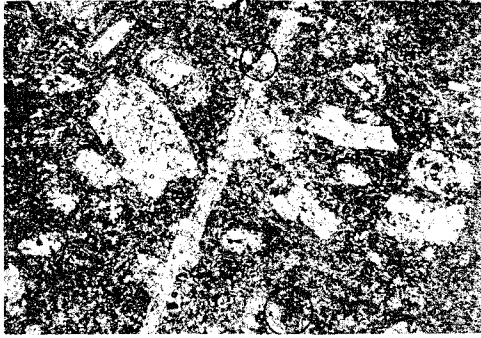


Figure 2. 48 In the Foça Alkaline Lavas, the High-Ca Plagioclase Phenocrysts are Commonly Found as Partly or Completely Converted into Calcite. The Long Side of the Photograph is 4.8 mm in Length.

Amphiboles with brown pleochroism, in minor amount, and rare biotites and olivines are also observed as mafic constituents. The clinopyroxene phenocrysts have low extinction angle of $5-25^{\circ}$ and show pale to dark green pleochroism indicating augite to aegyrine in composition (Figure 2.49). The pyroxene phenocrysts and especially those with the light green pleochroism, alteration is pronounced and they are partly to completely replaced by calcite indicating that they are augite in composition with high calcium content (Figure 2.50).

Boundary relations: To the 2 km southeast of Eski Foça, the massive lava flows of the Foça alkaline volcanics overlie the thick pyroclastic sequence of the Foça volcanic complex. The contact relations, however, are not clearly observed in this area. Around Bağarası village, on the other hand, the unit gradationally overlies the Pyroclastic flows. Along this contact 1 m-thick interlayers of the mafic lava flows are observed in the pyroclastic sequence and upward these pyroclastic rocks are overlain by the massive lava flows of the Foça alkaline volcanics (Figure 2.23). Upward, the mafic lava flows are overlain by the massive rhyolite lavas of the Foça rhyolites in the second mafic lava flow overlying the rhyolitic flows at the uppermost part. Between Horozgediği and Ilıpınar villages (Plate 1), the lava flows of the Foça alkaline volcanics and the Foça volcanoclastics. The Aliğa limestones overlie both the Foça alkaline volcanics and the Foça pyroclastics at this locality (Figure 2.51).

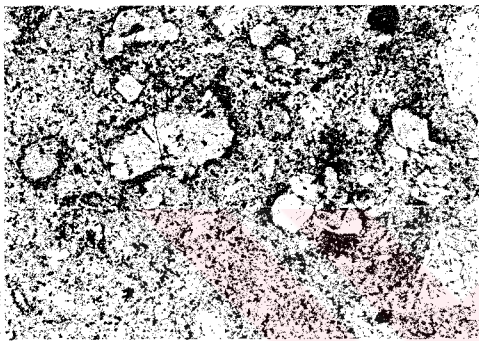
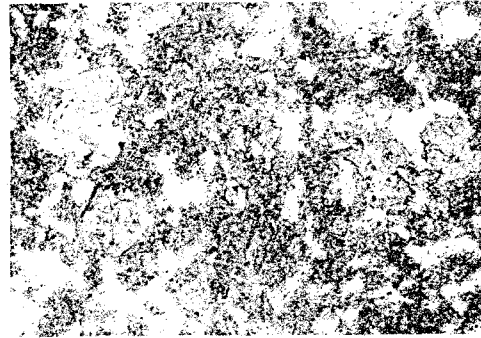
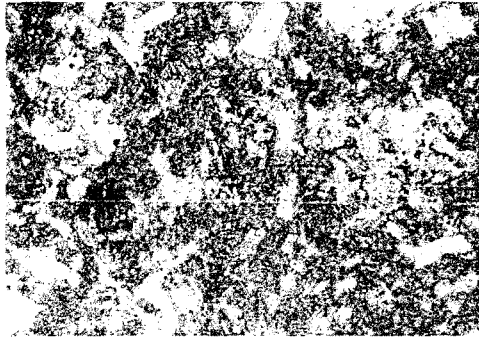


Figure 2. 49 The Dominant Mafic Mineral, Observed in Foça Alkaline Lavas, is the Aegyrine-Augite-Type Cylinopyroxenes with Significant Low Extinction Angle and Light to Dark Green Plechroism. The Long Side of the Photograph is 3.7 mm in Length.

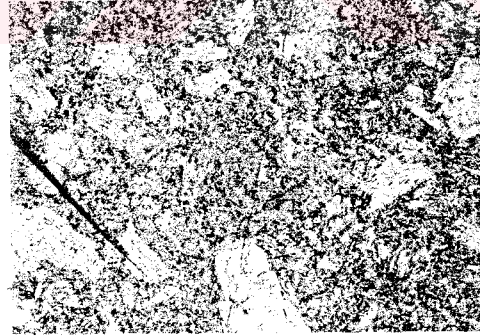
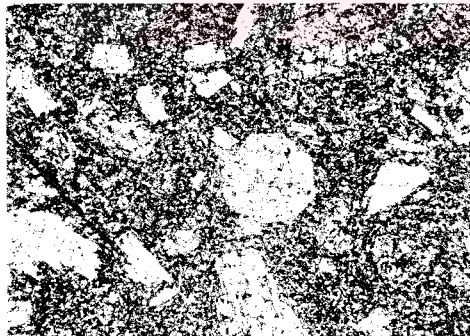


Figure 2. 50 Photomicrograph Showing the Augite-Type Cylinopyrosene Phenocrysts with High-Calsium Content, Converted into the Calcite. The Long Side of the Photograph is 4.1 mm in Length.



Figure 2.51. Field Photograph Showing the Coherent Lava Flows of the Foça Alkaline Volcanics, Overlain by the Aliğa Limestone Unit.

Urla K17 c2; 92 800 / 86 950

Along the Bozköy section (Figure 2.52), a thin lava flow of the Foça alkaline volcanics unit intercalates with the Foça pyroclastics and the whole section is overlain graditionally by the Aliğa limestone unit. To the west of Samurlu village (Plate 4), the lateral equivalents of the Aliğa limestone unit is overlain inturn by the Foça alkaline volcanics implying the simoultaneous formation of the lacustrine deposition and the alkaline volcanism.

On the Eski-Yeni Foça road, around Seyrekzeytinlik area, and on the Bağarası Eski Foça road, the dykes of the Foça alkaline volcanics cutting the volcanoclastic sequence along a sharp and high angle contacts are observed (Figure 2.53).

The intergraditional relations between the Foça alkaline volcanics, the Pyroclastic flows and the Foça rhyolites clearly indicate the bimodal characteristics of the volcanism in the area.

2. 2. 4. Age of the Foça volcanic complex

The volcanoclastic rocks of the Foça volcanic complex corresponds the Foça Tuff Unit of Kaya (1981), and alkaline mafic lavas and dykes are equivalents of the Foça alkaline sequence of Savaşçın (1978). The whole Foça volcanic complex corresponds to the Volcanic and Volcano-Sedimentary Unit of Savaşçın and Güleç (1992). There are some radiometric age determinations in these units and lateral equivalents of them, and some age interpretations based on this relative stratigraphic positions (Figure 2.14). Fytikas et al. (1979) reported an 12-7 m.y age for the scattered shosonitic rocks from the Aegean Sea to

BOZKÖY SECTION



Figure 2. 52 Cross section from the Bozköy village showing the gradational contact between the Foça volcanics and the Aliğa Limestone units. Section line is shown in Plate 2.



Figure 2. 53 Mafic Alkaline Dykes with High-Angle Cross Cutting Contact in the Foça Pyroclastic Flows Subunit
Urla K 17 c1; 82 150 / 80 050.

the East of Afyon and the Foça alkaline volcanics take place in this alkaline suite indicating the Late Miocene age. Previously, Savaşçın (1978) reported an 16.5 m.y age for the alkaline suite which indicates the Middle Miocene age. It is commonly believed that the volcanic activity in western Anatolia developed in two main stages. The first stage was calcalkaline in nature and occurred from the Late Oligocene-Early-Middle Miocene and the second stage was alkaline in nature and developed from Middle-Late Miocene to prehistoric times (Borsi et al., 1972; Fytikas et al., 1976; Fytikas et al., 1979; Yılmaz, 1990; Savaşçın & Erler, 1994). Fytikas et al.(1979) suggested that the volcanic cycle was completely exhausted between the Lower and Middle Miocene. Yılmaz (1989) and Yılmaz (1990), on the other hand, pointed out a transitional change from the calcalkaline to alkaline regimes at the end of the Middle Miocene. In the Foça area, the graditional contacts between the calcalkaline Foça volcanoclastic rocks and the Foça alkaline volcanics clearly indicate that the alkaline volcanism started in the later stages of the calcalkaline stages, but probably they evolved bimodally during the Middle Miocene time. The chemical affinities of these different series will be discussed in detail in chapter 3.

2. 3. ALIĞA LİMESTONE

In the Foça Peninsula, between Horozgediği and İlipınar villages and around Aliğa (Plates 2, 3), white to yellow coloured, commonly well-bedded limestones crop out. The most detailed mapping of this unit was carried out and documented by Kaya (1981).

The Aliğa limestone unit is composed of medium to thick bedded limestones and clayey limestones. The average thickness of bedding varies from 20 to 80 cm and the total thickness of the unit is up to 100 m. Rare stromatolites and gastropoda-rich levels are observed in the unit. The Aliğa limestone is observed as 40 cm to 20 m-thick lenses in different levels of the Yuntdağ volcanics and the Foça volcanic complex in the study area. 2.5 km to the WSW of Samurlu village (Plate 4), the massive lava flows of the Helvacı andesite unit are interlayered with 50 cm to 3 m-thick lacustrine limestone lenses of the Aliğa unit (Figure 2.54). Similarly, the volcanoclastic parts of the Yuntdağ volcanics are also interlayered with the Aliğa limestones. On the southern flank of the Bozdivlit Mt. (Plate 4), the fine ash horizons are interlayered with about 50 cm-thick lacustrine limestone lenses (Figure 2.55). Upward along the same section another thin lense of lacustrine limestone, interdigitates with the massive lava flows of the Çaltılı andesites. Around Samurlu and Güzelhisar villages (Plate 4), the Aliğa limestone conformably and gradationally overlies the Yuntdağ volcanics and the Foça volcanic complex (Figure 2.53). Along this contact, 1-3 m-thick limestone lense is observed in the Pyroclastic flows of the Foça volcanic complex. Similarly, around Bozköy village (Plate 2), the Aliğa limestone unit gradationally overlies the Foça volcanic complex which is characterized by the limestone, pyroclastic flow and lava alternations along the contact zone (Figure 2.52). Between Ilıpınar and Horozgediği villages (Plate 2), on the contrary, the Aliğa limestones spread over the different subunits of the Foça volcanic complex along a sharp contact which resemble slight angular (Plate 3). However, it is clear that the lateral equivalents of the Aliğa limestone unit, Yuntdağ volcanics and the Foça volcanic complex are gradationally pass into the each other even in the study area. So that, in this local area, angular relations probably caused by syntectonic activity. So that, local subsidence caused an enlargement of the lake boundary, in which carbonate deposition was taking.

SAMURLU SECTIONS

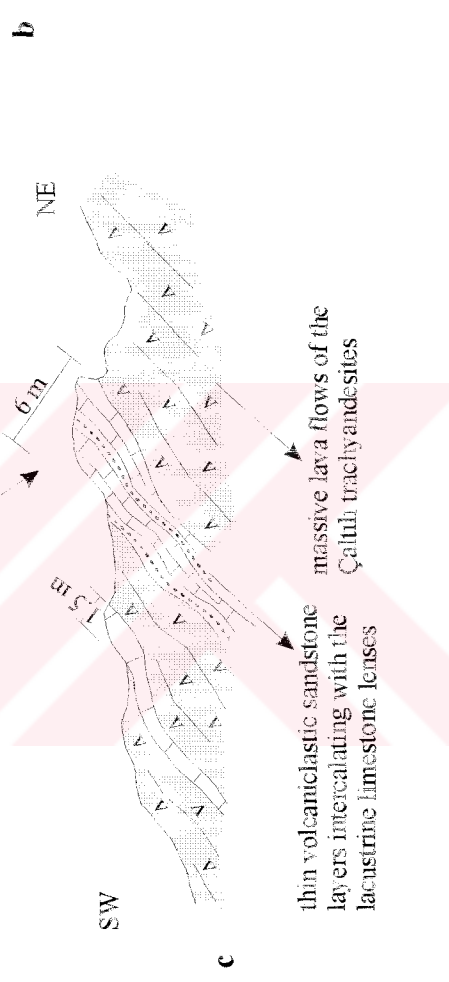
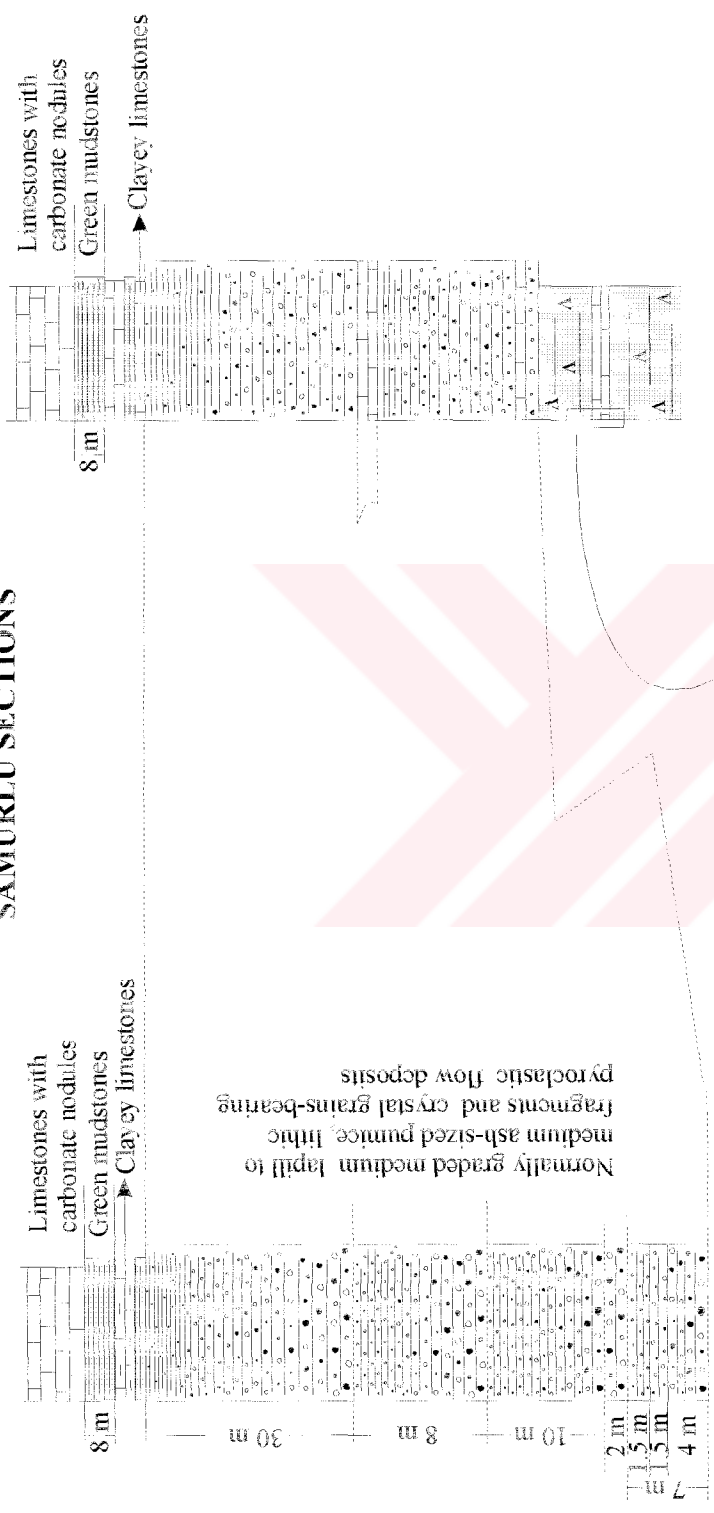


Figure 2. 54 Cross section from the Samurlu village showing the gradational contact between the Foça volcaniclastics and the Aliğa limestone units. Section line is shown in Plate 3.

ÇALTILI SECTION

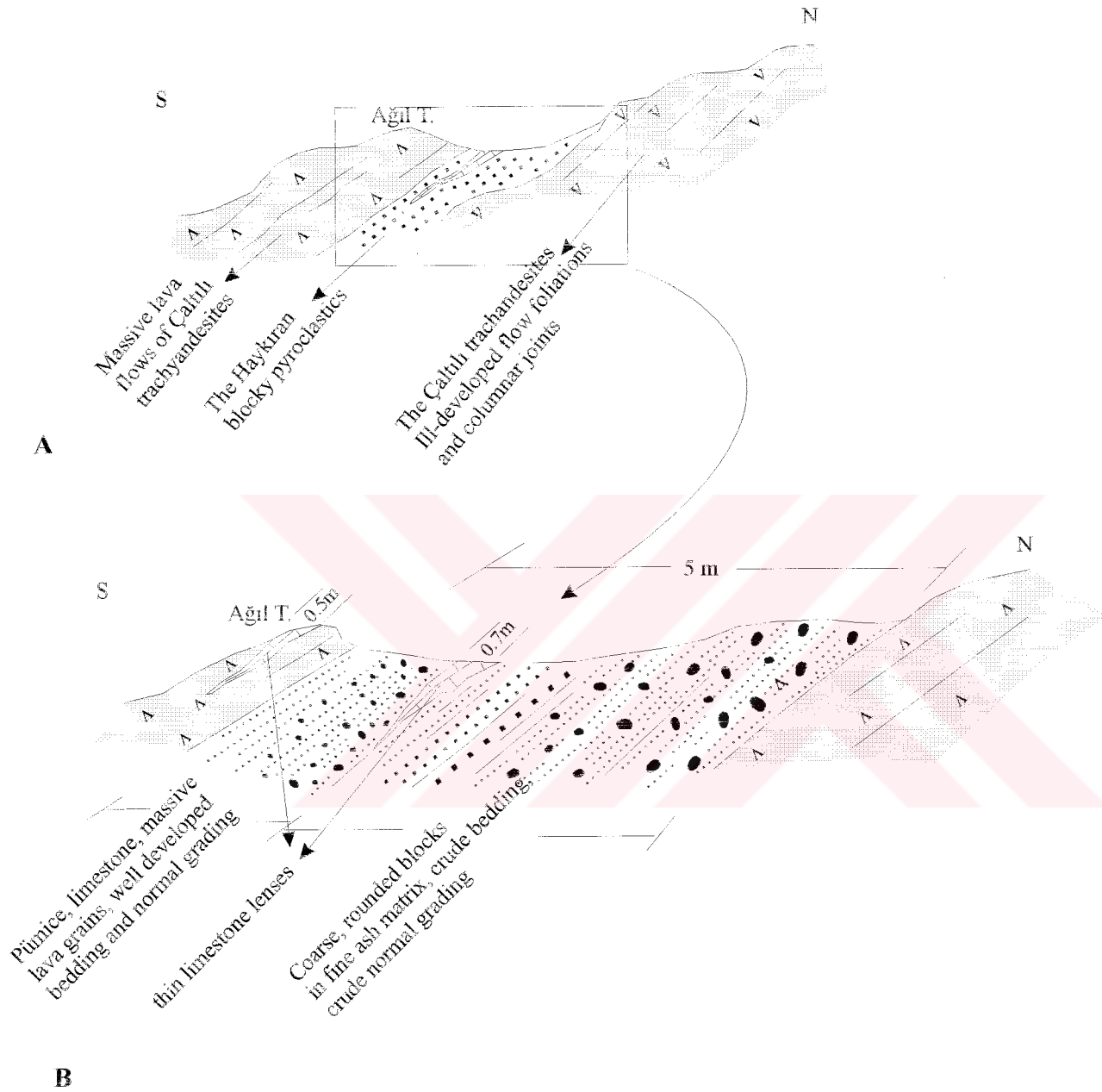


Figure 2. 55. Cross section from the southern flank of the Bozdivlit Mt. showing the lacustrine limestone lenses in the Foça volcanoclastics. Section line is shown in Plate 4.

CHAPTER THREE

GEOCHEMISTRY

In the Aliğa-Foça region, the Yuntdağ volcanics are mainly made up of the andesitic to dacitic lava flows of the Helvacı andesites, lava flows of the Çaltılı andesites and the coarse grained pyroclastic flow deposits of the Haykiran blocky pyroclastics. Dykes and subvolcanic stocks of the same volcanic cycle cut these units and form another unit of the Yuntdağ volcanics. The Foça volcanic complex, on the other hand, show a typical bimodal petrographic and chemical affinity characterized by rhyolitic volcanic, subvolcanic and volcanoclastic suites which dominate the Foça volcanic complex and accompanying trachytic-trachyandesitic lavas and dykes.

In this study, the geochemical affinities of the coherent facies of this wide-spread volcanic succession are examined and 95 samples were analysed. In this chapter major and trace element contents of the 71 samples from the Yuntdağ volcanics will be given, 16 of which are from the Çaltılı andesites, 9 from the Dumanlıtepe dykes and 46 are from the Helvacı andesites. The geochemical analyses of 24 samples from the Foça volcanic complex are also made; 14 samples of which are from the alkaline volcanic rocks and 10 samples from the rhyolites.

3. 1. YUNTDAĞ VOLCANICS

3. 1. 1. Helvacı andesites

46 representative and relatively fresh rock samples, collected from the Helvacı andesites are examined geochemically. The results of the major and trace element analyses of the Helvacı andesite are given in Table 3.1 in which the SiO_2 ratios range from 55.84 % to 69.43 %, Al_2O_3 from 14.55 % to 19.31 %, CaO from 1.75 % to 7.98

%, Na₂O from 1.62 % to 4.46 % and K₂O from 1.674 % to 4.941 %. On the Na₂O+K₂O vs SiO₂ diagram of Cox, Bell and Pankhurst (1979), the Helvacı andesites are plotted mainly in trachyandesite, andesite and dacite areas (Figure 3.1). Similarly on the Zr/TiO₂*0.0001 vs Nb/Y and SiO₂ vs Zr/TiO₂*0.0001 diagrams of Winchester and Floyd (1977), the samples of the Helvacı andesites gather mainly in the andesite area and a few samples are in trachyandesite, and rhyodacite / dacite areas (Figure 3.2a, b).

To show the chemical affinities of the Helvacı unit, the samples are plotted on the Na₂O+K₂O vs SiO₂ diagram of Irvine and Baragar (1971) in which most of the samples show subalkaline characteristics (Figure 3.3). On the same diagram only a few samples are located just on the line separating the alkaline and subalkaline areas (Figure 3.3). On the FeO / Na₂O+K₂O / MgO triangle of Irvine & Baragar (1971) (Figure 3.4a) and SiO₂ vs FeO / MgO diagram of Miashiro (1974) (Figure 3.4b), the samples show a significant calc-alkaline affinity. In the K₂O vs SiO₂ diagram of Gill (1981) the Helvacı andesites are scattered in the High-K, Acidic Andesites area (Figure 3.5).

In table 3. 2, the average chemical composition of some high-K, calc-alkaline andesites formed in different tectonic settings, are given to be compared with the Helvacı andesites. As seen in table, the major element contents of the Helvacı andesites are clearly comparable with the high-K, acid orogenic andesites which is indicated also in the K₂O / SiO₂ diagram of Gill (1981) (Figure 3.5). The major oxide contents are also comparable with those of the Active Continental Margins' Andesites of Andes. Particularly in point of the Na₂O, K₂O, MgO and CaO, the Helvacı andesites are clearly differ from the High-K, Basic Orogenic andesites and Island Arc Andesites.

Finally, both the chemical characteristics and the field occurrences of the Helvacı andesites show a rough similarity with the active continental margin andesites. The detailed discussion on the tectonic settings of the units will be given in Chs. 5 and 6.

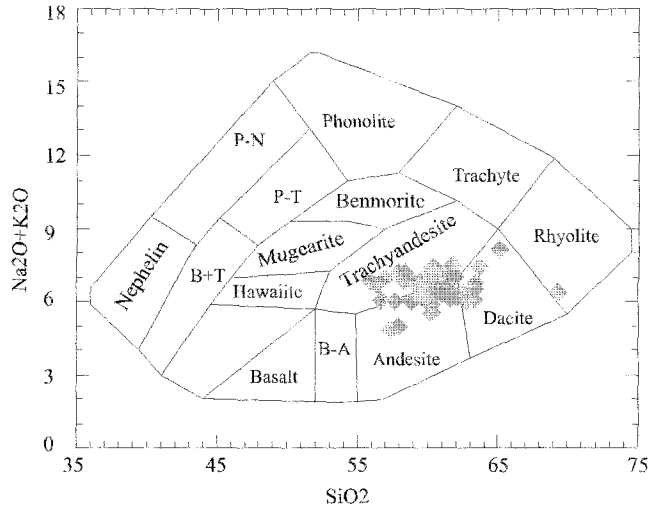


Figure 3. 1. $(\text{Na}_2\text{O} + \text{K}_2\text{O})$ vs SiO_2 variation of the Helvacı Andesites. Most Samples are Plotted in the Trachyandesite, Andesite and Dacite Areas. Diagram was constructed by Cox et al (1979)

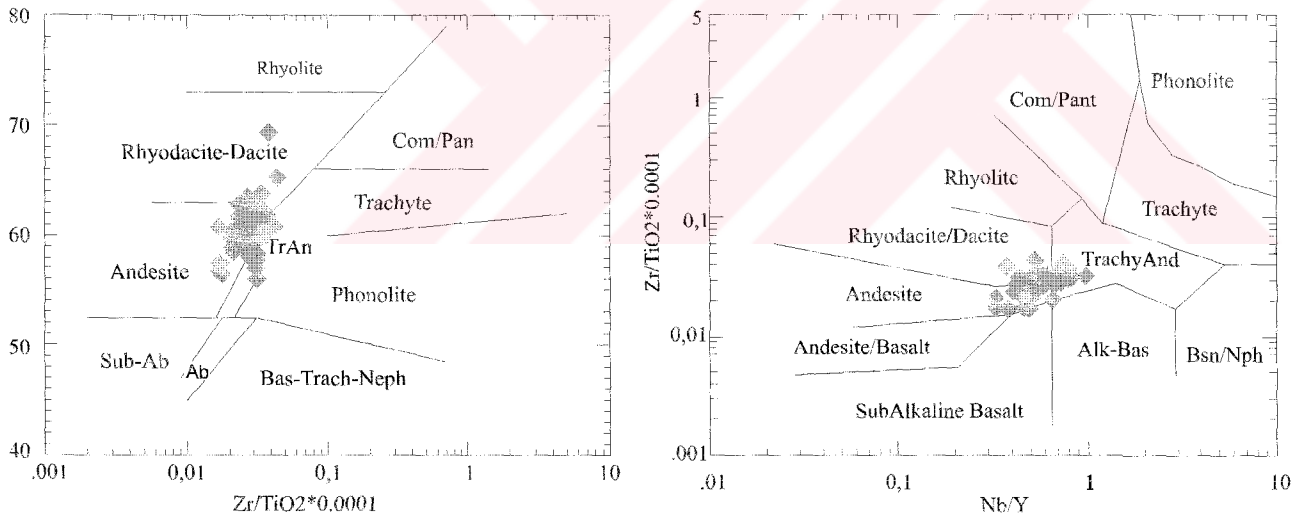


Figure 3. 2. Frequency of the Samples from the Helvacı Andesites in Nomenclature Diagrams of Winchester and Floyd (1977) which are based on the Trace Element Contents. **a.** SiO_2 vs $\text{Zr} / \text{TiO}_2 * 0.0001$, **b.** $\text{Zr} / \text{TiO}_2 * 0.0001$ vs Nb / Y . Samples are Characteristically gathered in the Andesite, Trachyandesite and Rhyodacite/Dacite Areas

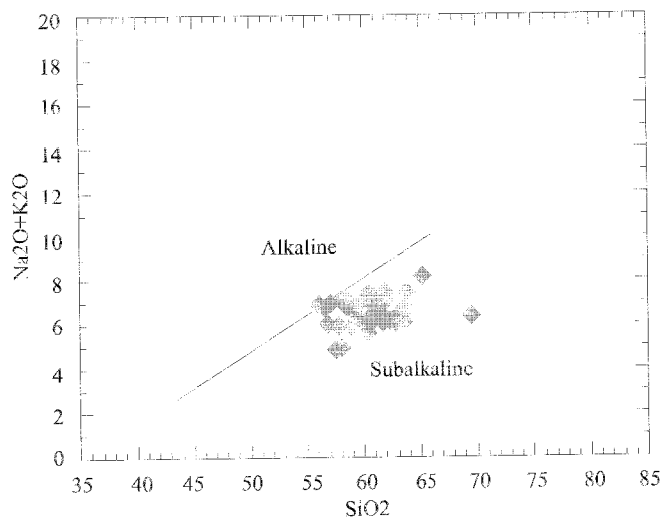


Figure 3. 3. The Chemical Affinity of the Helvacı Andesites. In the $\text{Na}_2\text{O}+\text{K}_2\text{O}$ vs SiO_2 Diagram of Irvine & Baragar (1971), They are Subalkaline in Nature

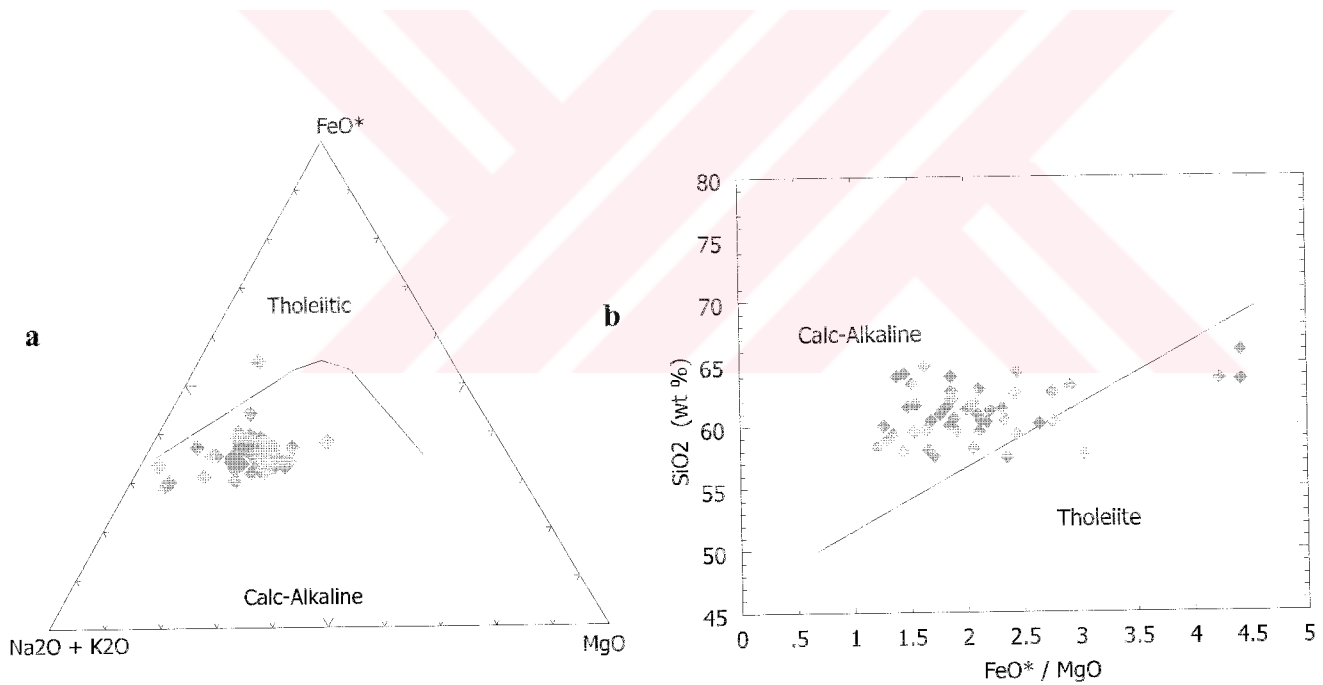


Figure 3. 4. Frequency of the Helvacı Andesites in **a.** $\text{FeO} / (\text{Na}_2\text{O}+\text{K}_2\text{O}) / \text{MgO}$ Triangle of Irvine & Baragar (1971) and **b.** $\text{SiO}_2 / \text{MgO}$ Diagram of Miashiro (1974). In both Diagrams the Helvacı Andesites Show Calc-Alkaline Chemical Affinity

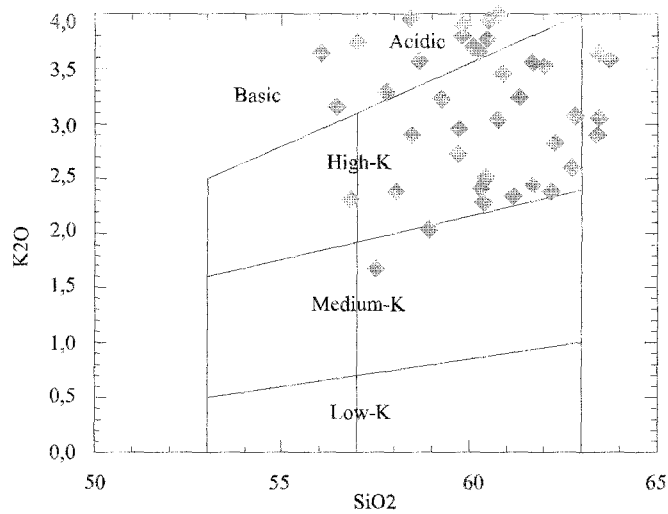


Figure 3. 5. The Frequency of the Helvacı Andesites in K₂O vs SiO₂ Diagram of Gill (1981).
Samples are scattered in High-K, Acidic Andesite Area.

Table 3. 2. The Average Major and Trace Element Composition of the Helvacı Andesites and Some Other Typical Andesite Types

	Average chemical composition of the Helvacı andesites	Representative andesite analyses		Average composition of orogenic andesite types (Gill, 1981)		Andesites of active continental margins from Andes (Ewart, 1982)	Island-Arc, high-K calc-alkaline andesites from Sunda Arc (Foden, 1983)	Island-Arc andesites of the south-west Pacific SWP (Ewart, 1982)
		high-K, basic Peccerillo & Taylor (1976)	high-K, acidic Lopez-Escobar et al. (1976)	high-K, basic	high-K, acid			
SiO ₂	60.68	55.2	59	54.6	59.4	59.89	61.59	59.09
Al ₂ O ₃	16.42	15.9	16.5	17.7	16.9	17.07	16.85	16.83
Fe ₂ O ₃ ^t	5.63	7.3	5.3	7.8	6.2	6.31	5.84	6.98
MgO	2.59	5.5	3.7	3.9	3.1	3.25	1.90	3.83
CaO	5.23	9.6	4.8	7.6	6.0	5.67	4.42	7.05
Na ₂ O	3.35	2.9	4.0	3.3	3.3	3.95	4.82	3.41
K ₂ O	3.27	2.7	2.4	2.1	2.5	2.47	3.00	1.70
TiO ₂	0.771	0.92	0.72	0.91	0.3	0.95	0.86	0.73
MnO	0.077	-	-	0.18	0.12	0.13	0.17	0.13
P ₂ O ₅	0.271	-	0.26	0.30	0.24	0.31	0.47	0.23
Nb	14.43	7	-	-	-	-	-	6.3
Zr	229.9	111	-	-	-	195	244	138
Y	24.40	22	-	-	-	12.2	45	24.7
Sr	523.29	583	190	-	-	648	405	516
Rb	130.52	68	126	-	-	75.4	69	41.2
Th	18.08	5.3	5.8	-	-	-	-	-
Pb	29.29	12	-	-	-	-	-	9.9
Zn	64.46	66	-	-	-	-	-	-
Cu	28.78	-	-	-	-	40	-	51.8
Ni	28.91	45	60	-	-	38.6	1	34.4
Cr	58.15	220	213	-	-	48.4	27	87.4
V	129.66	190	-	-	-	48.4	-	154
Ba	1139.75	670	310	-	-	886	-	479
Sc	17.01	-	-	-	-	-	-	-
Ce	84.34	33	38	-	-	66.8	-	44
Nd	34.58	-	-	-	-	-	-	-
La	44.28	15	19	-	-	38	-	25.4

3. 1. 2. Çaltılı andesites

The Çaltılı andesites are exposed mainly between the Helvacı and Yanık villages (Plate..) and to the north of Aliğa, around Çaltılı village (Plate...). In this study 9 relatively fresh samples from the unit, were chemically analysed. The major and trace element composition of the unit is given in table 3. 3. As seen in table, the SiO_2 ratios of unit range from 59.48 % to 62.07 %, Al_2O_3 from 13.67 % to 15.02 %, CaO from 5.6 % to 6.18 %, Na_2O from 2.82 % to 3.12 % and K_2O from 2.48 % to 2.81 %. On the $\text{Na}_2\text{O}+\text{K}_2\text{O}$ vs SiO_2 diagram of Cox. et al. (1979), the samples of the Çaltılı andesites are plotted in the Andesite area (Figure 3.6). Similarly on the SiO_2 vs $\text{Zr}/\text{TiO}_2*0.0001$ and $\text{Zr}/\text{TiO}_2*0.0001$ vs Nb/Y diagrams of Winchester & Floyd (1977) the Çaltılı andesites are gathered in the Andesite area (Figure 3.7a, b). In the field observations the Çaltılı andesites typically have a basaltic appearance with its dark colour and aphanitic texture. In thin sections, on the other hand, they have very low olivine and pyroxene content compared with the amphiboles and biotites which may indicate andesitic-trachyandesitic character (Ch. 2.1.3). In addition to petrographic features, the above mentioned chemical composition of the unit indicates their andesitic character rather than basaltic nature.

On the $\text{Na}_2\text{O}+\text{K}_2\text{O}$ vs SiO_2 diagram of Irvine & Baragar (1971), the Çaltılı andesites are plotted in the Subalkaline Volcanics area (Figure 3.8). On the $\text{FeO} / \text{Na}_2\text{O}+\text{K}_2\text{O} / \text{MgO}$ triangle of Irvine & Baragar (1971) (Figure 3.9a) and SiO_2 vs FeO / MgO diagram of Miashiro (1974) (Figure 3.9b), the samples of the Çaltılı andesites are gathered in the Calc-Alkaline Volcanics' area. Similar with the Helvacı andesites, the Çaltılı andesites are plotted in the Acidic High-K Andesites' area in the K_2O vs SiO_2 diagram of Gill (1981) (Figure 3.10) which all show the close chemical affinity between the Helvacı and Çaltılı units. In Table 3.4, the chemical compositions of some representative andesites types found in the literature and that formed in different tectonic settings, are also given for comparison. The similarity between the major element composition of the Çaltılı andesites and the High-K, Acidic Orogenic Andesites of Gill (1981) and Active Continental Margins' Andesites of Ewart (1982) is clear which also indicate the close chemical composition and hence tectonic setting of the Çaltılı and Helvacı units. In addition to the major element contents, the trace

Table 3. 3. Major and Trace Element Composition of the Çaltılı Andesites. Samples, Signed by (*), are After Altıntaş (1997)

	29 a *	30 a *	33 a *	34 a *	35 a *	36 a *	37 a *	38 a *	39 a *	1088 c	1088 h	1089 a	1093 a	1093 b	1095 a	1095 b
SiO ₂	60,00	60,62	60,37	59,48	61,21	60,99	60,86	60,35	62,07	59,79	57,83	59,02	59,26	58,35	58,67	59,83
Al ₂ O ₃	14,33	14,59	14,42	13,67	15,02	14,54	14,33	14,32	14,47	16,12	16,77	16,95	16,69	16,37	16,27	16,47
Fe ₂ O ₃ ^T	6,32	6,44	6,4	7,1	6,1	6,16	6,23	6,4	5,96	5,27	5,28	4,89	5,13	5,22	5,28	5,02
MgO	5,3	4,55	5,11	5,11	4,04	3,92	4	4,89	4,08	2,88	3,08	2,63	2,36	2,7	2,6	2,06
CaO	6,18	6,06	6,06	6,35	5,8	5,88	5,99	5,99	5,6	4,75	5,01	4,52	4,87	5,98	5,03	6,2
Na ₂ O	2,84	3,11	2,86	2,98	3,1	3,12	2,97	2,82	2,99	2,93	3,26	3,56	3,04	3,32	3,35	3,48
K ₂ O	2,61	2,71	2,65	2,75	2,66	2,68	2,81	2,81	2,48	3,841	3,116	3,338	3,23	2,016	3,014	2,88
TiO ₂	0,52	0,57	0,57	0,52	0,58	0,57	0,47	0,61	0,52	0,673	0,651	0,652	0,616	0,604	0,593	0,599
MnO	0,127	0,125	0,125	0,135	0,117	0,12	0,122	0,125	0,112	0,069	0,122	0,087	0,095	0,12	0,12	0,182
P ₂ O ₅	0,25	0,25	0,22	0,24	0,24	0,24	0,22	0,24	0,22	0,256	0,173	0,179	0,158	0,155	0,153	0,157
LOI	1,6	1,3	1,56	1,85	1,52	2,04	2,32	1,6	1,7	2,87	4,19	3,58	4,42	4,6	4,49	3,07
total	100,07	100,32	100,34	100,18	100,38	100,26	99,76	100,15	100,2	99,45	99,47	99,4	99,88	99,43	99,56	99,96
Nb	6,7	13,6	5,7	11,5	6,7	5,3	5,7	9	10	18,27	11,7	11,7	10,8	11,4	11,2	11,2
Zr	135,6	140,1	146,2	128,1	137,6	118,6	132,4	146	120,8	280,2	172,2	173,9	170,2	170,3	168,5	169,6
Y	21,5	23,9	27,56	24,2	28,8	20,7	26,1	21,4	27,9	23,74	19	18,4	19,1	18,4	19,7	18,8
Sr	625,1	603,8	620,3	642,7	571,6	568,4	598,7	631,8	544,4	92,3	546,9	541,9	439,8	513,9	558,1	524,7
Rb	83	82,6	89,1	88,1	78,9	89,8	74,9	84,9	74,5	158,9	92,6	100	105,1	40,5	106,5	101,3
Th	nd	nd	nd	20,2	nd	nd	nd	6,2	nd	28,4	13,4	12,9	13,2	13,4	13,4	13,2
Pb										32,4	29,9	35	33,2	30,3	30,9	32,3
Zn										63,6	61,9	62	66	71,6	64,2	66,2
Cu	33,6	51,8	30,6	49,9	39,3	25,1	32,1	26,5	33,4	32,3	15,9	16,3	25,8	18,5	23	24,1
Ni	57,1	43,7	51,2	62	33	29,9	29,4	50,6	32,2	22,3	27,3	24,6	36,4	29,6	42,2	41,5
Cr	44,3	50,7	84,8	125,8	38,8	53	27,5	56,2	53,1	60	58,9	57	87,9	72,7	82,9	81
V										108,9	120,4	118,9	110,1	114,7	115,3	114,7
Ba	1219,4	1241,4	1054,3	1257,7	1258,7	1081,3	1113,5	1169,1	1017,7	1006	1446	1629	1246	915,3	1573	969,9
Ce										16,5	17,8	14,4	16,9	16,7	16	16
Se	89,3	98,8	90,4	93,6	88,9	87,4	87,6	88,3	80,1	106,3	70,9	69,6	49,9	51,7	56,4	56,4
Nd										39,3	24	25,1	19	23,3	21,2	22,9
La	14,5	12	32,6	12,2	nd	8,4	46,5	27,2	13,2	62,1	38,3	37,3	65,4	33,3	34,6	31,3

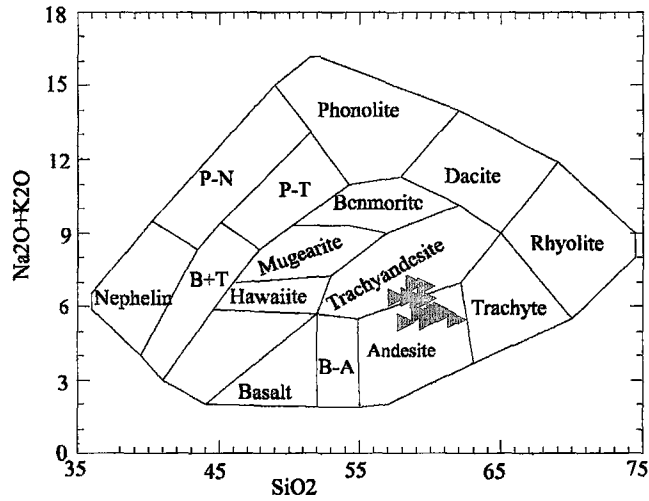


Figure 3. 6. (Na₂O + K₂O) vs SiO₂ variation of the Çaltılı Andesites. All Samples are Gathered in the Andesite and Trachyandesite Areas. Diagram was constructed by Cox et al (1979)

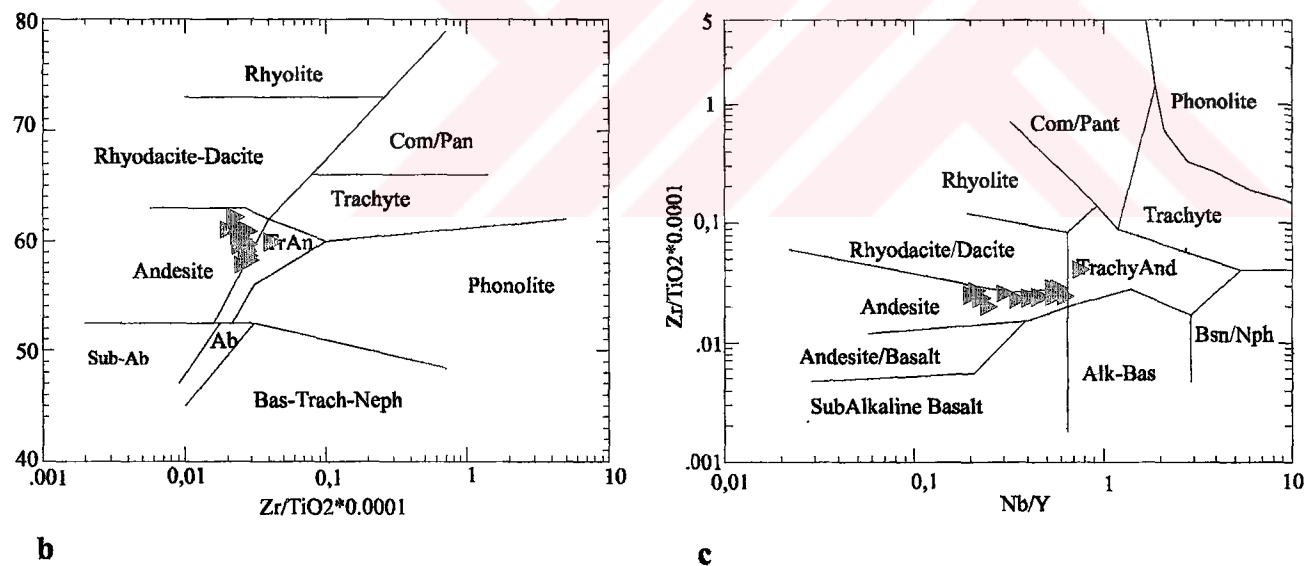


Figure 3. 7. Frequency of the Samples from the Çaltılı Andesites in Nomenclature Diagrams of Chester and Floyd (1977) Which are Based on the Trace Element Composition. **a.** SiO₂ vs Zr / TiO₂*0.0001, **b.** Zr / TiO₂*0.0001 vs Nb / Y. Samples are Characteristically gathered in the Andesite Area

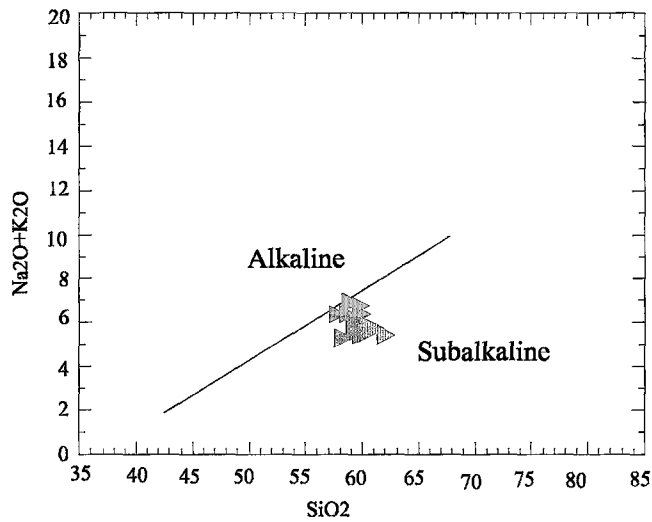


Figure 3. 8. The Chemical Affinity of the Çaltılı Andesites. In the $\text{Na}_2\text{O}+\text{K}_2\text{O}$ vs SiO_2 Diagram of Irvine & Baragar (1971), They are Subalkaline in Nature

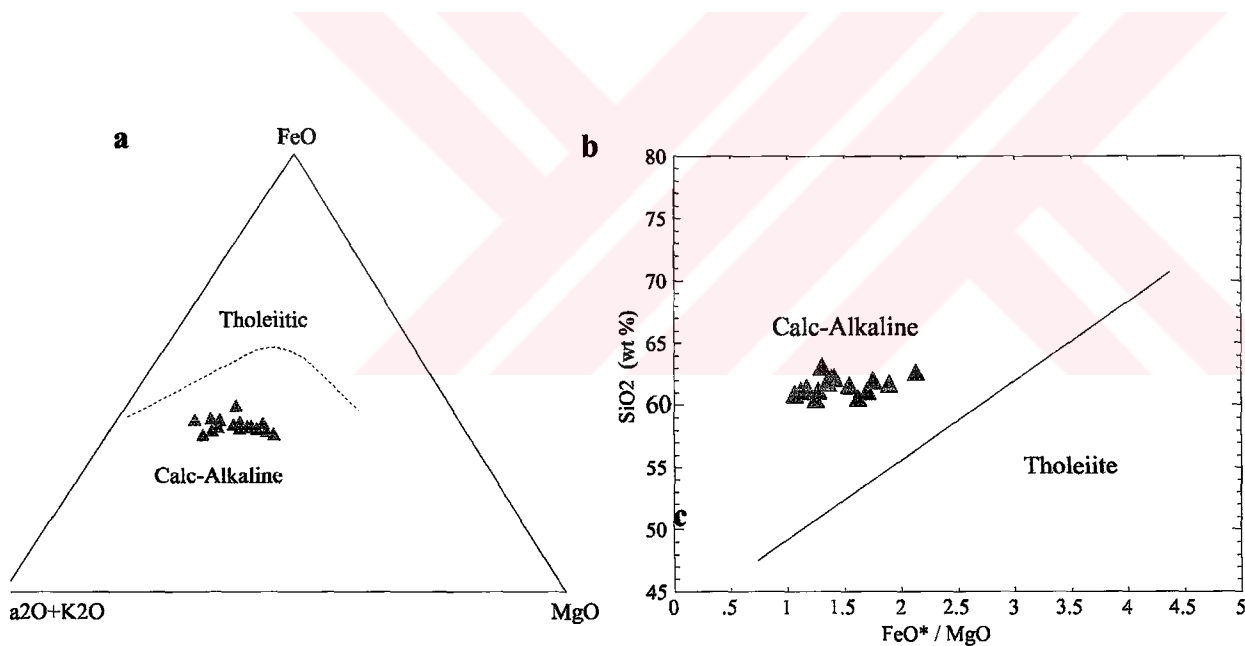


Figure 3. 9. Frequency of the Çaltılı Andesites in **a.** $\text{FeO} / (\text{Na}_2\text{O}+\text{K}_2\text{O}) / \text{MgO}$ Triangle of Irvine & Baragar (1971) and **b.** $\text{SiO}_2 / \text{MgO}$ Diagram of Miashiro (1974). In both Diagrams the Helvacı Andesites Show Calc-Alkaline Chemical Affinity

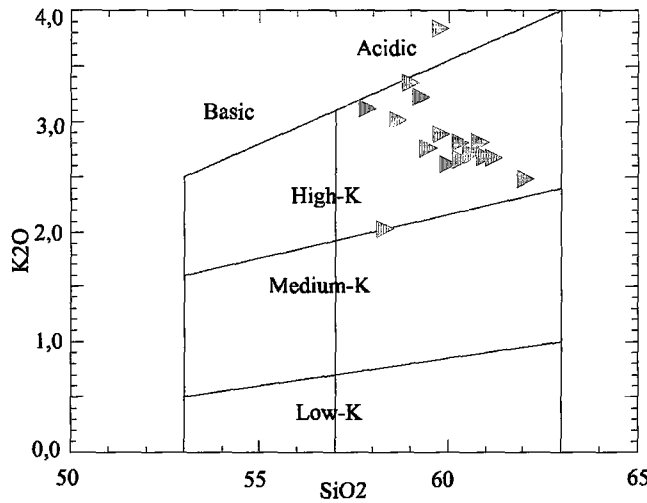


Figure 3. 10. The Frequency of the Çaltılı Andesites in K₂O vs SiO₂ Diagram of Gill (1981). Samples are gathered in High-K, Acidic Andesite Area.

element composition of the Çaltılı andesites also resemble with the Active Continental Margins' andesites (Table 3. 4). Besides that, the major and trace element composition of the Çaltılı andesites are significantly different from the Island Arc, the High-K, Acidic Andesites (Table 3. 4).

3. 1. 3. Dumanlıtepe dykes

To the NE of Helvacı and Hatundere villages, around Dumanlıtepe, petrographically andesitic, trachyandesitic dykes and one subvolcanic stock cut the andesitic lava flows of the Helvacı unit and the Haykıran blocky pyroclastics. In this study 9 representative samples from the different parts of this unit were geochemically analysed. The major and trace element composition of the unit is given in Table 3. 5 in which SiO₂ content varies from 56.25 % to 63.62 %, Al₂O₃ from 15.16 % to 16.29 %, CaO from 3.95 % to 6.11 %, Na₂O from 2.44 % to 3. 47 % and K₂O from 2.602 % to 4.374 %. The Na₂O, K₂O and SiO₂ content of the Dumanlıtepe dykes show that they are andesite, trachyandesite and dacite in composition (Figure 3.11). On SiO₂ vs Zr/TiO₂*0.0001 and Zr/TiO₂*0.0001 vs Nb/Y diagrams of Winchester & Floyd (1977) the Dumanlıtepe dykes are classified as the andesite, trachyandesite and dacite (Figure 3.12 a,b).

On the $\text{Na}_2\text{O}+\text{K}_2\text{O}$ vs SiO_2 diagram of Irvine & Baragar (1971), the Dumanltepe dykes show subalkaline characteristics (Figure 3.13). On the $\text{FeO} / \text{Na}_2\text{O}+\text{K}_2\text{O} / \text{MgO}$ triangle of Irvine & Baragar (1971) (Figure 3.14a) and SiO_2 vs FeO / MgO diagram of Miashiro (1974) (Figure 3.14b), the samples are plotted in the Calc-Alakaline area which all indicate the close chemical similarity between the Dumanltepe dykes, Helvacı andesites and partly the Çaltılı andesites. In Table 3. 6 the average chemical compositions of the Dumanltepe dykes, Helvacı andesites and the Çaltılı andesites are given in which the close similarity in both the major and trace element compositions among these three units are seen. The Harker-type variation diagrams showing the general trends of changes of the major

Table 3. 4. The Average Chemical Composition of the Çaltılı Andesites and Some Typical Andesite Types

	Average chemical composition of the Çaltılı andesites	Representative andesite analyses		Average composition of orogenic andesite types (Gill, 1981)		Andesites of active continental margins from Andes (Ewart, 1982)	Island-Arc, high-K calc-alkaline andesites from Sunda Arc (Foden, 1983)	Island-Arc andesites of the southwest Pacific SWP (Ewart, 1982)
		high-K, basic, Peccerillo & Taylor (1976)	high-K, acidic, Lopez-Escobar et al.(1976)	high-K, basic	high-K, acid			
O_2	59.91	55.2	59	54.6	59.4	59.89	61.59	59.09
Fe_2O_3	15.33	15.9	16.5	17.7	16.9	17.07	16.85	16.83
Mn_2O_3	5.82	7.3	5.3	7.8	6.2	6.31	5.84	6.98
MgO	3.70	5.5	3.7	3.9	3.1	3.25	1.90	3.83
CaO	5.64	9.6	4.8	7.6	6.0	5.67	4.42	7.05
Na_2O	3.10	2.9	4.0	3.3	3.3	3.95	4.82	3.41
K_2O	2.84	2.7	2.4	2.1	2.5	2.47	3.00	1.70
TiO_2	0.58	0.92	0.72	0.91	0.3	0.95	0.86	0.73
InO	0.11	-	-	0.18	0.12	0.13	0.17	0.13
ZrO_2	0.20	-	0.26	0.30	0.24	0.31	0.47	0.23
Nb	10.02	7	-			-	-	6.3
Rb	156.89	111	-			195	244	138
Sr	22.45	22	-			12.2	45	24.7
Y	568.8	583	190			648	405	516
Ba	90.6	68	120			75.4	69	41.2
Th		5.3	5.8					
U	29.88	66	-			40		51.8
Ni	38.31	45	60			38.6	1	34.4
Cr	64.66	220	213			48.4	27	87.4
Zn		190	60			125		154
Ga	1199.85	670	310			886	-	479
Ge	79.1	33	38			66.8		44
As	31.26	15	19			38		25.4
Sb		12	-			-		9.9

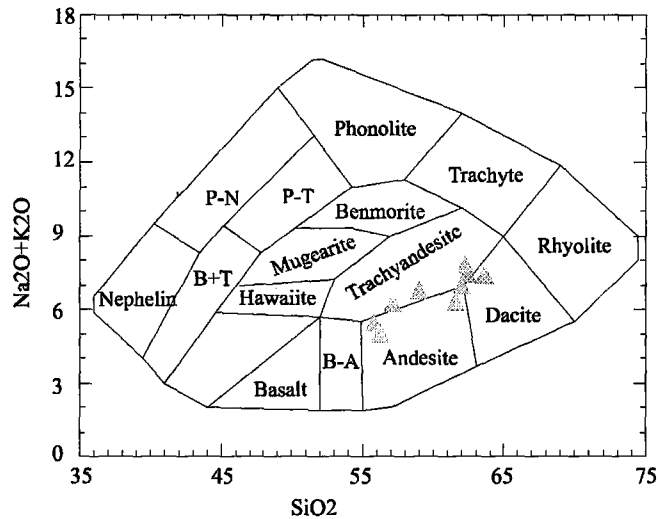


Figure 3. 11. $(\text{Na}_2\text{O} + \text{K}_2\text{O})$ vs SiO_2 variation of the Dumanltepe Dykes. Most Samples are Plotted in the Trachyandesite, Andesite and Dacite Areas. Diagram was constructed by Cox et al (1979)

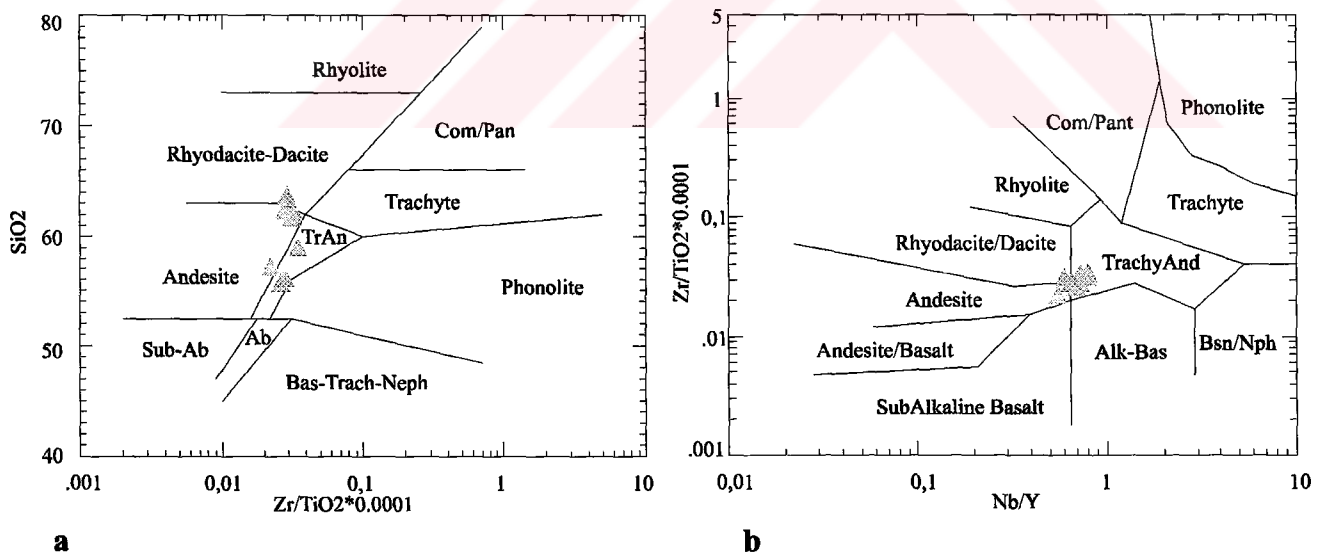


Figure 3. 12. Frequency of the Samples from the Dumanltepe Dykes in Nomenclature Diagrams of Winchester and Floyd (1977) which are based on the Trace Element Contents. **a.** SiO_2 vs $\text{Zr} / \text{TiO}_2 * 0.0001$ **b.** $\text{Zr} / \text{TiO}_2 * 0.0001$ vs Nb / Y . Samples are Characteristically Plotted in the Andesite, Trachyandesite and Rhyodacite/Dacite Areas

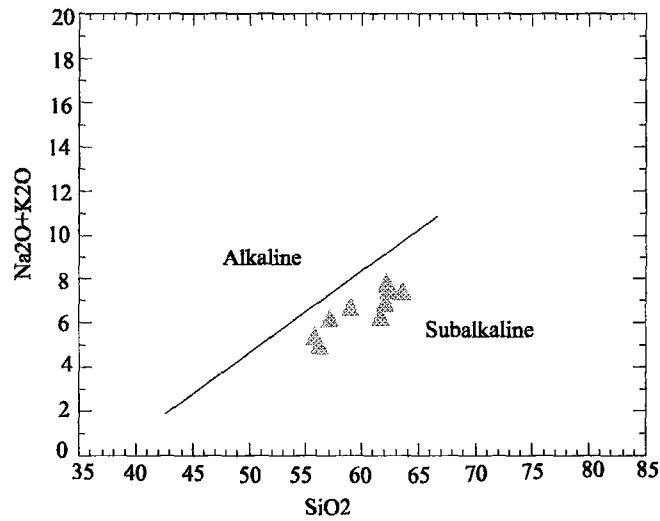


Figure 3. 13. The Chemical Affinity of the Dumanlıtepe Dykes. In the $\text{Na}_2\text{O}+\text{K}_2\text{O}$ vs SiO_2 Diagram of Irvine & Baragar (1971), They are Subalkaline in Nature

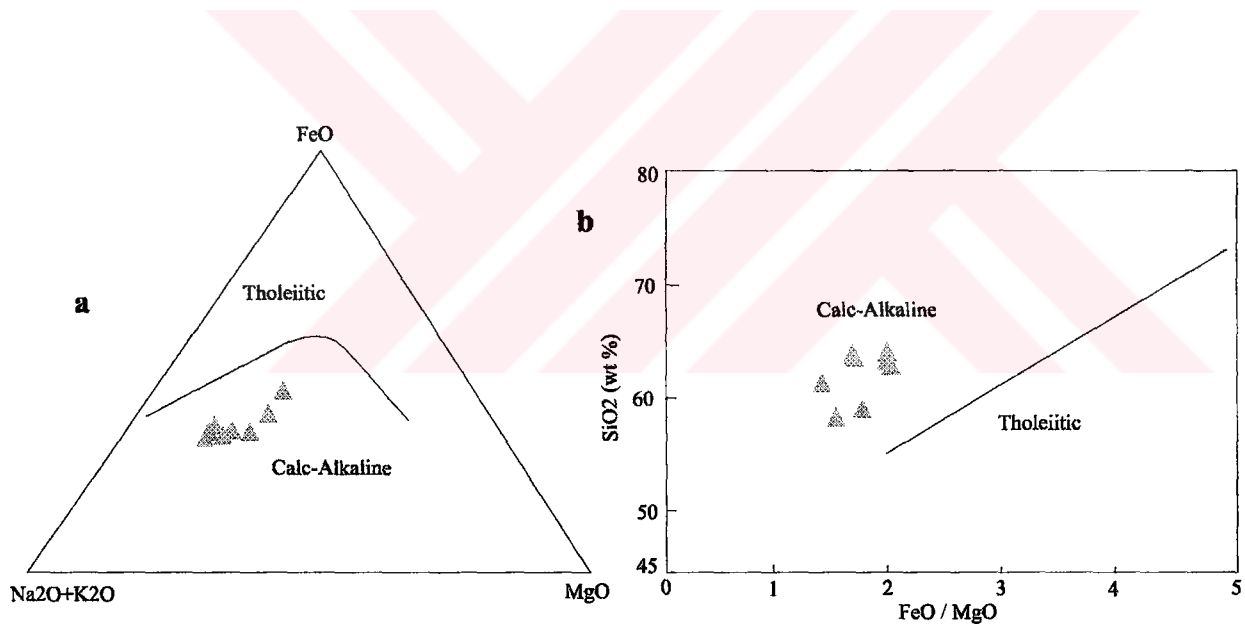


Figure 3.14. Frequency of the Dumanlıtepe Dykes in **a.** $\text{FeO} / (\text{Na}_2\text{O}+\text{K}_2\text{O}) / \text{MgO}$ Triangle of Irvine & Baragar (1971) and **b.** $\text{SiO}_2 / \text{MgO}$ Diagram of Miashiro (1974). In both Diagrams the Helvacı Andesites Show Calc-Alkaline Chemical Affinity

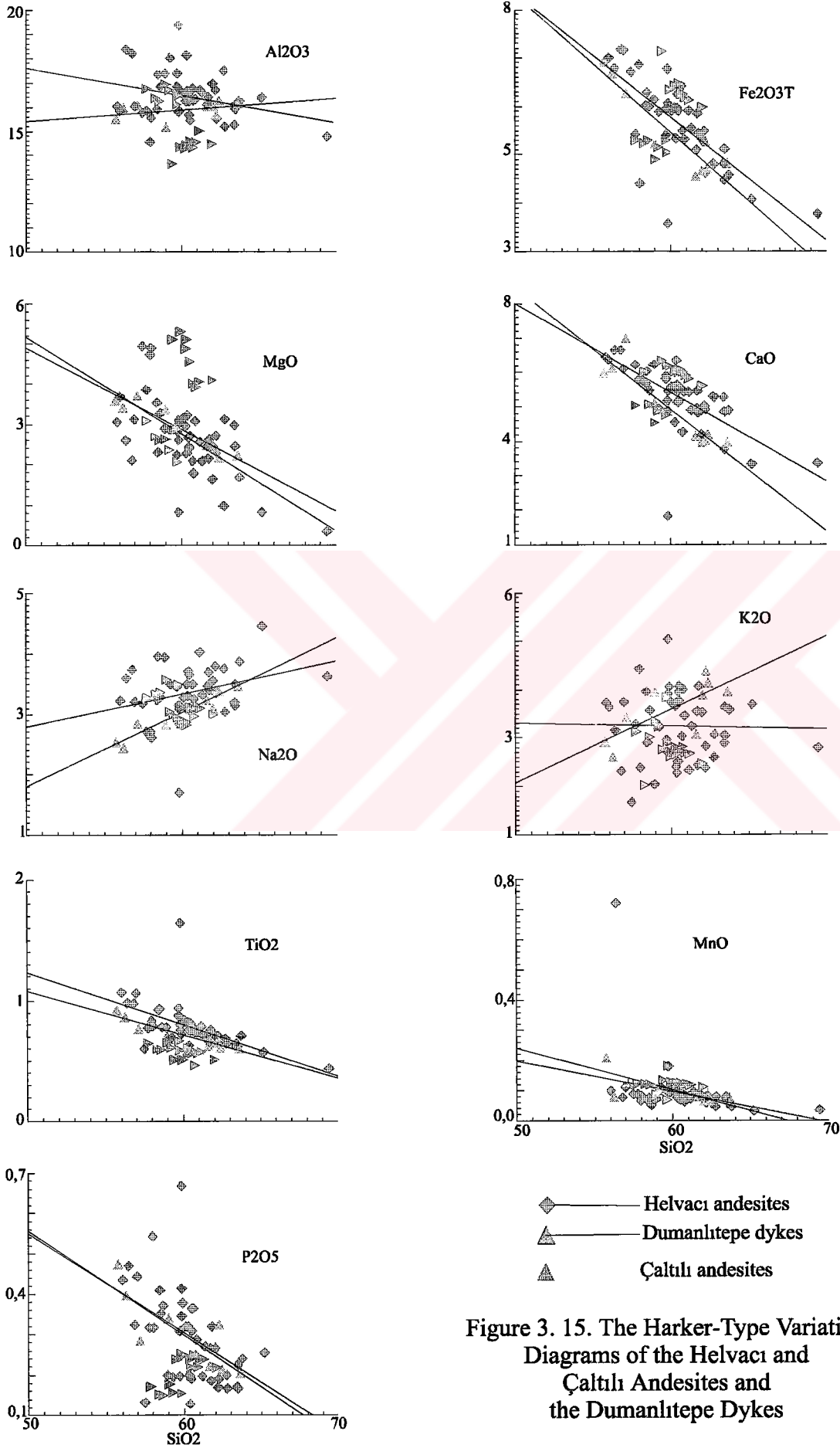


Figure 3. 15. The Harker-Type Variation Diagrams of the Helvacı and Çaltılı Andesites and the Dumanlıtepe Dykes

Table 3.5. Major and Trace Element Composition of the Dumanltepe Dykes

	1202 a	1202 b	1202 c	1204 a	785	787	788	790 a	790 b
SiO ₂	61,63		56,25	58,97	62,03		62,26	62,41	63,62
Al ₂ O ₃	16,07		15,96	15,16	16,02		15,65	16,29	16,15
Fe ₂ O ₃ ^T	4,56		6,68	5,23	4,67		5,26	4,73	4,81
MgO	2,47		3,43	3,38	2,51		2,38	2,17	2,22
CaO	4,15		6,11	5,08	3,96		4,02	4,19	3,95
Na ₂ O	3,23		2,44	2,83	3,1		3,41	3,38	3,47
K ₂ O	3,08		2,602	3,951	3,894		4,374	4,138	3,96
TiO ₂	0,627		0,869	0,711	0,652		0,697	0,611	0,603
MnO	0,08		0,081	0,085	0,066		0,088	0,066	0,075
P ₂ O ₅	0,223		0,395	0,339	0,268		0,326	0,215	0,206
LOI	3,35		4,71	3,67	2,24		0,97	1,22	0,94
total	99,46		99,54	99,4	99,41		99,44	99,43	100,01
Nb	12,6	15,4	16,2	17,2	15,8	12,3	16,6	13,4	13,4
Zr	198,4	244,9	243,7	245,6	216,3	174	221,4	173	173
Y	21,1	22,4	22,3	21,5	22	22,1	21,1	20,7	20,4
Sr	419,8	821,8	682	565,4	430	607	540,4	389,7	393,8
Rb	108,1	64	46,5	165,6	162,3	144	172,1	154,2	155,4
Th	19	20,7	20,5	30,8	25,6	17,1	26,2	22,6	23,4
Pb	26,9	28,1	30,5	27,7	30,6	23,6	30,7	28,7	28,2
Zn	56,9	71,8	67,4	54,9	47,6	60,4	54,3	51,9	51,1
Cu	16,3	46,4	47,3	39,6	29,1	39,2	36,1	18,2	17,5
Ni	16,2	22,5	22,6	36,2	16,4	39,3	54,5	14,3	14,1
Cr	27,2	36,6	33,5	80	22,8	88,9	125,6	14	15,8
V	111,6	171,2	182,1	119,2	117,4	148,1	115	100,7	100,7
Ba	865,4	1926,8	1581,9	1230,5	1196,9	1060,8	1309,2	922	899,5
Sc	15,1	21,1	20	17,1	14,9	18,8	16,2	12,3	11,5
Ce	82,4	91,4	85,5	92	92,6	74,4	90,8	78,1	82
Nd	29,5	35,6	33	35,2	33,8	33,1	31,9	27	18,1
La	44,3	44	53,9	49,4	50	35,2	42,6	41,9	43,3

element contents (Figure 3. 15) indicate that, the Helvacı andesites and the Dumanltepe dykes show similarity on all major elements except on Al₂O₃ and K₂O contents. The Çaltılı andesites, on the other hand, show negative correlation in comparison with the Helvacı andesites and the Dumanltepe dykes. In Figure 3.15, the negative correlation in Al₂O₃, K₂O, Fe₂O₃^T, MgO CaO Na₂O, K₂O and P₂O₅ contents of the Çaltılı andesites and the other subunits of the Yuntdağ volcanics, is significant indicating the different chemical evolution of these units. Since the Çaltılı andesites form the stratigraphically uppermost parts of the Yuntdağ volcanism (Ch. 2), such kind of a different chemical evolution may be the indicator of a chemical differentiation in the magma chamber during the activity.

In the Harker-type variation diagrams, it is noted that, the Çaltılı andesites show a different differentiation by itself which is characterized by the prominent grouping of these samples (Figure 3.15). The samples 29a, 30a, 33a, 34a, 35a, 36a, 37a, 38a and 39a are

collected from the aphanitic, significantly columnar jointed parts of the Çaltılı andesites. The other samples, on the other hand, are from the Foça Peninsula and overlain by the rhyolitic Foça pyroclastic sequence (Plate 1). The presence of a significant difference between these two sample groups show that magmatic differentiation had taken place even in the Çaltılı andesites compared to its earlier and later phases.

The spider diagrams constructed by the trace element composition of these three units are given in Figure 3.16. In Figure 3.16a, the chondrite normalized trace element composition of the Helvacı and Çaltılı andesites and the Dumanlıtepe dykes are given in which the very similar trace element composition and the same anomalies are clear. In the figure, between these three units, the same chemical evolution is seen. In Figure 3.16b MORB normalized trace element compositions of the units are given which similarly show the nearly same chemical evolution between the Helvacı and Çaltılı andesites and the Dumanlıtepe dykes. In this diagram, on the other hand, a minor negative anomalies in all trace elements in the Çaltılı andesites representing a minor differentiation, is seen. As well as the field observations (Chs. 2,4), the similar chemical composition of the Helvacı andesites and the Dumanlıtepe dykes indicate that these two units were derived from the same magma and had the same chemical evolution. The Çaltılı andesites, on the other hand, should have been developed by a minor chemical differentiation as indicated by the trace element composition (Table 3.6 & Figure 3.16b).

3. 2. FOÇA VOLCANIC COMPLEX

3. 2. 1. Foça rhyolites

The Foça rhyolites are massive rhyolitic bodies formed mainly as massive flows, rhyolitic dykes and rhyolitic domes. In this study, 10 samples from these different rhyolitic rocks are chemically analysed and major and trace element compositions of them are given in Table 3.7. The SiO₂ ratios range from 73.31 % to 82.15 %, Al₂O₃ from 9.3 % to 13.55, CaO from 0.18 % to 2%. Na₂O from 1.95 % to 3.76 % and K₂O from 3.97 % to 6.29 %. In Figures 3.17 & 18, the nomenclature diagrams for the Foça rhyolites are given.

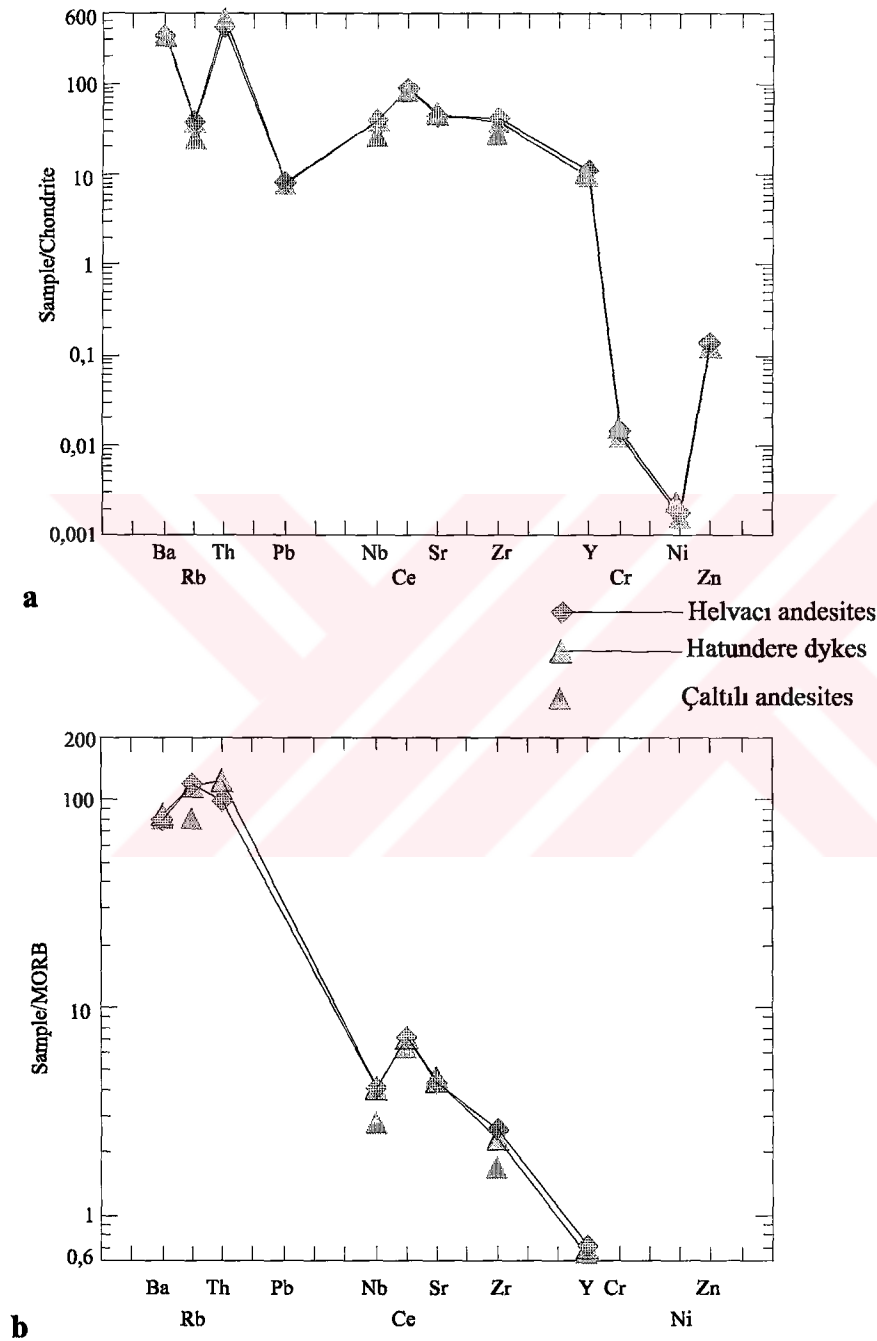


Figure 3. 16. **a.** Chondrite and **b.** MORB-Normalized Spider Diagrams of Helvacı and Çaltılı Andesites and the Hatundere Dykes Showing the Chemical Similarities and Differences Between These Three Units

Table 3. 6. Average Major and Trace Element Composition of the Dumanlıtepe Dykes, Helvacı and Çaltılı Andesites

	Dumanlıtepe dykes	Helvacı andesites	Çaltılı andesites
SiO ₂	60.95	60.68	59.91
Al ₂ O ₃	15.9	16.42	15.53
Fe ₂ O ₃	5.13	5.63	5.82
MgO	2.65	2.59	3.70
CaO ₂	4.49	5.23	5.64
Na ₂ O	3.12	3.35	3.10
K ₂ O	3.714	3.27	2.84
TiO ₂	0.681	0.771	0.58
MnO	0.077	0.077	0.11
P ₂ O ₅	0.281	0.271	0.20
Nb	14.76	14.43	10.02
Zr	210.3	229.9	156.89
Y	21.51	24.40	22.45
Sr	538.87	523.29	568.8
Rb	130.24	130.52	90.6
Th	22.87	18.08	nd
Cu	32.18	28.78	29.88
Ni	26.23	28.91	38.31
Cr	49.37	58.15	64.66
V	129.55	129.66	
Ba	1221.44	1139.75	1199.85
Sc	16.33	17.01	
Ce	85.46	84.34	79.1
Nd	30.8	34.58	
La	44.95	44.28	31.26
Pb	28.33	29.60	
Zn	57.36	64.43	

The Na₂O, K₂O and SiO₂ composition of the samples indicate rhyolitic nature (Figure 3.17). On the Q/P diagram of Debon & Le Fort (1983), on the other hand, they are plotted in the Rhyolite area (Figure 3.18a). On the SiO₂ vs Zr/TiO₂*0.0001 diagram of Winchester & Floyd (1977), the samples are in rhyolite area (Figure 3.18b). On the Na₂O+K₂O vs SiO₂ diagram of Irvine & Baragar (1971) the unit is subalkaline in nature (Figure 3.19) and on the FeO / Na₂O+K₂O / MgO triangle of Irvine & Baragar (1971), they show a calc-alkaline affinity (Figure 3.20). In most of the previous studies, carried out in the Foça region, the rhyolitic association is considered as an alkaline in nature (Savaşçın, 1978; Savaşçın & Erler, 1994). In this study, however, it is clearly seen that the wide spread rhyolitic association cropping out in the Foça region and the neighbouring areas are calc-alkaline in nature.

Table 3. 7. Major and Trace Element Composition of the Foça Rhyolites

	1007	1008	1042 d	1046 e	1089	1143	1145	979 a	980	998
SiO ₂	77,69	77,1	74,28			82,15		73,31	78,03	73,34
Al ₂ O ₃	11,47	11,54	13,55			9,3		13,44	12,12	13,52
Fe ₂ O ₃ ¹	0,97	1,2	1,1			0,21		1,67	0,34	1,71
MgO	0,07	0,11	0,08			0,13		0,57	0,16	0,16
CaO	0,45	0,48	0,18			0,43		2	0,4	0,84
Na ₂ O	3,3	3,33	1,95			3,4		3,34	2,28	3,76
K ₂ O	4,702	4,588	6,294			4,78		3,972	4,603	5,131
TiO ₂	0,12	0,143	0,134			0,092		0,285	0,09	0,233
MnO	0,013	0,012	0,004			0,007		0,023	0,01	0,026
P ₂ O ₅	0,015	0,073	0,018			0,021		0,095	0,011	0,045
LOI	0,63	0,84	1,85			1,05		0,77	1,6	0,64
total	99,53	99,43	99,45			99,65		99,49	99,44	99,41
Nb	36,5	35,8	21,6	18,5	32	9,7	10	13,4	16,7	29,8
Zr	92,6	126,5	120,9	106,4	133,4	60,2	60,3	162,7	58,6	152,9
Y	21,4	24,3	14,3	12,2	18,5	14	14,7	16,6	12,5	19,9
Sr	47,5	64,3	48,8	69,3	52,6	78,8	100,7	303,4	51,8	118,5
Rb	286,7	266,6	237,7	243,3	252,6	97	101	132,3	260,4	254,4
Th	38,1	62,7	38	34,7	38,5	9	11,3	12,1	22,6	39,6
Pb	54,7	50,3	46,3	37,7	62,5	31,5	29,7	29,4	51,9	52,5
Zn	14,1	18	21,4	9,1	26,2	9	11,1	28,4	10,7	22,8
Cu	nd	nd	0,4	0,7	2,4	nd	nd	2,2	nd	3,1
Ni	6,9	6,9	7,9	6,1	8,4	6,4	6	7,7	6,1	8
Cr	nd	nd	nd	nd	nd	nd	nd	0,6	nd	nd
V	118,7	17	12,3	9,2	17,1	3,3	9,3	24,3	8,5	15,8
Ba	133,6	227,4	532,3	541,9	316,7	1143,1	1302,6	1131	165,4	374,5
Sc	0,6	1,9	0,2	2,9	1,6	1,8	2,4	3,3	2,3	2,4
Ce	63	89,5	72,8	62,9	80,1	51,7	50,4	59,7	26,6	66,9
Nd	21,7	24,8	16,9	16,5	22,1	14,1	15,9	22,1	6,7	17,1
La	32,3	48,8	43,9	40,5	43	27,7	28,6	41,5	6,3	38,9

On the Nb vs Y diagram of Pearce, Harris & Tindle (1984), the Foça rhyolites are found in the Volcanic Arc Granitoids (VAG)+Syn-Collisional Granitoids (SynCOLG) area and Within Plate Granitoids (WPA) area (Figure 3.21a). On the Rb vs Y+Nb diagram of Pearce et al. (1984), the samples are plotted at the intersection point of Syn-COLG, VAG and WPG areas but mostly in VAG (Figure 3.21b). These authors, proposed these tectonic discrimination diagrams for granitoidic rocks, and stated a problem for application of these diagrams to the magmatic associations which are gathered around the triple point (Pearce et al., 1984). According to them, the associations gathered at the intersection point of VAG, SynCOLG and WPG areas may probably be formed in a post-collisional setting, and for such associations making tectonic discrimination would be difficult. Thus, these diagrams would not be the best choices to approach the tectonic setting of the Foça rhyolites but the field features of them which will be discussed in following sections.

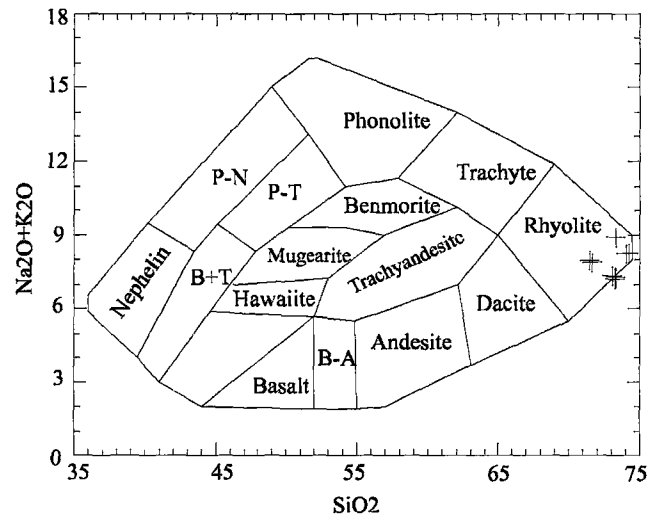


Figure 3. 17. (Na₂O + K₂O) vs SiO₂ variation of the Foça Rhyolites. Samples are Plotted in the Rhyolite Area. Diagram was constructed by Cox et al (1979)

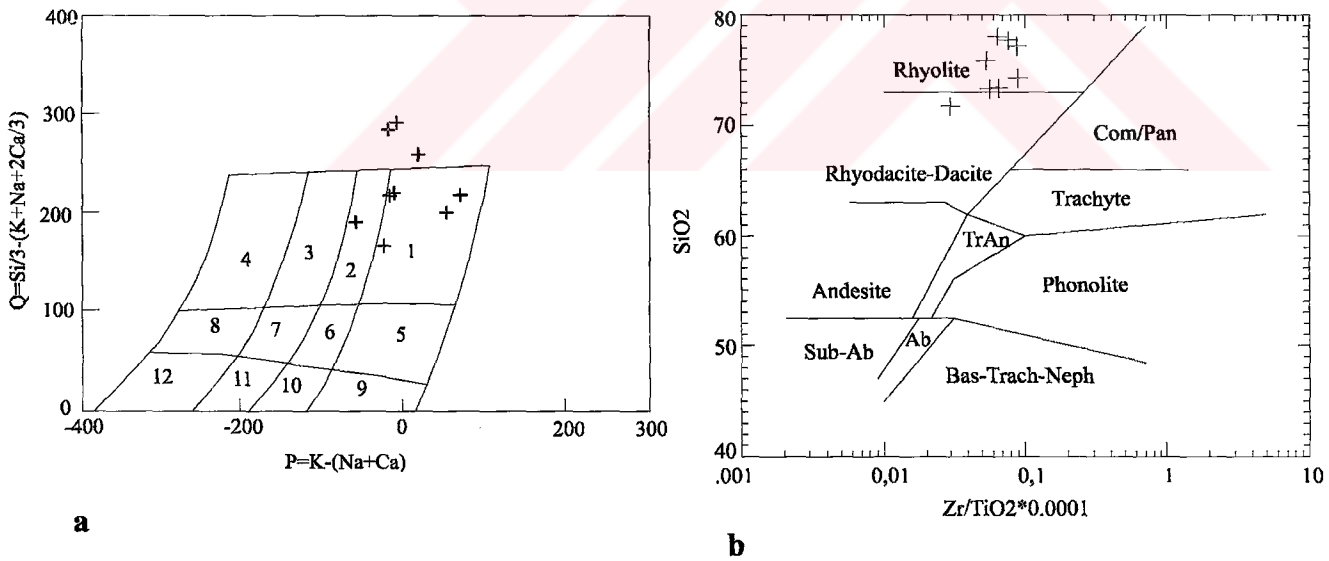


Figure 3. 18. Frequency of the Samples from the Foça Rhyolites in Nomenclature Diagrams Which are Based on the Trace Element Contents. a. Si/3-(K+Na+2Ca/3) vs K-(Na+Ca) Diagram of Debon & Le Fort (1983), b. Zr / TiO₂*0.0001 vs Nb / Y Diagram of Winchester and Floyd (1977). Samples are Characteristically Gathered in the Rhyolite Area

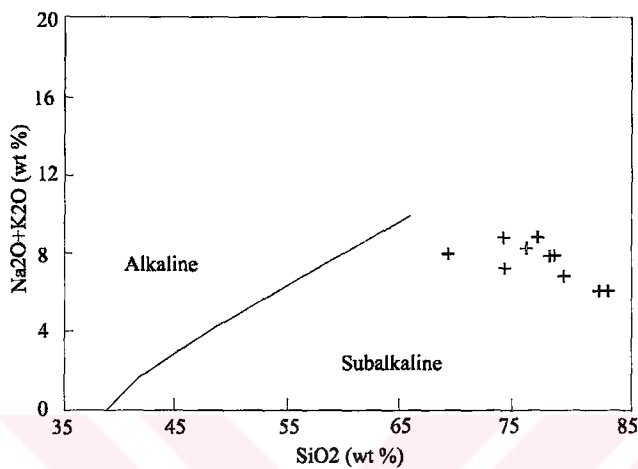


Figure 3.19. The Chemical Affinity of the Foça Rhyolites. In the $\text{Na}_2\text{O}+\text{K}_2\text{O}$ vs SiO_2 Diagram of Irvine & Baragar (1971), They are Subalkaline in Nature

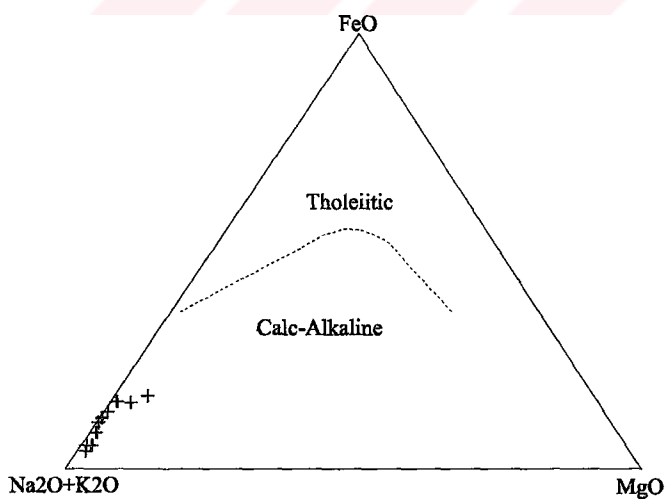
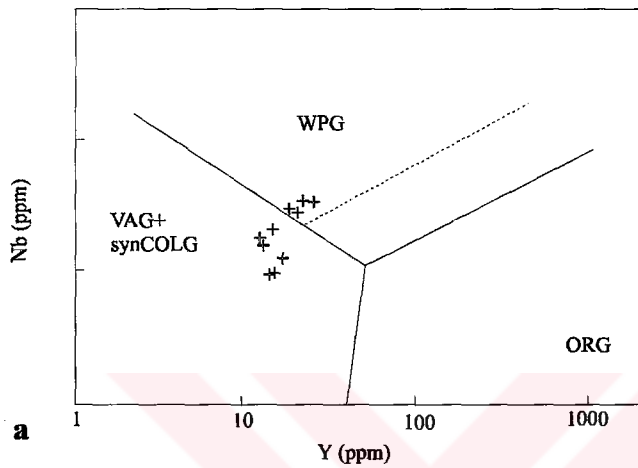
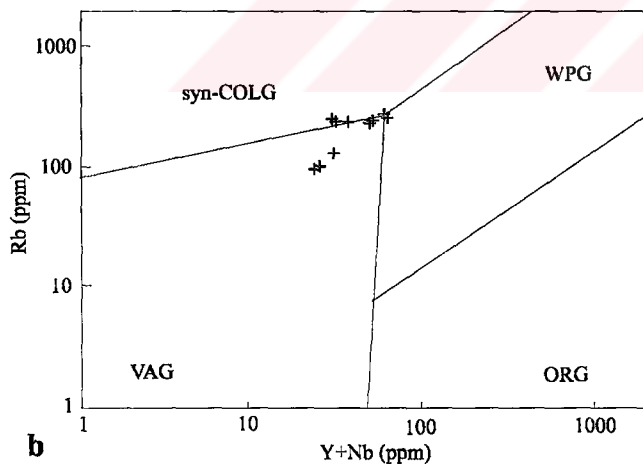


Figure 3.20. Frequency of the Foça Rhyolites in $\text{FeO} / (\text{Na}_2\text{O}+\text{K}_2\text{O}) / \text{MgO}$ Triangle of Irvine & Baragar (1971) in Which the Foça Rhyolites Show Calc-Alkaline Chemical Affinity



a

SynCOLG: Syn Collisional Granitoids
 VAG: Volcanic Arc Granitoids
 WPG: Within Plate Granitoids
 ORG: Oceanic Ridge Granitoids



b

Figure 3. 21. a. Nb vs Y and b. Rb vs Y+Nb (Pearce et al., 1984) variations of the Foça Rhyolites. Samples are Mostly Plotted in the Intersection Point of Syn-Collisional, Volcanic Arc and Within Plate Granitoids' Areas

3. 2. 2. Foça alkaline volcanics

In the Foça Peninsula, the alkaline volcanic rocks are found around Bağarası village, between Bağarası and Eski Foça and Between Eski and Yeni Foça towns (Plates...). Chemical analyses of 22 representative samples of these alkaline volcanic rocks were made in this study. In Table 3. 8 the major and trace element composition of the Foça alkaline volcanics are given. Their SiO₂ ratios range from 47.42 % to 61.14 %, Al₂O₃ from 12.75 to 19.46 %, MgO from 0.1 % to 8.66 %, CaO from 1.09 % to 11.18 %, Na₂O from 1.71 % to 8.93 %, K₂O from 1.92 % to 9.34 %. In Figures 3.22 & 23, the nomenclature diagrams, using major and trace element contents are shown. On the Na₂O+K₂O vs SiO₂ diagram of Cox et al. (1979), the rocks are mainly trachyandesitic and andesitic in nature. Two samples which were collected from the west of Bağarası village, and one sample representing the alkaline dykes, are plotted in the phonolite area, and some other samples are scattered in the hawaiite, benmorite and basalt areas (Figure 3.22).. On the SiO₂ vs Zr/TiO₂*0.0001 diagram of Winchester & Floyd (1977), the samples are classified as andesite, trachyandesite and alkaline basalt areas (Figure 3.23a). In this figure the samples from Bağarası village are plotted in the phonolite area as well. The sample representing the alkaline dykes, on the other hand, is plotted in the trachyandesite area. On Zr/TiO₂*0.0001 vs Nb/Y diagram of Winchester & Floyd (1977), most of the samples are gathered in the trachyandesite, andesite and basalt areas (Figure 3.23b). In this diagram two samples, from Bağarası village, also show phonolitic character and similarly with the Figure 3.23a, sample from the alkaline dykes, is plotted in trachyandesite area (Figure 3.23b).

On the Na₂O+K₂O vs SiO₂ diagram of Irvine & Baragar (1971), the samples from the Foça alkaline volcanics are mainly located in alkaline area and partly in subalkaline area (Figure 3.24). In the previous studies the alkaline nature of these volcanics is also stated (Savaşçın, 1978; Kaya & Savaşçın, 1981; Savaşçın & Erler, 1994; Ercan et al., 1985).

In Table 3.9 the average major and trace element compositions of the Foça alkaline volcanics and some volcanic suites of continental rift and within plate settings from various areas of the world, are given. In the table, similarity of the SiO₂, total Fe₂O₃, TiO₂, Zr, Y, Th, values of trachytic components and Al₂O₃, Na₂O, Nb, Zr, Zn, Sc values of phonolitic components with the continental rift and within plate alkaline suites can be seen.

In the western Anatolia, it is commonly believed that the alkaline volcanism is related with the N-S directed tensional tectonic regime and accompanying rifting (Savaşçın, 1978; Fytikas et al., 1980; Innocenti et al., 1982; Savaşçın, 1982; Fytikas et al., 1984; Seyitoğlu & Scott, 1991) which may explain the similarity of the chemical compositions of the Foça alkaline volcanics with the alkaline continental rift volcanics and within plate volcanics (Table 3. 9). In these studies, on the other hand, it is noted that there was a volcanic gap between the former calc-alkaline volcanism which is originated from the compressional tectonic regime of Oligo-Miocene time (Şengör, Satır & Akkök, 1984; Şengör, Görür & Şaroğlu, 1985; Innocenti et al., 1982; Fytikas et al., 1984) and later alkaline suite. In the Foça area, however, the bimodal character of volcanism show that the Foça Region is an area where the change from the calc-alkaline nature to the alkaline one and hence, from the compressional tectonic setting to the tensional one is observed. Probably that is why in Tables 3. 2, 4 & 9, the geochemical compositions of both the calc-alkaline and the alkaline suites show some minor differences from the characteristic examples of them

Table 3. 8. Major and Trace Element Composition of the Foça Alkaline Volcanics

	SiO ₂	Al ₂ O ₃	Fe ₂ O ₃	MgO	CaO	Na ₂ O	K ₂ O	TiO ₂	MnO	P ₂ O ₅	LOI	Nb	Zr	Y	Sr	Rb	Th	Pb	Zn	Cu	Ni	Cr	V	Ba	Se	Ce	Nd	La	
109 d	53,41	16,91	5,46	0,31	5,13	4,26	6,59	0,827	0,357	0,290	6,29	99,83	11,7	147,1	21,4	419,1	207	12,3	36,3	29,2	61,4	162,8	135,1	1371	23,2	75,5	24	34,9	
109 g	51,03	14,95	6,68	5,18	8,21	1,39	2,85	0,778	0,214	0,258	7,86	99,40	9,4	137,4	17,8	595,8	74,4	11,4	29,9	38,1	58,4	131,8	177,9	722,6	24,6	64	23,5	33,7	
109 h	51,47	15,35	6,56	4,9	8,62	1,71	2,245	0,696	0,119	0,17	7,65	99,49	10	140,3	17,8	635,2	53,4	10,8	33,3	43,3	56,4	141,6	176,6	739,3	26,5	67,9	29,8	35,6	
1086	59,55	17,38	5,42	1,92	5,44	4,05	3,751	0,847	0,047	0,281	0,72	99,41	18,2	288,1	20,6	524,3	158,6	16,3	24,7	22	34,1	41,5	111,6	1024	12,5	92,5	34,6	58,4	
1025	47,42	15,41	8,52	8,66	11,18	3,07	2,148	1,178	0,148	0,373	2,28	100,4	15,5	176,6	24,6	619,3	101,7	12,5	18,8	63	49,9	118,7	371,8	191,4	610	23,1	94,3	40,6	49,7
1026 a	58,3	19,46	4,7	0,16	1,48	8,93	7,2	0,099	0,179	0,037	1,14	99,69	83,8	854	52,7	53,1	370,7	68,6	63,3	120,6	7	5,2	nd	2,6	0,4	238,9	70,6	131,2	
1026 b	57,3	19,07	4,58	0,1	1,38	7,63	5,98	0,102	0,136	0,036	1,51	97,83	83,9	782,5	50,1	91,5	354,9	55,5	77,8	118	7,4	5,9	nd	6,5	35,8	nd	257,4	74,4	132,4
1043	51,85	15,73	7,51	6,41	7,69	3,69	3,373	0,981	0,147	0,306	1,71	99,4	22,4	253,9	27	524,4	108,4	20,8	50,4	32,6	90	336,8	149,9	645,5	18,7	126,9	46,1	60,8	
1063 e	61,14	18,15	4,45	0,71	1,09	4,48	9,34	0,67	0,083	0,245	1,59	99,94	34,4	346,9	31,1	131,8	299,1	32,2	56,4	79,8	6,5	6,1	nd	28,3	1202	4,6	168,2	57,5	95,9
1071	59,03	16,93	5,02	2,75	5,81	4,05	3,179	0,72	0,101	0,263	1,71	99,56	18,9	219,3	19,7	556,3	144,2	20	28,1	53,1	23,7	20,4	30,1	107,8	928,8	11,1	85,3	24	47,1
935	51,95	16,33	7,07	7,08	8,64	3,29	1,923	0,857	0,116	0,264	2,52	100,1	13,8	167,5	20	515,1	60,5	12,7	17,1	66,2	48,9	133,3	346,8	164,3	680,4	20,5	72,5	26,1	39,6
937	49,57	12,75	7,06	6,03	11,06	3,1	2,361	1,822	0,113	0,556	4,95	99,48	30,3	453,1	21,5	575,8	150,8	7,4	7,2	66,3	32,8	103,8	620,8	176,3	408,4	21,2	104,4	45,4	nd
941	54,56	16,31	5,91	5,12	7,02	3,8	2,607	0,835	0,11	0,407	2,89	99,47	22,8	273	22,1	637,1	134,4	16,6	21,4	61,4	32,1	131,9	218,3	123,7	919,6	16,5	84,6	33,8	42,8
947 a	53,08	17,22	5,79	4,03	8,64	3,8	2,679	0,947	0,97	0,352	3,03	99,67	23,1	231	20,1	636	95,8	11,5	18,1	57,4	33,8	91,7	204,4	129,5	790,3	18	68	29,8	37,6

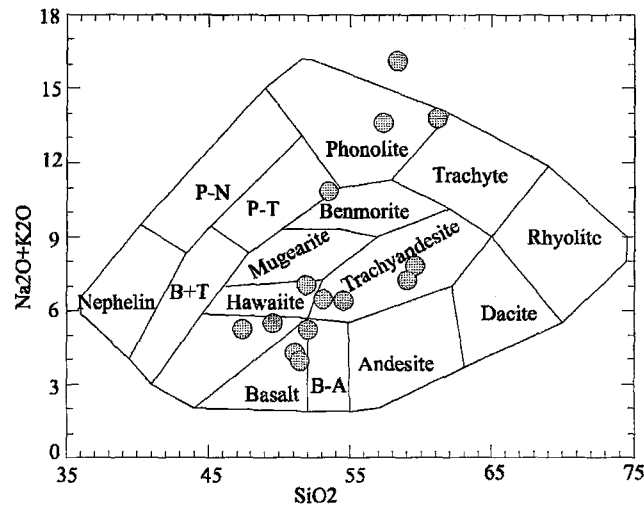


Figure 3. 22. (Na₂O + K₂O) vs SiO₂ variation of the Foça alkaline volcanics. Most Samples are Plotted in the Trachyandesite, Andesite and Basalt Areas and the Others are Scattered in Hawaiiite and Mugaerite Areas. Samples, Plotted in Phonolite Area are from the West of Bağarası Village and One of Them is from Alkaline Dykes Diagram was constructed by Cox et al (1979)

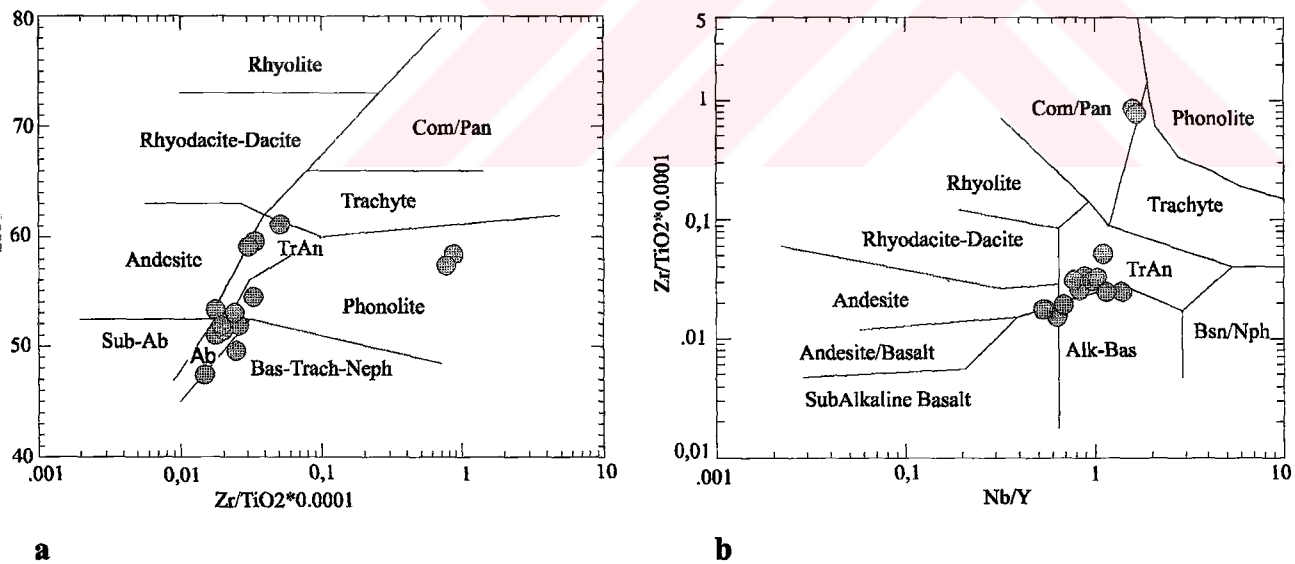


Figure 3. 23. Frequency of the Samples from the Foça Alkaline Volcanics in Nomenclature Diagrams of Winchester and Floyd (1977) which are based on the Trace Element Contents. **a.** SiO₂ vs Zr / TiO₂*0.0001, **b.** Zr / TiO₂*0.0001 vs Nb / Y. Samples are Characteristically gathered in the Trachyandesite and Alkaline Basalt Areas. Sample from the Alkaline Dykes is plotted in Trachyandesite Area. Phonolitic Samples are typically found in these Graphs as well

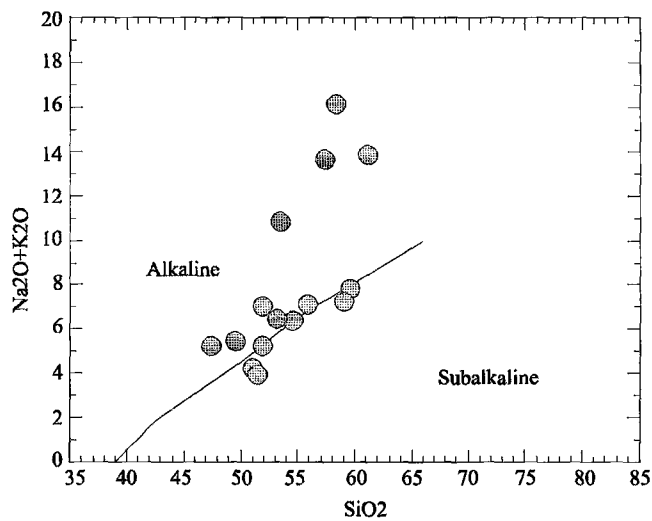


Figure 3. 24. The Chemical Affinity of the Foça Alkaline Volcanics. Samples are Mostly Plotted in Alkaline Area in the Na₂O+K₂O vs SiO₂ Diagram of Irvine & Baragar (1971). The Other Samples Take Place Close to the Separation Line of Alkaline and Subalkaline Areas.

Table 3. 9. Average Major and Trace Element Composition of the Foça Alkaline Volcanics and Some Typical Within Plate Alkaline Rocks

	Average chemical composition of the Foça alkaline volcanics	Average chemical composition of the Foça alkaline lavas except phonilitic components	Average chemical composition of the phonilitic components of the Foça alkaline lavas	Chemical composition of the basanite-phonolite suite of continental rift zone magmatism from Mt Kenya. Price et al. (1985)	Within Plate alkaline basalts. Sun (1980)
SiO ₂	53.57	52.97	58.91	55.74	
Al ₂ O ₃	16.52	15.54	18.89	18.26	
Fe ₂ O ₃ ^T	6.08	6.45	4.57	6.14	
MgO	3.75	4.76	0.32	1.01	
CaO	6.51	7.93	1.31	2.57	
Na ₂ O	4.03	3.28	7.01	8.53	
K ₂ O	3.99	3.05	7.50	4.82	
TiO ₂	0.82	0.95	0.29	0.85	
MnO	0.19	0.218	0.13	0.25	
P ₂ O ₅	0.27	0.31	0.106	0.41	
Nb	27.99	17.82	67.3	145	53
Zr	320.18	226	661.13	545	220
Y	26.27	21.13	44.63	33	30
Sr	477.02	567.12	92.13	881	800
Rb	166.132	117.18	341.56	94	22
Th	22.40	13.84	52.1	15	3.4
Pb	37.59	25.92	65.83	12	
Zn	74.18	66.52	106.13	107	
Cu	30.33	35.12	6.96	11	
Ni	63.54	81.8	5.73	<1	
V	131.9	149.45	124.6	23	
Ba	756.3	803.6	419.9	1324	380
Sc	15.87	19.616	2.5	3	
Ce	114.24	85.06	221.5	167	72
Nd	40.46	32.51	67.5		

CHAPTER FOUR

VOLCANIC FACIES and STRUCTURES

Volcanic terrains consist of a great variety of rock types. They include lavas, explosive pyroclastic deposits, volcanic autoclastic deposits and deposits resulting from the sedimentary processes that operate in volcanic terrains. Early studies on the rock types in volcanic terrains have been roughly dividing the volcanic rocks into lavas and explosively erupted pyroclastics. However, such a subdivision now sounds too simplified, and can be expanded into a more detailed subdivision of lavas, pyroclastics, autoclastic deposits and redeposited volcanic sediments or epiclastics.

Since it is possible to see many different kinds of rock types in volcanic terranes, recognition of the origins of rock types in volcanic terranes, is difficult, and in ancient terranes, additionally, because of the deep alteration, metamorphism or deformation, it is much more complicated to recognize the origin of these rocks.

In field, some physical appearance of different rock types, for example sedimentary structures such as the presence or absence of layering, grading or cross-stratification, may make possible to distinguish them. In some cases, however, an association consisting of two or three different rock types may have distinctive internal depositional structure and a unique field appearance. In this case this unique appearance of this association may distinguish this unit from the others. The term “**facies**” is used for such distinctive intervals or associations of rocks in outcrop. The facies approach is a useful way of identify and describe of distinctive associations. Although the concept is most commonly applied in sedimentology, it is also applicable in volcanic successions, and is even used by metamorphic grades based on significant marker minerals or association of minerals.

In the chapter of “An introduction of facies analyses in volcanic terranes”, Cas and Wright (1982) explain the “facies concept” and need of facies analyses as follows:

...A facies is therefore a body or interval of rock or sediment which has a unique definable character that distinguishes it from other facies, or intervals of rock or sediment. The definable character may be compositional or textural, or may be based on the sedimentary structures or fossils present. A facies is the product of a unique set of conditions in the depositional environment. These conditions may be physical, chemical or biological in origin, and may include such factors as the topography and bathymetry; the mechanisms and rates of material release, transport and deposition; the climate and weather; the nature of the source materials (both chemically and physically); the prevailing chemical condition; and the floral-faunal influences.

A facies can be defined at any scale. At a regional level stratigraphic units such as groups, formations or members are effectively facies because they have an overall lithological character that distinguishes them from other groups, formations or members. At a more local scale, facies may be defined at the scale of an outcrop by an interval of several or more beds, or by both. The degree of detail used in subdividing a stratigraphic succession into facies will largely be controlled by the aims of the study, the information available and the level of the understanding that is sought...

Selley (1978) nominated five facies descriptors:

geometry

lithology

sedimentary structures

paleocurrents or sediment movement patterns

fossils

In the light of the explanations of Cas & Wright (1982), in the following section first the field occurrences and petrographic features of the volcanic facies of the study area will be presented and then the field features of the volcanic vents will be mentioned.

4. 1. FACIES OF YUNTDAĞ VOLCANICS

The Yuntdağ volcanics crop mainly out around Menemen, Aliğa and to the north and northeast, around Çaltılıdere, Şakran and Yuntdağ villages (Ch. 2, Plates 4, 5, 6). In this unit four subunits are distinguished which have been mentioned in Ch. 2. In this succession, 5 main volcanic facies are defined which are 1. Flow banded andesite, 2. Columnar jointed andesite, 3. Flow breccias, 4. Block and ash flow deposits and 5. Grain supported, andesite lava-scoria facies .

4. 1. 1. Flow banded lavas (Facies 1)

Description: The Flow banded lava facies forms thick lava flows of the Helvacı unit and the Çaltılı trachyandesites. This facies is composed of the non-vesicular, pink, gray to black coherent lava flows with well-developed 1 to 10 cm-thick flow banding. Texture is prominently porphyritic with 20-50 % of euhedral to subhedral phenocrysts in glassy to microlitic matrix (Figure 2.3). The detailed mineralogical compositions of units are given in Ch. 2. In microlitic parts of the matrix, trachytic flow texture which is characterized by the elongated microlites, is clear (Figure 2.4). In field exposures, the flow foliation is distinguished by pink and gray coloured lava alternations and transported lava fragments (Figure 2.2). In addition to that, laterally discontinues, wavy banding also characterize the flow foliation.

Interpretation: Flow banded lavas, characterize the coherent facies of the Yuntdağ volcanics which forms the thick lava flows. The prominent porphyritic texture, observed both in the Helvacı andesites and Çaltılı andesites, elongation in microlites in matrix and transported angular lithic fragments in glassy matrix in Helvacı andesites are all indicatives of well developed flow process in coherent lava facies.

4. 1. 2. Subvolcanic andesites (Facies 2)

Description: The Hatundere dykes which correspond the subvolvanic equivalent of the andesitic Yuntdağ volcanics, clearly cut the coherent lava flows of the Helvacı andesites and

blocky pyroclastics. Maximum 2 km-long, radially-organized, planar dykes with high-angle contacts and a small stock characterize the subvolcanic facies. In this facies characteristic textural changes from the periphery of dykes to the centre, from glassy to porphyritic texture, are observed. 2 to 15 cm-wide andesitic inclusions from the andesitic host rock, with resorbed periphery, are also characteristics of these subvolcanic intrusions (Figure 2.14).

Interpretation: Textural changes in the hatundere dykes from the glassy, at the periphery, to the porphyritic texture, at the centre, and their significant high-angled, cross-cutting contacts with lava flows (Figure 2.13) and blocky pyroclastics indicate that they were emplaced after the formation of Helvacı andesites and Haykıran blocky pyroclastics between Helvacı, hatundere and Çukurca villages. Resorbed rims of the andesitic enclaves in the subvolcanic dykes indicate also that they were included by the subvolcanic volcanism in cold state. Semi-radial field occurrence of the Hatundere dykes and subvolcanic stock at the central part of these dykes (Plate 5) show that the area was the centre of the extrusion of the Yuntdağ volcanism. As will be discussed later, this central part was converted to a caldera structure as the volcanism evolved. (For details, see ch. 4. 2. 1).

4. 1. 3. Columnar jointed andesite (Facies 3)

Description: The columnar jointed andesite facies form the dark gray to black, aphanitic lava flows of the Çaltılı andesites interdigiting with the Helvacı andesites in the upper parts around Helvacı and Hatundere villages (Ch. 2, Plate 5). Although petrographically they are andesitic in nature, in all field outcrops they have a basaltic appearance with black colour, aphanitic texture and mafic phenocryst content. The facies shows well developed flow banding which are 1 to 10 cm in thickness in 15 cm to 2 m individual flow units. Aphanitic and fine grained porphyritic textures with 40 % of plagioclase, pyroxene, amphibole, biotite, olivine and sanidine phenocrysts and 60 % of microlitic and glassy matrix, are common in this facies (Figure 4.1). Where matrix is microlitic, flow texture is characterized by the elongated microlites (Figure 4.2). To the north of Aliğa, around Çaltılıdere village this facies is characterized by the prominent columnar jointing of 10 to 40 cm in diameter.

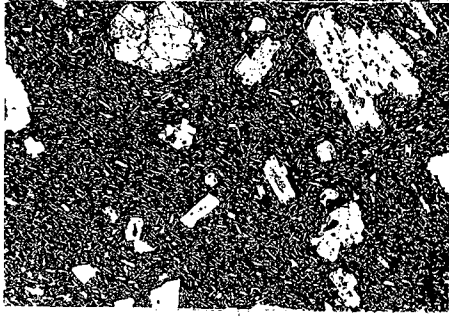


Figure 4. 1 The Typical Porphyritic Texture in the Çaltılı Andesites with Abundant Plagioclase and Pyroxene Phenocrysts in Microlitic Matrix. The Long Side of the photograph is 4.7 mm in Length.

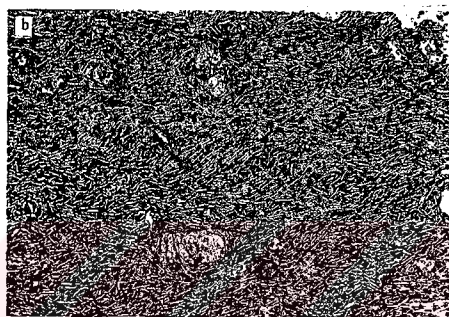
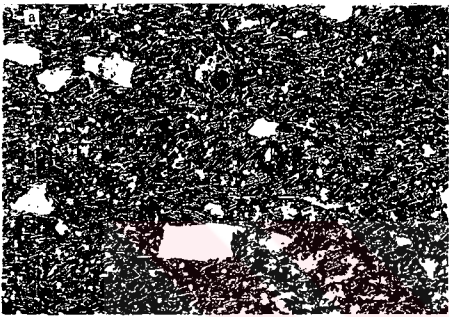


Figure 4. 2 Trachytic Texture in Columnar Jointed Andesites Characterized by the Elongated Microlites in Matrix. **a.** Cross Polarized Light, **b.** Parallel Polarized Light. The Long Side of the Photograph is 3.2 mm in Length.

Interpretation: The columnar jointed andesite facies corresponds the lava flows of the Çaltılı andesite unit. The well-developed trachytic texture both in porphyritic and aphanitic textures characterize the long-ranged flowing process. Columnar jointing which is typical for this facies are interpreted here as the evidence of the long term cooling of lava flows and hence the subaerial environment. Both in the Helvacı and the Çaltılı andesite units, the lacustrine limestone lenses are observed interlayering with the massive lava flow (Ch.2) indicating the presence of the short-term, local and probably shallow lacustrine environments during the effusive volcanism.

4. 1. 4. Flow breccias (Facies 4)

Description: The Flow breccia facies corresponds the autobrecciated andesite lavas of the Helvacı and Çaltılı andesite units. Among Helvacı, Hatundere and Çukurköy villages, accompanying with the lava flows of the Helvacı andesites, the facies have its widest

exposures which are dominated by the porphyritic andesite to dacite lava clasts. Texture is commonly grain supported in which poorly-sorted clasts with jagged ends and of 1 to 10 cm in diameter, are bounded by massive coherent andesitic lava matrix (Figure 4.3). There is no textural change from the centre of clasts to the edge. In some outcrops, matrix / grain ratio is very low where clasts are bounded by another clast and rough jig-saw fit texture is observed indicating relatively short-ranged flowing. The Flow breccia facies passes into the coherent lava flows of the Helvacı andesite unit almost in every outcrop where lower or upper contact is seen. In the Çaltılı andesites, the Flow breccia facies is observed as well accompanying with the coherent lava flows in which gray to black aphanitic, ragged lava clasts supporting the one another.

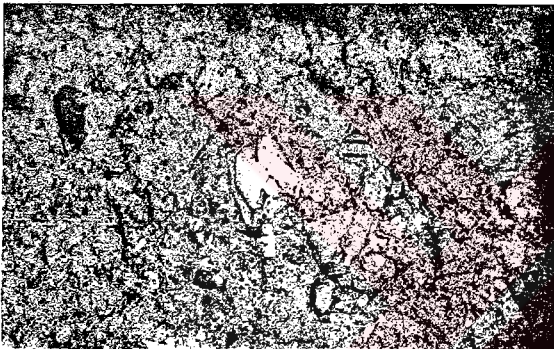


Figure 4. 3 Brecciated Texture, Observed in Flow Breccia Facies Typified by the Angular Clasts Set in a Coherent Lava Matrix.

Interpretation: The Flow breccia facies corresponds the autobrecciated parts of the lava flows. Monolithic clast composition, lava matrix or grain supported texture in which all clasts are fixed to each other and rough jig-saw fit texture and gradational contact with the massive lava flows are indicatives of the autobrecciation during lava flowing. The porphyritic texture, observed entirely in the clasts, and lack of altered or glassy periphery are interpreted as the subaerial environment of autobrecciation. The jagged ends of clasts, poorly-sorted texture and angular morphology of grains indicate the very short-term transportation.

4. 1. 5. Block and Ash flow deposits (Facies 5)

Description: In the Yuntdağ volcanic succession, nearly in all outcrops, thick lava flows of the Helvacı and Çaltılı andesite units are interlayered with the laterally discontinues, coarse grained volcanoclastic deposits which are all named here as the Haykiran blocky pyroclastics (Ch.2). The Block and ash flow facies correspond the volcanoclastic facies of this unit which

is made up of the fine pebble to boulder-size andesitic lava clasts from the Helvacı and Çaltılı andesite units, in fine to medium ash matrix (Figure 4.4).

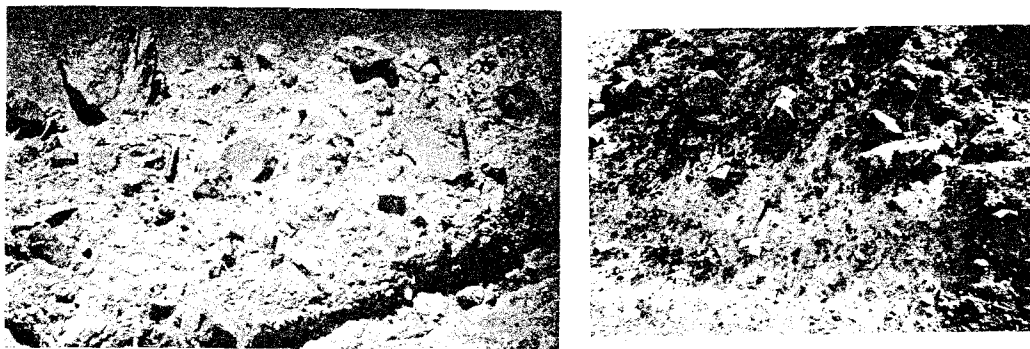


Figure 4. 4 The Block and Ash Flow facies is characterized by the Poorly Sorted Pebble to Boulder Size Lava Clasts Set in Ash-Size Matrix.

Where the lower contact is observed, the block and ash flow deposits are overlain by the coherent lava facies along commonly a rough irregular contact (Figure 4.5). In some outcrops, on the other hand, the dilute, fine ash horizons are observed in the lowermost parts (Figure 2.8). The facies is typically monolithic and made up of pink andesite clasts of the Helvacı unit or gray to black andesite clasts of the Çaltılı unit, depending on the eruption cycle during which the facies were formed. Block and ash flow facies forms typically the topographic

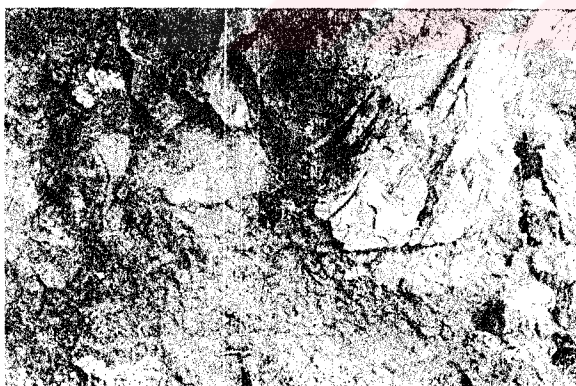


Figure 4. 5 The coherent Andesite Lavas Along an Irregular Contact

levées, include steep flow fronts and have the large surface blocks. Poorly-rounded and sorted coherent lava grains typically show porphyritic texture with plagioclase, biotite and amphibole phenocrysts of 2 to 7 mm, in pink to gray-dark gray matrices. No textural change in clasts from centre to the periphery, is observed, nor the significant alteration. These angular

to poorly-rounded clasts are set in white to yellow, partly altered ash matrix which is made mainly up of the pumice, crystal and lithic fragments. Texture is matrix supported in all outcrops. Rough bedding is the unique sedimentary structure, observed in places in this facies (Figure 4.6). In the most parts, the block and ash flow facies show unorganized internal structure except rare normal grading within individual flow units (Figure 4.6). Coherent lava flows of the Helvacı and Çaltılı units interlayering with the block and ash flow facies are found in some exposures (Figure 4.7).



Figure 4. 6 Poorly Developed Bedding is the Unique Sedimentary Structure, Observed in the Block and Ash Flow facies

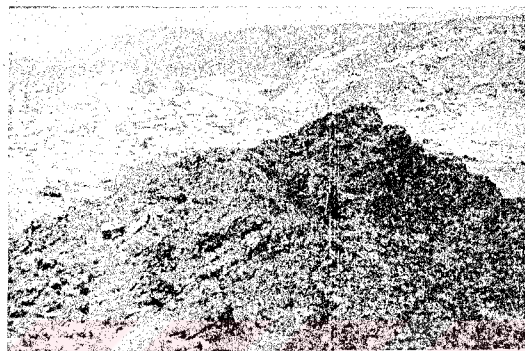


Figure 4. 7 Coherent Lava Flows Interlayering with the Thick Block and Ash Flow deposits.

Interpretation: “Block and ash flow deposits” term was defined by Cas and Wright (1987) as the topographically controlled unsorted pyroclastic flow deposits having an ash matrix and containing large, non-vesicular, cognate lithic fragments. In addition to the field features, the textural features of the block and ash flow facies, defined here, fit their definition. The authors also noted that, homogenous clast composition, hot blocks and gas segregation pipes are the field criteria to distinguish the pyroclastic block and ash flow deposits from types of sedimentary debris flow deposits. In addition to the field features, the matrix supported texture, pebble to boulder-size, poorly-sorted and angular clasts, fine ash matrix, unorganized internal structure and lacking of sedimentary structures of the block and ash flow facies of this study, reflect the typical textural features of the debris flow deposits (McPhie, Doyle and Allen, 1993). However, in this case, although there is no gas segregation pipes and significant data showing hot emplacement, clasts are clearly juvenile and monolithic composition is

characteristic. So that, the facies is interpreted as the pyroclastic block and ash flow facies generated by the explosive cycles of the volcanism and inbetween coherent lava flow cycles.

Textural features of the block and ash flow facies make deposits resemble also to the lahars. Fischer (1984) defines lahars as rapid, water-supported flows of volcanoclastic particles generated on volcanoes and Smith and Lowe (1991) suggest that, in many cases, they move partly or entirely as debris flows and their deposits show the characteristics of the debris flow deposits. However, there is no significant data showing that the block and ash flow facies of the Yuntdağ volcanism was water-supported, and that they are resedimented volcanoclastic facies in which case, heterolithic composition, relatively well-sorted texture, relatively well-rounded clasts are expected.

Finally, McPhie et al. (1993) noted that, in ancient sequences, it is difficult to establish a primary origin for poorly sorted, ungraded, pyroclast-rich, monomict mass-flow deposits that lack evidence of hot emplacement. However, the volcanoclastic rocks observed interdigitating with coherent lava flows of the Helvacı and Çaltılı units, and comprising monolithic, poorly-sorted, porphyritic andesite blocks in white to pale green ash matrix are interpreted here as the pyroclastic block and ash flow facies.

4. 1. 6. Grain supported, andesite lava-scoria facies (Facies 6)

Description: Between Helvacı, Hatundere and Çukurköy villages, close to the one of the central vents of the Yuntdağ volcanics which will be detaily defined in the next section, in local paleovalleys, highly grain-concantrated, pyroclastic flow units crop out. These paleovalley-fill volcanoclastic rocks are characterized by crude bedding with dip of 20-30⁰ (Figure 4.8). The thickness of beds vary from 30 to 50 cm. Poorly-developed reverse grading is the most typical textural feature observed in individual beds. Coarse lapilli to cobble-size clasts are composed mainly by the highly vesicular scoria and coherent andesite lava clasts of the Helvacı unit. Poorly sorted texture is clear. Angular to subrounded clasts are generally welded indicating hot emplacement. Matrix/grain ratio is significantly low so that

grains are supported by other grains. The matrix is made up of coherent lava or fine ash. In flow front, plastically deformed and overturned, foliated lava flow planes are observed (Figure 4.8). The total thickness of facies reaches up to 8 m.

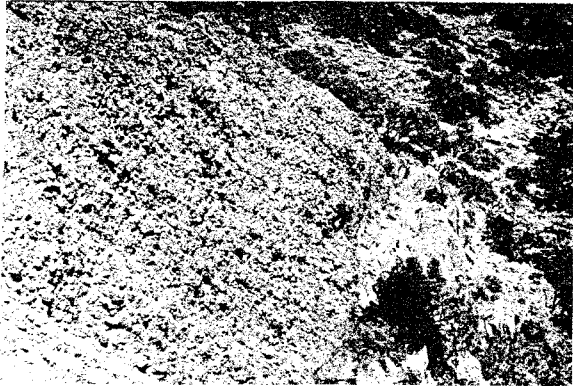


Figure 4. 8 Field Photograph Showing the Grain Flow Deposits with Poorly Developed Bedding of 20-30°. Note the Steepened Lava Flows in Flow-Head.

Interpretation: The grain supported andesite scoria facies is characterized mainly by the bedded, poorly sorted and typically grain supported andesite scoria and coherent lava clasts. The welded boundaries between the clasts indicate hot stage emplacement and hence a pyroclastic origin. The facies is observed on the inward edges of one of the probable central vents of the Yuntdağ volcanics (Section 4. 2). The textural features, such as poorly-developed sorting, angular to subrounded grain shape, grain supported texture, reverse grading, are those of defined for the grain flow deposits (McPhie et al., 1993; Cas & Wright, 1987). Abundant scoria content of the facies indicate the explosive nature of the volcanism. In the light of these observations, the grain supported andesite scoria facies should have been formed by the inward pyroclastic grain flows along edges of the central vents during the explosive Yuntdağ volcanism.

4. 2. MORPHOLOGY AND VOLCANIC STRUCTURES IN YUNTDAĞ VOLCANISM

In the large areas among Menemen, Aliğa, Yuntdağ and Osmançalı (Plates...), depending on the paleotopography, the long-ranged coherent lava flows and pyroclastic flow deposits of the Yuntdağ volcanics are observed as horizontally to 20-35° dipped planar flows. All around this area, the Yuntdağ volcanics are dominated mainly by the coherent lava flows of the Helvacı and Çaltılı units. The volcanoclastic equivalents of the same volcanism interfingers with these lava flows as relatively short-ranged and laterally discontinuous pyroclastic flow units. In the study area, two different central vents of the Yuntdağ volcanism are distinguished

which can be defined by their significant morphologies, alterations and volcanic features. These volcanic centres are **1. The Dumanlıdağ caldera** and **2. The Yuntdağ caldera**. The Dumanlıdağ caldera can be distinguished by its significant volcanic structures and morphology. The Yuntdağ caldera, on the other hand, is deeply eroded and it is defined only by its deeply altered lithology and less prominent surface features.

4. 2. 1. Dumanlıdağ caldera

The Dumanlıdağ volcanic cone and caldera were first defined geomorphologically by Ögdüm (1983). He stated in this study, that the Dumanlıdağ caldera has been originated as a volcanic cone in Late Miocene and then collapsed and turned into a caldera form in Pliocene. The Dumanlıdağ caldera is located between Helvacı, Hatundere and Çukurköy villages (Plate 5, Figure 4.9). In this area, coherent lava flows of the Helvacı andesites and the block and ash flow deposits of the Haykırın blocky pyroclastic unit dominate the rock association and Dumanlıtepe dykes form the other common rock type cropping out in the central parts of the caldera. The Dumanlıdağ caldera is characterized by the circular-semicircular low topographic depression distinguished by both the circular map view of strikes of the flow foliation planes (Plate 4, Figure 4.9) and field view. The caldera is approximately 6 km in radius. In the north edge, a steep caldera wall is characteristic along which pinky andesitic lava flows and interdigitating block and ash flow deposits, dip outward. In the eastern edge, on the other hand, around Dumanlıtepe, in addition to the outward dipping of the flow foliation planes, high angle, circular boundary fault of the caldera and inward dipped block and ash flow deposits on the footwall of the fault characterize the Dumanlıdağ caldera. In the southern edge, similar to the eastern part, two high-angle faults with 70 to 80° dips, control the caldera formation and along this edge, lava flows and volcanoclastic deposits dipped to the south, toward the Menemen Plain, are clearly observed around Ballık and Keklikkaya Hills. In the central part of the Dumanlıdağ caldera, the most typical volcanic structures are the semi-radial dykes and a subvolcanic stock of andesite composition which cut both the coherent lava flows of the Helvacı and Çaltılı andesites and the volcanoclastic deposits of the Haykırın blocky pyroclastics unit (Figures 2.13,15). Probably because of the shallow erosion, alteration is not a prominent feature for the Dumanlıdağ caldera. Argilic alteration in fine ash horizons interlayering the lava flows and feldspar phenocrysts in coherent lavas, and Fe-

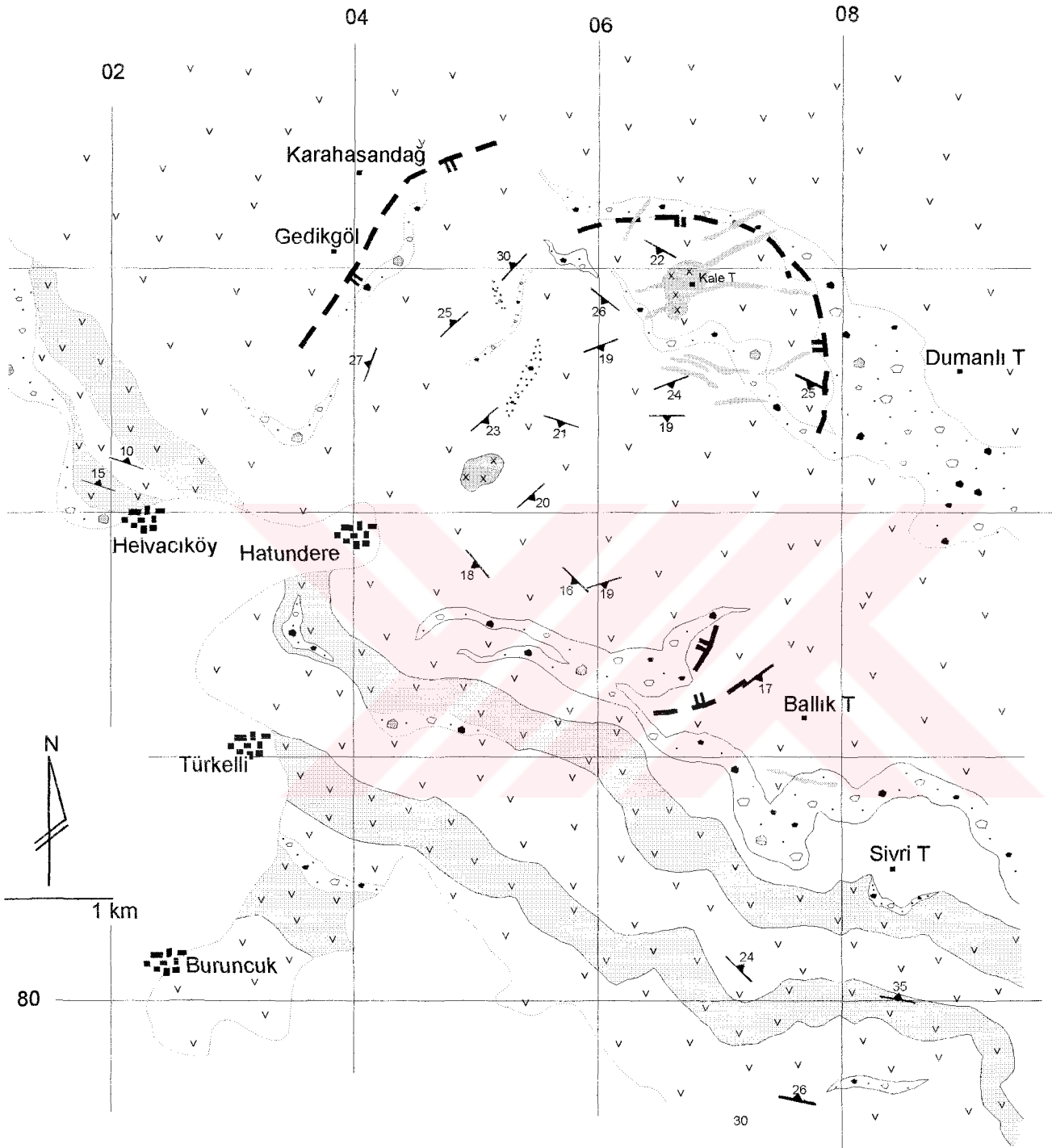


Figure 4. 9 Detailed Geological Map of the Dumanlıdağ Caldera. For Explanations, See Plate 7

oxidization are the most common alteration types observed in the central parts of the caldera. Chemical and petrographical composition of the lava and subvolcanic phases of this volcanism show close similarity indicating that the different volcanic phases were generated from the same magma (Chs. 2, 3).

Along the outer slopes of Dumanlıdağ caldera, in the wide areas, the coherent lava flows of the Helvacı and Çaltılı andesites and the volcanoclastic rocks of the Haykırın pyroclastics unit show generally low-dipped and/or horizontal morphology depending on the paleotopography. In these areas, coherent lavas form the topographic highs and the volcanoclastic parts correspond the lowlands.

4. 2. 2. Yuntdağ caldera

The Yuntdağ caldera is located 5 km to the south of Yuntdağ town (Plate...), and form the second prominent vent of the Yuntdağ volcanism. In this area, contrary to the Dumanlıdağ caldera the boundary faults and radial subvolcanic equivalents of the volcanism are not well-preserved because of deep erosion. The concave morphology, on the other hand, can still be distinguished (Figure 4.9). The most distinct surface feature of the deeply eroded caldera is the presence of intense alteration observed in rock associations in the central part of the area (Figure 4.10). The map view of the alteration zone is circular in form with an approximate diameter of 4 km. Originally pink to gray lavas and volcanoclastics were altered to white, greenish white, green and red altered volcanics. The alteration is argillic in nature and strong chloritization in the mafic minerals, Fe-oxidization and clay-rich alteration are common. Besides that, sulfur-rich springs had caused yellowish color in outcrops. In the Yuntdağ caldera and the adjacent areas, the Yuntdağ volcanics are represented dominantly by fresh lava flows of the Helvacı andesites which are intercalated with the black lava flows of the Çaltılı andesites and the Haykırın blocky pyroclastics. In the caldera center and around, the aphanitic dark lavas of the Çaltılı andesites show distinct concoidally weathered surfaces which form the sphere-like surface view for this unit. Generally horizontal or low-dipped flow foliations in lava flows and beddings in volcanoclastics, become more steeply dipped outward the caldera and reach 30° dips at the periphery.



Figure 4. 10 The Central Parts of the Yuntdağ Caldera. The Concave Morphology is Significant. Altered Central Part is Exposed Because of the Deep Erosion.

4. 3. FACIES OF THE FOÇA VOLCANIC COMPLEX

In an area covering Yeni Foca, Eski Foça and Bağarası towns (Plate 1), the Foca volcanic complex forms extensive outcrops and consists dominantly of felsic volcanoclastic rocks. Three rhyolite dome structures are present in this area (Figure 2.17). The Yeni Foca dome is about 500 m in diameter and circular in map form. The north and northeastern parts of the dome and associated volcanoclastic rocks are covered with the sea (Figure 2.17). The Bağarası rhyolite, on the other hand, covered by a younger alkaline lava flows of the Foça alkaline volcanics unit and only the internal parts of the massive rhyolite facies are observed (Figure 2.17). In this area two different rhyolite lava flow units are observed indicating the progressive extrusion phases. The Eski Foça composite dome is much larger in areal extent and consists of a center where rhyolitic magma poured upward to the surface from three local areas. The western and northwestern parts of this dome pass into the related volcanoclastic facies and form open outcrops to observe the internal and lateral variations of the massive rhyolites and volcanoclastic sequence. The strikes of the blanketing volcanoclastic sequences are also circular around the rhyolite domes and dip outward with an angles of 15 to 25 degrees (Figure 2.17). These dome-shaped outward dipping volcanoclastic covers are common around the Eski Foca and Yeni Foca domes.

The characteristics of the Eski Foca composite dome as viewed from three different areas, are presented in the following section. One of these areas contains a small dome located in the central part of the composite dome and is shown in figure 4.11. The second area is also located in the central part of the dome, along a section between Eski Foca and Bağarası towns (Figure 2.31) where a massive dome and covering volcanoclastic series are observed. The

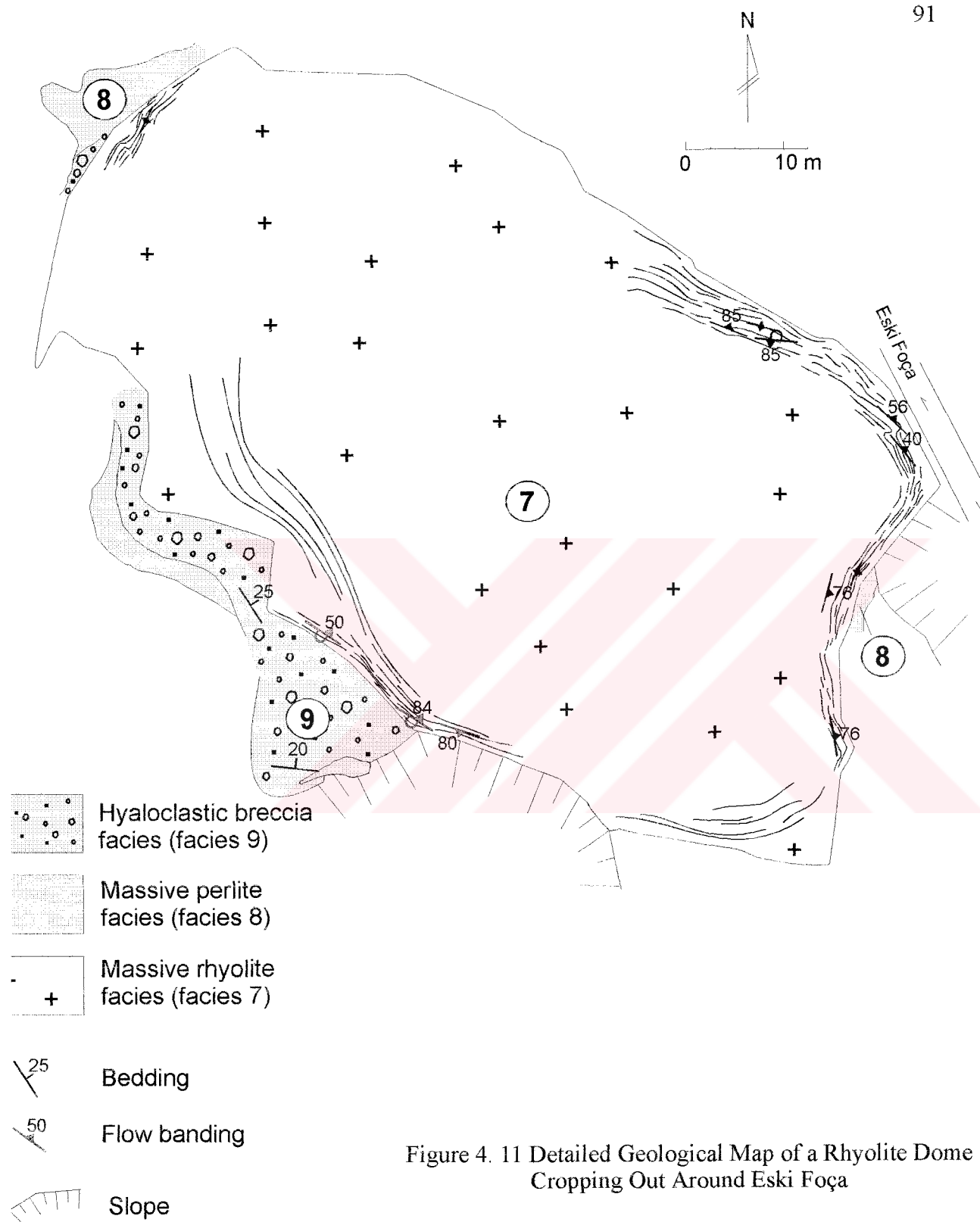


Figure 4. 11 Detailed Geological Map of a Rhyolite Dome Cropping Out Around Eski Foça

third area is located at the periphery of the dome and underlain only by pyroclastic facies. Along two measured sections (Figure 2.39), peripheral pyroclastic facies are described. In these three areas 12 different volcanic facies are differentiated which are shown by numbers 6 to 17 on the related maps and cross sections. The Massive rhyolites facies of this sequence corresponds the Foça rhyolites subunit of the Foça volcanic complex the Coherent alkaline lava facies (Facies 17) corresponds the Foça alkaline volcanics subunit and the rest corresponds the Foça volcanoclastics subunit of the Foça volcanic complex (Ch. 2). The Massive perlites facies corresponds the Perlites unit, distinguished in the Foça volcanoclastics subunit and the other facies correspond the Pyroclastic flows unit of the Foça volcanoclastics (Ch. 2).

4. 3. 1. Eski Foça Area

The first area is a small oval-shaped dome with a diameter of about 100 m and located to the 2 km southeast of Eski Foca town (Figure 2.17 and 4.10). From the center to the periphery of the circular dome 3 different facies are observed.

4. 3. 1. 1. Massive rhyolites (Facies 7)

Description: Massive rhyolite facies form the dome-shaped rhyolite intrusion in the Eski Foça Area (Figures 2.28 and 4.12) the central part of which is composed of porphyritic massive rhyolites. The porphyritic rhyolites are composed of about 20 % phenocrysts of euhedral and embayed quartz and K-feldspar (Figure 4.13). The average length of the phenocrysts is about 2 mm and they are set in a devitrified and recrystallized granophyric aggregate (Figures 2.24 and 4.14.). This granophyric and crystallized matrix, in places, is grown into the phenocrysts (Figure 2.23). The internal part of the core is massive but along the periphery well developed flow foliation is observed (Figure 4.15). The strikes of the flow foliations surround the periphery of the massive rhyolite core and their dips are generally outward with 56 to 85 degrees (Figure 4.11). In some places the foliations are vertically inclined, and along the southwestern edge of the dome they are overturned and dip 50 degrees towards the center (Figure 4.11). Along this boundary, the pyroclastic sequence also displays

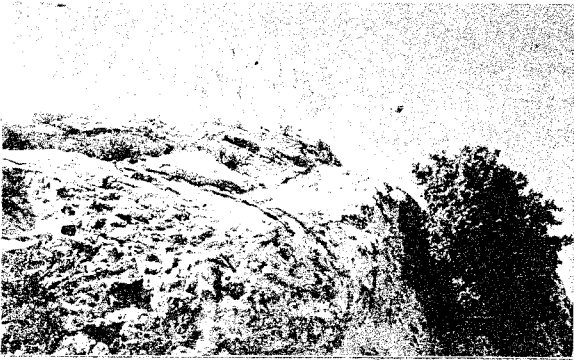


Figure 4. 12 The Steeply Dipped Periphery of the Dome-Shape Rhyolite Intrusion



Figure 4. 13 In the Central Parts of Domes, Porphyritic Texture with Quartz and Feldspar Phenocrysts, Set in a Recrystallized and Partly Devitrified Matrix, is Characteristic. Arrow Show the Embayed Feldspar Phenocryst. **a.** Cross Polirized Light, **b.** Parallel Polirized Light. The Long Side of the Photograph is 7 mm in Length.

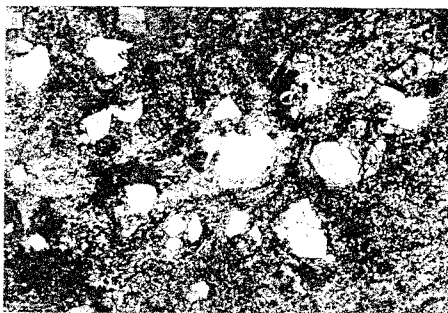


Figure 4. 14 Photomicrograph Showing the Porphyritic Texture in Massive Rhyolite Facies with Recrystallized Glassy Matrix. Flow Lamination in Matrix is Characteristic. **a.** Cross Polirized Light, **b.** Parallel Polirized Light. The Long Side of the Photograph is 5.6 mm in Length.

inward dip suggesting continuous updoming of the core and overturning of one side of the dome during the emplacement (Figure 4.16).



Figure 4. 15 Well-Developed Flow Lamination at the Periphery of Rhyolite Dome.



Figure 4. 16 During the Intrusion, Due to the Progressive Updoming, the Hosting Massive Perlites and Hyaloclastic Breccias Displays Inward Dips.

In the geological map of the area (Figure 2.17) the pyroclastic sequences have an average dip of 10 to 25 degrees around Eski Foça town. Only around and at the periphery of the rhyolite domes, higher dip angles of pyroclastic rocks and flow foliations are observed. Along the periphery and within the flow foliated zone of the dome in figure 4.11, the texture of the massive rhyolite facies is very fine grained and glassy. The origin of these glassy flow foliations will be discussed below.

Interpretation: The massive rhyolite facies characterize coherent lava intrusions or short-ranged rhyolite lava flows in the Foça volcanic complex. The relatively coarse-grained, porphyritic texture, in the central parts, indicate the relatively slow cooling and the glassy texture in the periphery, is caused by the rapid cooling because of the interaction with the cold

host rock and because of the intrusion into the shallow water environment. Within the surrounding cold environment, felsic magma cooled fast and an envelope of glassy textured massive rhyolites formed. Additional input of magma caused onion-like glassy envelopes around the core of the dome, so that the flow banded structures were developed at the periphery. The repeated flow bands were formed by the successive emplacement of magma in the central part of the dome. So that, the term of the “flow banding” in our usage implies both viscous magma flow and planar structures resulted from the successive cooling of magma at the periphery. Both the oval map view of the rhyolite body and the circular strikes of the flow foliation planes at the periphery indicate a dome-shaped emplacement.

4. 3. 1. 2. Massive perlites (Facies 8)

Description: In the eastern and northwestern parts of the dome (Figure 4.11), the massive rhyolite facies pass into the massive perlite facies which surrounds the dome in a circular to semicircular form (Figures 2.28 and 4.11). The maximum thickness of this zone is 5 m in the northwestern part of the dome. The massive perlites are grey to white in colour with glassy and conchoidally-fractured texture in the field. In the glassy parts, plastically deformed flow lamination is common (Figure 4.17). The perlitic texture is especially pronounced in thin sections (Figure 4.18). The contact of the massive rhyolite and massive perlite facies are typically diffuse.

Interpretation: The semicircular form of the perlite zone, surrounding the massive rhyolite body, and diffuse boundary relation with the massive rhyolite facies indicate that, massive perlites were formed by the hydration of the rhyolite body in a water-rich environment.

4. 3. 1. 3. Reassembled hyaloclastic breccias (Facies 9)

Description: Along the southwestern margin of the dome in figure 4.11, a breccia zone of 10 to 15 m in thickness surrounds the internally foliated massive rhyolite facies. This breccia zone is massive in appearance or in places, very crudely stratified (Figure 2.44) and consists



Figure 4. 17 Plastically Deformed Flow Lamination in Massive Perlite Facies

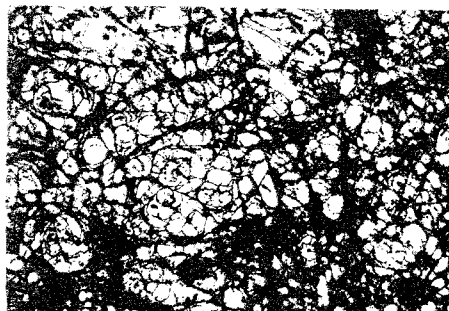


Figure 4. 18 Photomicrograph Showing the Perlitic Texture in Massive perlites. The Long Side of the Phtograph is 4 mm in Length

of poorly sorted and completely angular, coarse ash to cobble-sized clasts of massive rhyolite, flow-laminated rhyolite, massive perlite and some pumice clasts (Figure 4.19). Rims of the entire clasts are delicately surrounded by green alteration zones and these alteration rims pass into a greenish-white fine ash matrix imperceptively (Figure 4.19). The thickness of this facies varies laterally and change in short distances. The reassembled hyaloclastic breccias thin out and laterally pass into the massive perlite facies in the southwestern part of the body (Figure 4.11). Along the southwestern edge of the dome this zone is in direct contact with the massive rhyolite facies (Facies 7) and overlain by the massive perlite facies (Facies 8) (Figures 2.44 and 4.11). In some parts of the area where this zone overlays the massive perlite, the reassembled hyaloclastic breccias are interlayered with the massive perlite intercalations and the clast composition is predominantly glassy perlites with rare rhyolite particles (Figure 4.20). In rare side-by-side located angular clasts, the edges are observed to fit each other like in jig-saw-puzzle suggesting in-situ shattering and fragmentation. The strikes of the hyaloclastites are generally parallel to the flow foliation of the massive rhyolite facies and in the western side of the dome the reassembled hyaloclastic breccias are in places overturned and have inward dip about 50° (Figures 4.12,17).

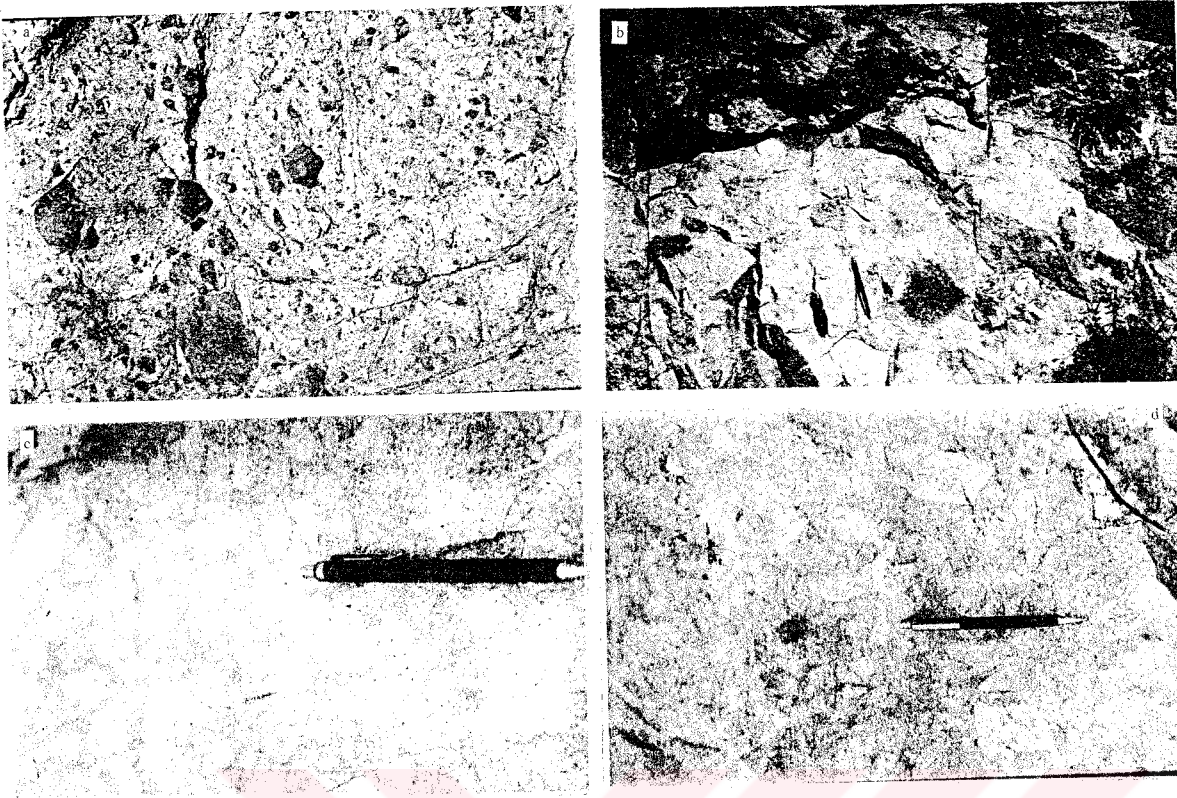


Figure 4. 19 Field Photographs Showing the Reassembled Hyaloclastic Breccias. **a.** Rhyolite and Perlie Fragments in Altered Fine Ash Matrix, **b.** Green Altered Rims of Grains Characterize the Subaqueous Brecciation and Alteration, **c.** Rhyolite Breccias, Set in a Partly Perlitized Matrix and **d.** Rhyolite Breccias in Green Altered Ash Matrix.

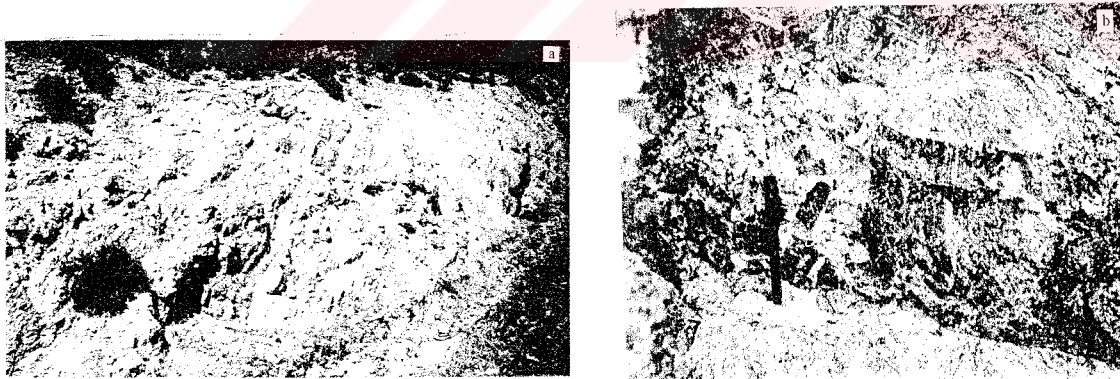


Figure 4. 20 **a.** Massive perlites Interlayering with the Reassembled Hyaloclastic Breccias, **b.** At the Contact Between Massive Perlites and the Reassembled Hyaloclastic Breccias, the Latter Becomes Richer in Perlitic Breccias.

Interpretation: The reassembled hyaloclastic breccia facies correspond to directly sedimented explosively brecciated clasts around the rhyolite domes. Very angular clast content, poorly developed sorting, juvenile nature of the all components and crude bedding show that this sedimentation was short-ranged and developed as a proximal pyroclastic flow. Juvenile pumice fragments, as clast and in matrix, indicate an explosive activity. Lateral graduation into the perlite horizons, alteration rims surrounding the coherent clasts and in matrix show that the reassembled hyaloclastic facies was formed cogenetically with perlites.

4. 3. 2. Eski Foça-Bağarası Area

This area is located in the central part of the Eski Foca composite dome, and is observed along the road-cut between Eski Foca and Bagarasi towns. This road-cut is 2 km from the town of Eski Foca and displays the massive rhyolite and interrelated volcanoclastic facies (Figure 2.31).

4. 3. 1. 1. Massive rhyolites (Facies 7)

4. 3. 2. 2. In-situ brecciated hyaloclastites (Facies 10)

Description: The Massive rhyolites facies is observed in several individual domes and dykes cutting the massive rhyolite bodies and the accompanying volcanoclastic sequence (Figures 2.26 and 4.21). In the massive rhyolites, changes from the porphyritic to glassy texture, from centre to the periphery is characteristic. Steeply dipped flow foliations surrounding the massive body, are also significant in this area. In the central parts, texture is porphyritic with about 20 % of euhedral to subhedral, embayed quartz and K-feldspar in glassy matrix. At the periphery, on the other hand, glassy texture with well-developed flow foliations (See section 4. 3. 1.1) are dominant. On both sides, the massive rhyolites gradually pass in to 1-2 m-thick monomictic in situ brecciated hyaloclastites which are characterized by the quench-fragmented, glassy rhyolite and rare perlite breccias in a coherent glassy groundmass (Figure 4.22). The most typical feature of the in situ hyaloclastic breccias is the jigsaw-fit texture, distinguished by the unmodified, angular clasts fitting each other side by side without reworking (Figure 4.22a,c). Grain size in the in situ hyaloclastic breccia zone

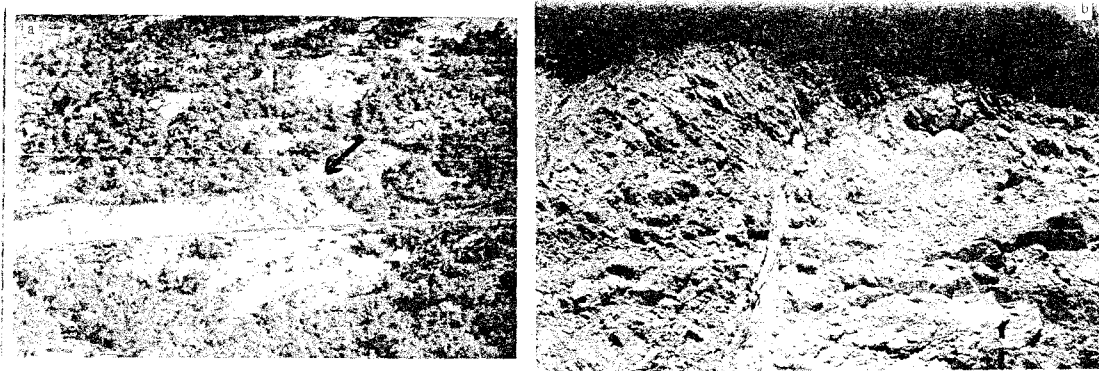


Figure 4. 21 The Massive Rhyolite Bodies Around Eski Foça. **a.** Rhyolite Dyke Cutting the Accompanying Pyroclastic Sequence, Arrow Show the Rhyolite Dyke, **b.** Rhyolite Dyke Intruded into Another Rhyolite Dome

varies from 0.5 up to 2 cm. Massive rhyolites and the surrounding in-situ brecciated hyaloclastites are covered in both sides by the massive perlites and the reassembled hyaloclastic breccia facies.

Interpretation: The steeply dipped contacts and flow foliations surrounding the massive core, porphyritic texture in the centre and the glassy texture at the periphery indicate a dome-shaped intrusive emplacement of the rhyolite body. Although there are several individual massive bodies, their similar petrological features (Chs. 2 and 3) suggest that the rhyolite bodies intruded as a composite dome. The in situ brecciated hyaloclastites surrounding the bodies and perlite clasts in this facies suggest that the rhyolitic magma intruded into a subaqueous environment which caused the quenched fragmentation and shattering without any reworking.

4. 3. 2. 3. Massive perlites (Facies 8)

Description: On the both sides of the, massive rhyolitic dome, there is a 20 m-thick perlitic cover zone (Figure 2.26). Gray-white coloured perlitic rocks have significant concoidal perlitic texture (Figure 4.18). The boundary between the massive perlite zone and the massive rhyolite body is gradational in this area. In the western part of the rhyolite dome, the perlite zone is interbedded with the lenses of accompanying reassembled hyaloclastic breccia facies.

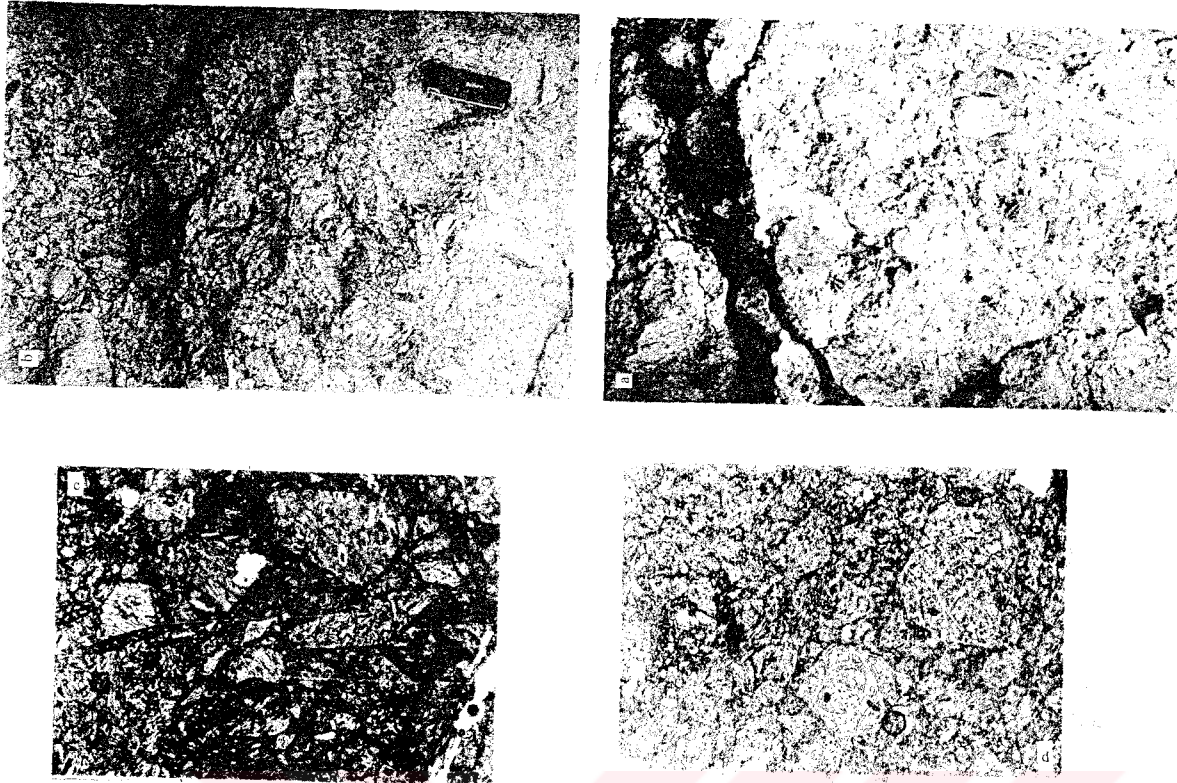


Figure 4. 22 In Situ Brecciated Hyaloclastites. **a.** Coherent Rhyolite Breccias, Set in a Coherent Matrix. Note the Jig-Saw Fit Texture, Characterized by the Angular Grains Fitting Each Other Side by Side, **b.** Coherent Nature of Both Breccias and Matrix is Characteristic for In Situ Brecciated Hyaloclastites, **c.** Photomicrograph Showing the Rhyolitic Nature of Breccias and Matrix and Jig-Saw Fit Texture, **d.** Perlitic Breccias are Also found in In Situ Brecciated Hyaloclastites. For Photomicrographs, the Long Side Of the Photograph is 5.5 mm in Length

Interpretation: Massive perlitic zones on both margins of the rhyolite dome indicate a diffuse hydration of coherent rhyolite lava. in a subaqueous environment. The perlitic fragments, observed in the in situ hyaloclastic breccia facies (Figure 4.22d), suggesting that the quenched fragmentation in the coherent lavas and the perlitization occurred simultaneously.

4. 3. 2. 4. Reassembled hyaloclastic breccias (Facies 9)

Description: Poorly sorted lapilli-size perlite, rhyolitic lava and pumice grains with high particulate concentrate texture of about 30-50 % grains in white to green, ash matrix characterize the reassembled hyaloclastic breccia facies in this area (Figures 2.34,44 and

4.19). Crude bedding and grading are the main sedimentary structures, observed in the field exposures (Figure 2.34). Altered margins in grains and matrix is the most significant feature for this facies (Figure 2.34a and 4.19). Where the reassembled hyaloclastic breccias overlie the massive perlites, boundary between these two facies is gradational which is characterized by the perlitic interlayers in reassembled hyaloclastites and increasing in the number of perlite clasts in them (Figure 2.35 and 4.20a,b).

Interpretation: Altered rims of the clasts and sericitic and chloritic intense alteration both in the clasts and matrix are pronounced in this facies. The sedimentary structures like bedding and grading and scoured lower boundaries suggest the flow mechanism and the high particulate concentration and the composition of the clasts indicate the generation by pyroclastic flow mechanism. Because of the deep alteration, the resultant rock is green in colour (Figure 4.19d) and very similar to palagonite tuffs that are defined for basaltic glass in ash deposits, formed in wet and hot conditions (Heiken & Wohletz, 1985; Jakobsson & Moore, 1980; Farrand & Singer, 1992). The subaqueous debris flow deposits of this rhyolitic sequence are similar to palagonite tuffs and have massive lava and glass grains with altered rims consisting of an aggregate of chlorite and sericite. The same alteration is also observed in the matrix (Figure 4.19). The gradual changes from the massive rhyolite dome to massive perlites and also thin brecciated and intensely altered facies indicate close affinity of their formations. Overturned and inward dipped bedding in nearvents indicate the progressive rising of the rhyolitic magma and accompanying updoming.

4. 3. 2. 5. Laminated mudstone (Facies 11)

Description: 20 cm to 3 m-thick, thinly laminated green and yellowish green mudstone-shale horizons are found in this sequence as lenses and interlayers. The laminated mudstones interlayer with the reassembled hyaloclastic breccias and small mud dykes are observed in the boundary zone, intruded into the overlying clastic sequence (Figures 2.32,37 and 4.23).

Interpretation: The finely laminated mudstone horizons interlayer with the Foça volcanoclastic sequence and they formed together in the same environment. Fine lamination, lateral continuity of individual laminae, and up to 3 m-thick and laterally continuous horizons indicate low energy lacustrine environment of deposition.



Figure 4. 23 Lacustrine Volcanic Mudstone Interlayers Observed in Reassembled Hyaloclastic Breccias

4. 3. 2. 6. Fine grained rhyolite pumice-lithic fragment facies (Facies 12)

Description: The fine grained rhyolite pumice-lithic fragment facies is about 3 m thick and overlies the reassembled hyaloclastic breccias and laminated mudstones (Figure 2.37). In this volcanoclastic facies crude bedding is observed with individual bed thickness of 15-30 cm. Poorly sorted and angular to subrounded polymictic particules indicating abrasion in a flow environment, include variety of textures even in a single outcrop, and are set in an ash matrix which ranges from tuffaceous to volcanigenic sandstones and mudstones. The main components are pumice, rhyolitic lava fragments, perlitic clasts and rare mafic lava clasts. Graded bedding is observed in this facies (Figure 4.24). The maximum grain size is 2 cm in the lower part and 0.5 cm in the upper part.



Figure 4. 24 Normal Grading in Fine Grained Rhyolite Pumice-Lithic Fragment Facies. Arrow Shows the Fining Direction in Grain Size. A New Flow Unit of Coarse Grained Rhyolite Pumice-Lithic Fragment Facies Overlie the Former One Along a Sharp but Irregular Contact.

Interpretation: The high particule concentrated matrix supported texture, sedimentary structures like grading and diffuse bedding and irregular to scoured lower boundary of the facies indicate a pyroclastic flow origin of it. Since the massive lava flow continued to rise, on the updomed areas, stability of the formerly deposited unconsolidated wet material should have been disturbed and started to flow down on to flanks of the eruption centre. As clearly indicated by the lacustrine mudstone intervals and the other subaqueous facies properties, mentioned above, this facies is interpreted as a subaqueous volcanoclastic debris flow deposits.

4. 3. 2. 7. Coarse grained rhyolite pumice-lithic fragment facies (Facies 13)

Description: The fine grained rhyolite pumice-lithic fragment facies is overlain by the coarse grained equivalents of itself along a scoured lower boundary (Figures 2.36 and 4.25). Lithologic features and the sedimentary structures of the facies are nearly the same with the fine grained rhyolite pumice-lithic fragment facies. Normal grading and diffuse bedding, about 20-50 cm in thickness, are clear. The average grain size significantly different between these two facies. The maximum grain size in coarse grained rhyolite pumice-lithic fragment facies is about 10 cm in the lower parts and 5 cm in the upper parts. Along the truncated lower boundary, the coarse grained facies cut the underlying fine grained facies and lacustrine mudstones (Figure 2.31.).

Figure 4. 25 The Irregular, Scoured Lower Contact of the Coarse Grained Rhyolite Pumice-Lithic Fragment Facies.

Interpretation: The coarse grained rhyolite pumice-lithic fragment facies is interpreted to be deposited by sublacustrine debris flow which were triggered by the disturbing of the stability in the flanks because of the rising rhyolitic dome.

4. 3. 2. 8. Lithic fragment-rich channel-fill facies (Facies 14)

Description: In the upper parts of the volcanoclastic sequence around the Eski Foça composite dome, the Foça volcanoclastic sequence become coarser grained and richer in lithic fragments (Figure 4.26a). In this area, the coarse grained lithic fragment-rich channel fill facies, interlayering with fine ash horizons with distinctly scoured basal boundaries, characterizes the Foça volcanoclastics (Figure 4.26). The facies is typified by the coarse ash to cobble-sized lithic fragments and volcanic glass (Figure 4.26a). Poorly sorted grains are characteristically angular. High grain concentration is the most distinguishable field feature of the facies. Grain supported texture is dominant. Where matrix supported texture is observed, matrix/grain ratio is significantly low and white, fine ash matrix is rich in altered pumice and glass clasts. Crudely reverse-graded beds generally have 20-30° dips (Figure 4.26c).

Interpretation: The textural properties of the lithic fragment-rich channel-fill facies such as poorly developed sorting of angular clasts, grain supported texture, reverse grading in slightly dipped bedding and significantly scoured lower boundaries suggest that they were formed by short-ranged debris flows developed on the updomed areas caused by the explosive and gravitational instability of formerly extruded material or material derived from the explosive column collapse. Steep sides of scoured channels and chaotic internal arrangement of blocks and matrix suggest subaerial extrusion and flowing of this facies.

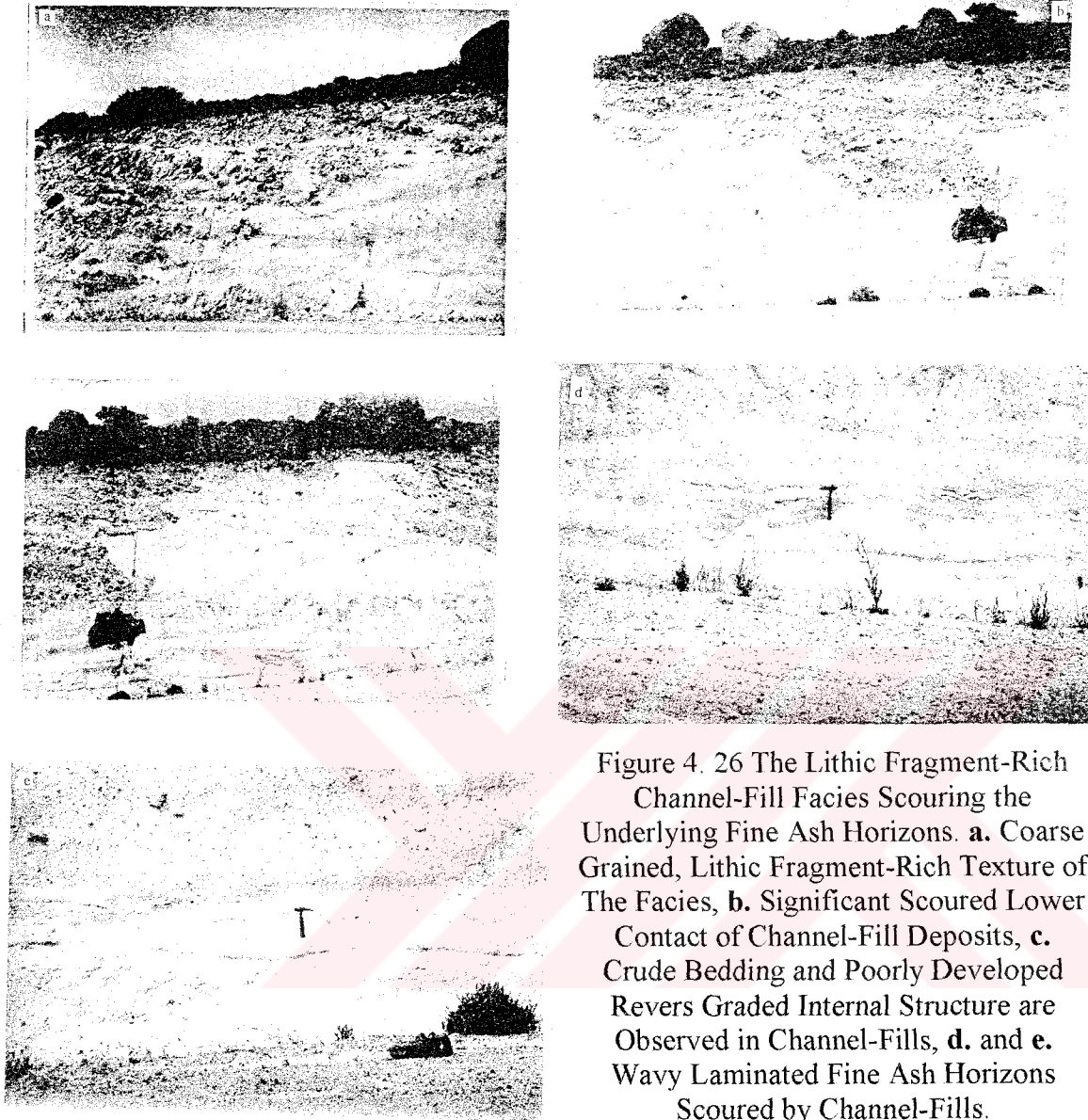


Figure 4. 26 The Lithic Fragment-Rich Channel-Fill Facies Scouring the Underlying Fine Ash Horizons. **a.** Coarse Grained, Lithic Fragment-Rich Texture of The Facies, **b.** Significant Scoured Lower Contact of Channel-Fill Deposits, **c.** Crude Bedding and Poorly Developed Revers Graded Internal Structure are Observed in Channel-Fills, **d.** and **e.** Wavy Laminated Fine Ash Horizons Scoured by Channel-Fills.

4. 3. 3. Eski Foça-Yeni Foça Area

The third area examined in this study, is located to the northeastern part of the Eski Foca dome in which the accompanying volcanoclastic sequence form open outcrops. In this area two new facies are recognized which are the Subaqueous welded ignimbrite facies and the Brecciated perlite facies (Figure 2.39). The sequence of these two facies are vertically repeated and overlain by the lithic fragment-bearing volcanoclastic facies (Facies 9,11,12,13, Figure 2.39).

4. 3. 3. 1. Subaqueous welded ignimbrite facies (Facies 15)

Description: The diffusely to slightly welded subaqueous ignimbrite facies is composed of laminated, fine grained pyroclastic sequences and rare density current volcanoclastic intervals and forms the lowermost part of the pyroclastic sequence between Eski and Yeni Foça towns (Plate1, Figures 2.17,39). The ignimbrite sequences consist of angular fragments of coherent rhyolite lava and pumice and fine grained tuffaceous matrix (Figure 4. 27). The fragments which constitute about 30 % of these rocks, are primarily flattened pumices with subordinate angular glass shards and massive to banded rhyolite particles (Figure 4.28). Digitated ends of compacted and flattened pumices are still evident in thin sections. Both pumices and glass shards are deformed around volcanic particles (Figure 4.29). The internal pore spaces of the pumice fragments are entirely filled with microcrystalline quartz vertically along the complete thickness of this sequence (Figure 4.29,30). Siliceous nodules which are set in flow foliated fine pumiceous matrix and are, in fact, secondarily quartz-filled gas bubbles, are also common in this facies (Figure 4.31). Glass shard fragments are generally well-preserved. Rhyolitic lava grains are the second dominant component. Flow banding in glassy matrix surrounding the lithic fragments are also observed.

In the upper parts of the measured section (Figure 2.39), welding becomes less intense where flattening in pumice fragments and recrystallized quartz fill are less significant. Poorly developed columnar joints are observed in these slightly welded parts (Figure 4.32). There are beds of the density current deposits incorporated with the welded ignimbrites (Figure 2.39). In these density current deposits, 20 to 70 cm-thick, graded and cross bedded volcanic conglomerate and sandstone intervals are interlayered with very fine grained tuffaceous mudstones. In the sandstones, poorly developed Bauma sequences are observed with coarse grained pumiceous part along a tractional lower contact which passes upward into the cross-bedded sand-sized pumice particles. At the uppermost part, the sequence ends in planar laminated fine ash layers (Figure 4.33). In the cross stratified parts of the sandstones, bimodal paleocurrent directions are envisaged. The Reassembled hyaloclastic breccias, Fine grained and Coarse grained rhyolite pumice-lithic fragment facies interlayer the Subaqueous welded ignimbrite facies in different stratigraphic levels along the section and upward the Fine or in

places, Coarse grained rhyolite pumica-lithic fragment facies overlie the facies along an irregular contacts (Figures 2.39 and 4.34).

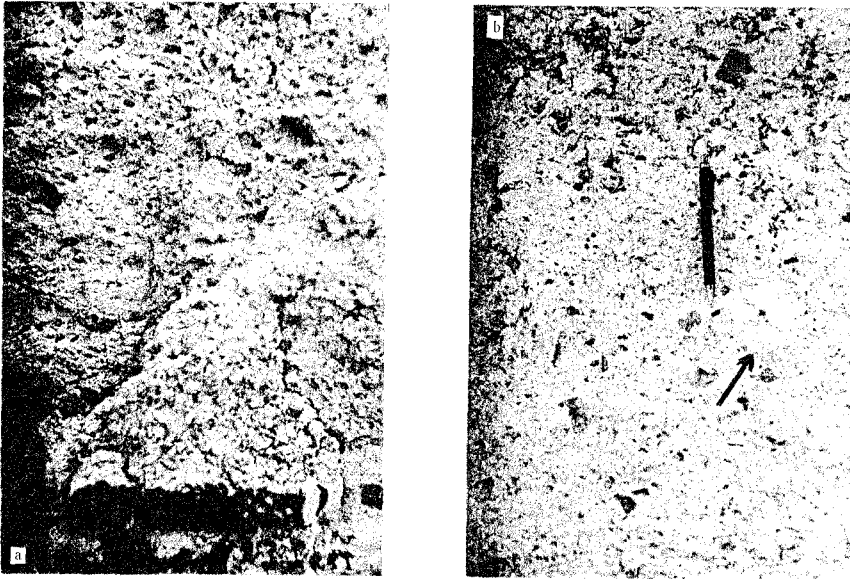


Figure 4. 27 Subaqueous Welded Ignimbrites. **a.** Facies is Rich in Pumice Fragments, (Urla K17 d2 77750 / 87750) **b.** Coherent Rhyolite and Pumice Fragments in Slightly Welded Ignimbrites. Although Welding is not Significant in Field Exposures, Slight Flattening is Still Evident in Vesicles in Pumice Fragments (Arrow). (Urla K17 d2 76925 / 84625)

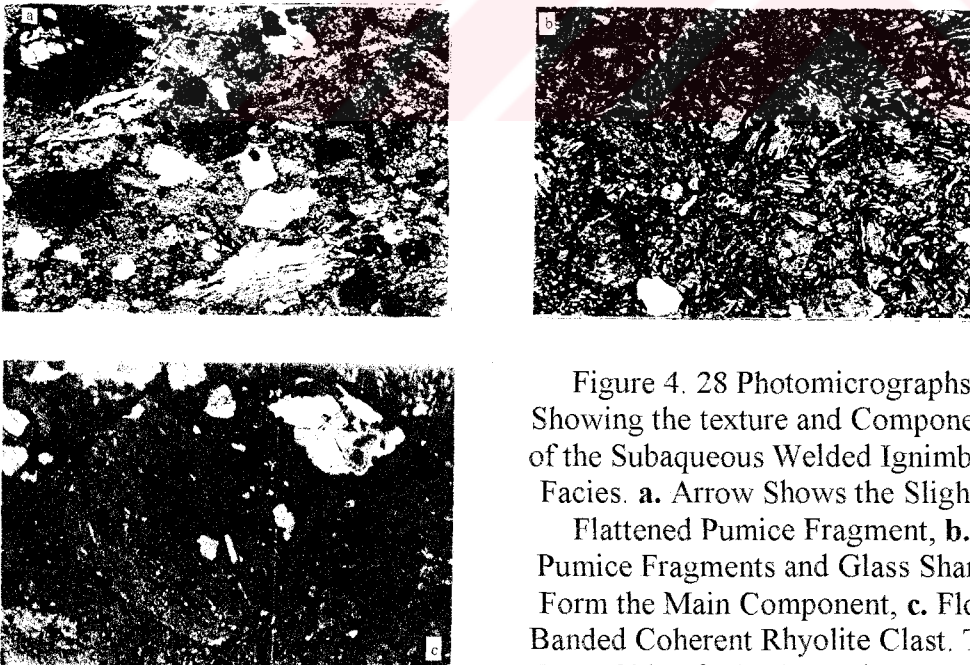


Figure 4. 28 Photomicrographs Showing the texture and Components of the Subaqueous Welded Ignimbrite Facies. **a.** Arrow Shows the Slightly Flattened Pumice Fragment, **b.** Pumice Fragments and Glass Shards Form the Main Component, **c.** Flow Banded Coherent Rhyolite Clast. The Long Side of All Three Photographs are 6 in Length.

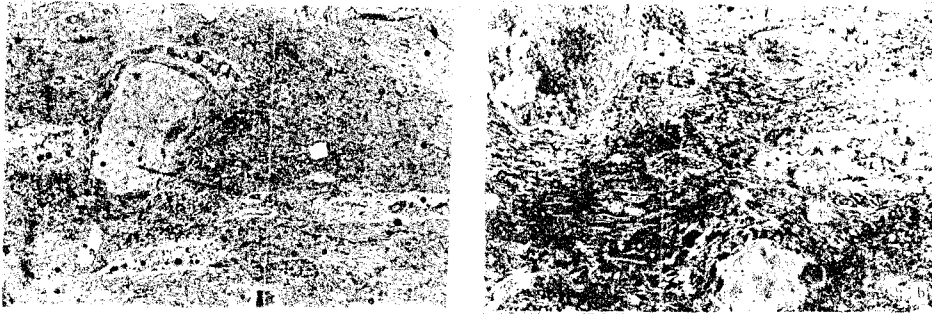


Figure 4. 29 Photomicrographs Showing the Flattened Pumice Fragments, Filled by Recrystallized Granoblastic Quartz. **a.** Flattened Pumice Fragments Wrapping the Lithic Rock Fragments, **b.** Flattening in Pumice Fragments and Plastically Deformed Structure Indicate the Slight Welding. The Long Side of the Photographs are 6 mm in length.

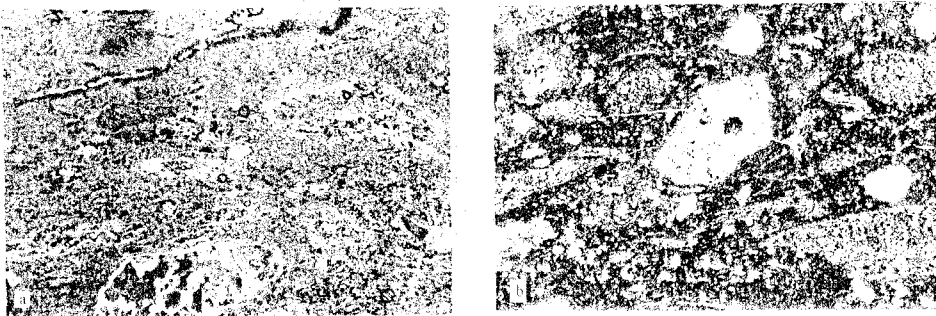


Figure 4. 30 The Pore Spaces of the Pumice Fragments are Filled by Recrystallized Granoblastic Quartz or Feldspar in Whole Sequence. The Long Side of the Photographs are 6 in Length.

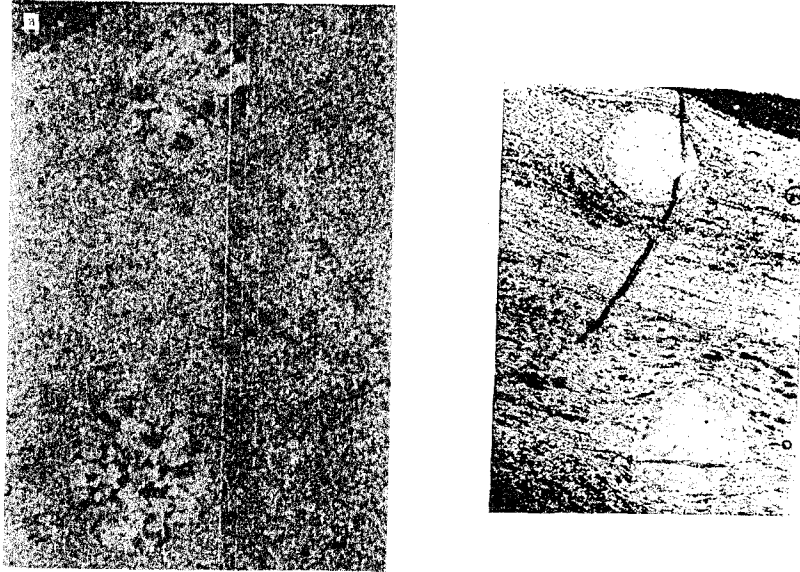


Figure 4. 31 Photomicrographs Showing the Siliceous Nodules, Observed in Subaqueous Welded Ignimbrites. Flow Foliation in Fine Matrix is Significant. See Text for Detailed Explanation. **a.** Cross Polarized Light, **b.** Parallel Polarized Light. The Long Side Of the Photograph is 3.5 mm in Length.

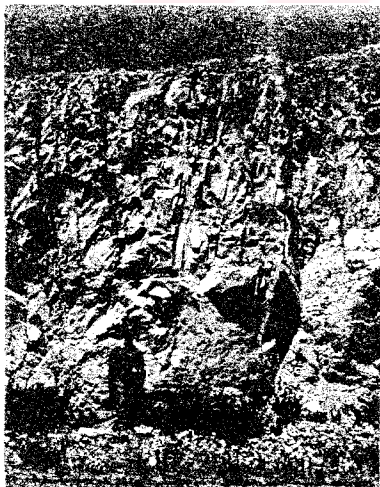


Figure 4. 32 Poorly developed Columnar Joints in Slightly Welded Upper Parts of the Subaqueous Ignimbrites.
 Urla K 17 d2; 76 700 / 86 250

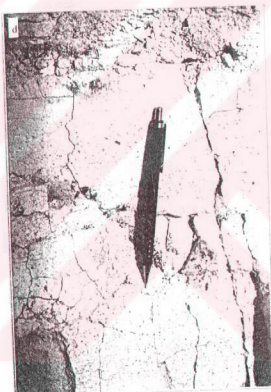
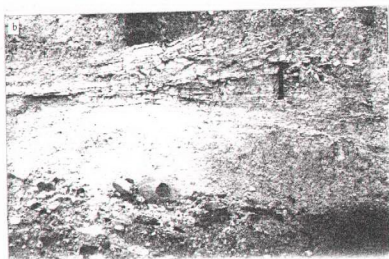
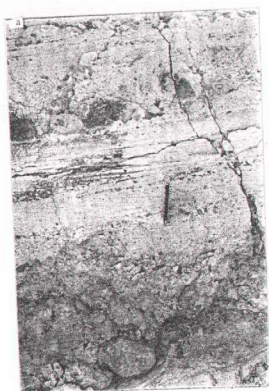


Figure 4. 33 Flowing-Related Sedimentary Structures in Subaqueous Ignimbrites. **a.** Baume-Like Sequences with Scoured Lower Contact. Normal Grading and Cross Stratification in the Middle Parts are Clear (İzmir K17 d2; 77750 / 87 750), **b.** Cross Stratification in Fine Grained Upper Parts (İzmir K17 d2; 77 800 / 79 325), **c, d, e.** Normally Graded Flow Units. Each Units Starts with Coarser Clasts Along an Irregular Lower Contact and Upward Pass into the Fine Ash Horizons (İzmir K17 c1; 85 275 / 79 375).



Figure 4. 34 Field Photograph
Showing the Coarse Grained
Rhyolite Pumice-Lithic Fragment
Facies Overlying the Subaqueous
Welded Ignimbrite Facies.
Urla K17 c1; 80875 / 87 525

Interpretation: In this section, the pyroclastic sequence is quite similar to the Eski Foça-Bağarası section. The main difference between these two sequences is the welding which is significant for the Eski-Yeni Foça section. Welding in subaqueous pyroclastic flow deposits has been controversial because of the supposition that cold water becomes thoroughly admixed with shattered fragments during the flow of subaqueous eruption (Sparks et al., 1980; Stix, 1991). Kokelaar (1992), on the other hand, suggests that the controversy over the occurrence of subaqueous welding of pyroclastic flow deposits has arisen not because of its rarity but because of the poor preservation potential of diagnostic microstructures and the difficulty of unequivocal demonstration of the paleoenvironment of deposition. The critical point in this discussion is that if the compaction which caused the resultant streaky texture, was really because of hot-state welding or post or syn-diagenetic burial compaction (Branney & Sparks, 1990). In the latter, the flattened clasts normally do not show viscous attenuated microscopic vesicular texture and individual shards are commonly not preserved. Kokelaar (1992) noted that the resultant streaky-textured rocks are not unequivocal in respect to discriminating welding from compaction. Allen (1988) suggested pumice and shard clasts which have been pseudomorphically replaced by microcrystalline quartz and feldspar aggregates by devitrification, are the best preserved welding fabrics. In addition to that, Kokelaar (1992) interprets the microcrystalline quartz-filled void spaces and pumices of volcanoclastic sequences as characteristics of subaqueous welding. In the Eski-Yeni Foça area, flattened magmatic gas bubbles (vesicles) in pumice fragments and shards, formed by fragmentation of highly vesicular magma, are common components and clearly are replaced by microcrystalline quartz (Figures 4.29,30,31) indicating the hot-state emplacement of ignimbrites.

Wright & Coward (1977) defined some siliceous nodules, filled by microcrystalline quartz, in Pitts Head tuff indicating shallow marine emplacement of ignimbrites. According to these authors, the nodules originally were gas bubbles and were filled by quartz in later stages of welding. So that, similar siliceous nodules in this facies (Figure 4.31) in Foça region, are interpreted as an evidence of subaqueous welding. Additionally, pumice fragments observed in this sequence in which the gas bubbles are filled by recrystallized granoblastic quartz, indicate the subaqueous emplacement (Wright and Coward, 1977; Cas et al., 1990; Kokelaar, 1992), and high particulate concentration indicates the pyroclastic flow mechanism. In the lower parts flattening in the pumice fragments, flow banding in pumiceous matrix and pumices and glass shards, deformed around volcanic particles indicate the plastic and probably not entirely cooled conditions during the compaction and intense welding.

In the upper parts of the flows, on the other hand, these structures become less significant and crude columnar joints are also observed indicating hot-state emplacement of a new subaqueous pyroclastic flow unit but less intense welding which probably is caused by the rapid cooling in the uppermost part because of the direct interaction with the water column and slow material income.

4. 3. 3. 2. Brecciated perlite (Facies 16)

Description: The subaqueous welded ignimbrite facies gradually passes upward into a 10 m-thick brecciated perlite (Figure 2.39a). The main components of these rocks are poorly sorted and angular rhyolitic lava grains, perlitites and pumice fragments. Partly to completely perlitized glassy matrix is also abundant. Rare dykes, up to 75 cm-thick, of the underlying pyroclastic unit cut this perlitic zone in which rhyolitic lava breccias and perlitic fragments are the dominant components (Figure 2.41). Grain supported texture is significant for these dykes (Figure 2.42).

Interpretation: The brecciated perlite intervals are formed in a subaqueous environment and originally composed of water-rich fine particles. Relatively slow cooling and high water contents of these sequence were the cause of perlitization. The textural features of dykes cutting the overlying perlitic zone, are similar to the gas segregation pipes recognized by

Walker (1971, 1972). Although they commonly are thinner than those observed in Foça area, Cas & Wright (1987) noted that these gas pressure rich pipes may attain up to 2 m in thickness. Walker (1971, 1972) suggested that gas segregation pipes are formed by volatiles streaming through the ash matrix of the flow during emplacement.

4. 3. 3. 3. Reassembled hyaloclastic breccias (Facies 8)

Description: In the volcanoclastic sequence, observed in the Eski Foça-Yeni Foça section (Figure 2.39), rocks, deposited in the reassembled hyaloclastic breccia facies, defined above, interlayer the subaqueous welded ignimbrites in different stratigraphic levels. In these parts, the reassembled hyaloclastic breccia facies is significantly green colour in most outcrops, because of the intense alteration (Figure 4.20d).

Interpretation: The reassembled hyaloclastic breccia facies, interlayered with the subaqueous welded ignimbrites, indicate that, during the subaqueous volcanism, because of the continuing lava extrusion and updoming the already extruded material became unstable and formed the debris flow deposits on the flanks and intense hydrothermal alteration caused the complete green colour of the resultant rock.

4. 3. 3. 4. Subaqueous ash fallout facies (Facies 17)

Description: In the Eski-Yeni Foça area well laminated mud beds consisting entirely of ash-sized pyroclasts are found in the Subaqueous welded ignimbrite facies. In these parts, the intraformational gullies, in facies 15, with significant scoured lower contacts (Figure 4.34) are filled by the mud-sized ash deposits. The entire deposits are very fine grained and normally graded. In the lower parts relatively coarse grained pumice and lithic fragments are present (Figure 4.35). Lamination in facies is characteristically mount the paleosurface (Figure 4.35).

Interpretation: The very fine grained pumiceous composition of the facies indicates that deposits were formed from a very efficient volcanic activity during the subaqueous welding. Thin laminations mounting the paleosurface are indicative of ash fall deposition mechanism and intraformational gullies are characterized the subaqueous environment.

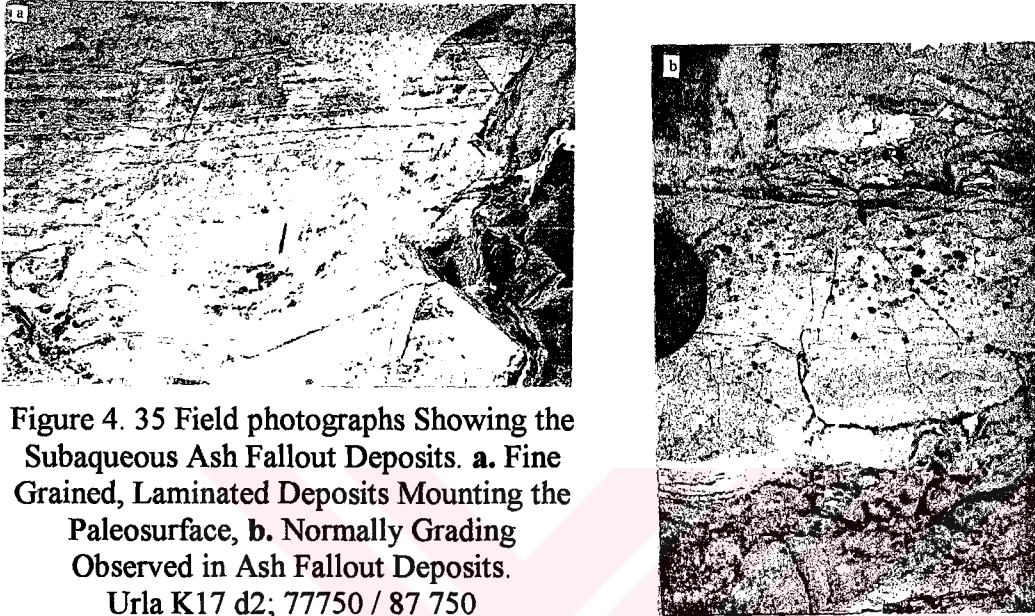


Figure 4.35 Field photographs Showing the Subaqueous Ash Fallout Deposits. a. Fine Grained, Laminated Deposits Mounting the Paleosurface, b. Normally Grading Observed in Ash Fallout Deposits. Urla K17 d2; 77750 / 87 750

McPhie et al. (1993) defines similar deposits as the phreatomagmatic ash fallout deposits in the Rotongaio Ash, AD. 186, Taupo, New Zeland (p. 161, Plate 39.5) and notes that the gullies indicate the presence of abundant surface water during ash deposition and that the very fine grain size is caused by the efficient phreatomagmatic explosive activity. These field features, defined by McPhie et al. (1993), are quite similar to those, observed in the Eski-Yeni Foça area so that, these deposits are interpreted as the subaqueous ash fallout deposits derived from the phreatomagmatic explosive activity and fall down in the subaqueous environment during the subaqueous welding.

4.3.3.5. Coherent alkaline lavas (Facies 18)

Description: The coherent alkaline lava facies corresponds the mafic lava flows of the Foça alkaline volcanics (Ch. 2) cropping mainly out in the Foça Peninsula. The coherent lavas are formed typically by the intensely flow laminated, aphanitic, dark green to black lava flows. In this facies, aphanitic texture is common in handspecimens. In thin sections, porphyritic and microcrystalline texture with elongated microlites, are also clear (Figures 2.46, 47).

Petrographically the coherent alkaline lavas are basaltic in composition with abundant clinopyroxene phenocrysts accompanied by amphiboles with brown pleochroism, rare biotites and olivines (Figure 2.50). According to their extinction angles and the other petrographical characteristics, the pyroxene phenocrysts are commonly augite to aegyrine in composition (Ch. 2, Figure 2.51). Because of their high Ca content, the pyroxene phenocrysts are commonly found as converted into the calcite (Figure 2.52). The main felsic mineral is euhedral, partly zoned plagioclases with typical polysynthetic twinning.

As indicated in Ch. 2. 2. 3, the coherent alkaline lava facies is observed in different stratigraphic levels, interlayering with the Foça volcanoclastics, in the Foça volcanic complex indicating the bimodal nature of the volcanism in the area.

Interpretation: The textural and petrographic features of the coherent alkaline lava facies indicate that, in the Foça area, during the acidic volcanism, an alkaline trachytic to basaltic volcanism was also active, and probably from another source, alkaline trachytic to basaltic lavas have been flowing the surface as evident by the prominent trachytic texture, observed in the coherent lavas.

4. 3. 3. 6. Alkaline dykes (Facies 19)

Description: In the Foça Peninsula, between Eski Foça-Bağarası and Eski-Yeni Foça Areas subvolcanic equivalents of the alkaline volcanism, are observed as 1-10 m-thick dykes cutting the Foça pyroclastic sequence (Figure 2. 55). The alkaline dykes, petrographically and geochemically are similar to the Coherent alkaline lavas (facies 18) and trachyandesite to basalt in composition as mentioned in Ch. 3. Although there is not enough number of outcrops to make statistical study, the dykes have N-S strike and 60-80° dip (Plate 1).

Interpretation: Mafic dykes in the same chemical and petrographic composition with the coherent alkaline lavas in the Foça alkaline volcanics indicate that the lava effusions occurred along N-S trending fracture zones and they are not related with any central volcanism. Their gradational stratigraphic relations with the Foça pyroclastic sequence indicate also that the alkaline volcanism occurred at the latest stages of the calc-alkaline rhyolitic Foça volcanism.

4. 4. MORPHOLOGY AND ERUPTION HISTORY OF FOÇA VOLCANIC COMPLEX

In the Foça peninsula rhyolite domes, intruded in several areas, and a thick rhyolitic volcanoclastic sequence surrounding the domes form the dominant rock association. In the Bağarası area the massive rhyolites are found as a stubby lava flow including two main lava intrusion phases characterizing two progressive pulses (Figure 2.15). In the Yeni Foça area, on the other hand, massive rhyolites show a dome shaped emplacement. In this later example, however, the rhyolite dome is partly located under the sea level and in the southern parts the relations with the accompanying volcanoclastic sequence are not well-exposed. In the Eski Foça area, and between Eski and Yeni Foça towns, the Foça volcanic complex have its best-preserved outcrops where both the internal structures of the massive rhyolites and the relationships with the surrounding volcanoclastic sequence are clearly observed. In this area, the massive rhyolites are found as a composite dome which is formed by the several individual rhyolite domes and dykes. The volcanoclastic sequence surrounding these rhyolite domes, with a circular shape and show significant outward changes in facies. Close to the domes the rhyolitic volcanoclastic sequence is characterized by the in situ and reassembled hyaloclastic breccia facies (Facies 9 and 10), and coarse and fine grained rhyolite pumice and lithic fragment rich facies (Facies 12 and 13). Outward, the subaqueous welded ignimbrite facies which is prominently finer grained, cover these central facies (Figure 2.15). Ondulated internal structure and the lateral facies changes make the succession exposing in wide areas all around the Foça peninsula. The internal structures, lithological characteristics and relations of the different volcanic and volcanoclastic facies of the felsic Foca volcanic complex indicate that it was formed by subaqueous emplacements from at least the Eski Foça, Yeni Foça and Bagarasi rhyolite domes. The rhyolitic magma extruded directly into a shallow water from these three centers.

The subaqueous domes were evolved and grew progressively (Figure 4.36), so that, in their central parts, the massive rhyolite facies formed in their interiors which is typified by the porphyritic texture with embayed quartz and feldspar phenocrysts in recrystallized or devitrified glassy matrix. Upon getting contact with cold water, magma quenched and shattered to form the in situ hyaloclastic breccias. Interaction between the massive rhyolites

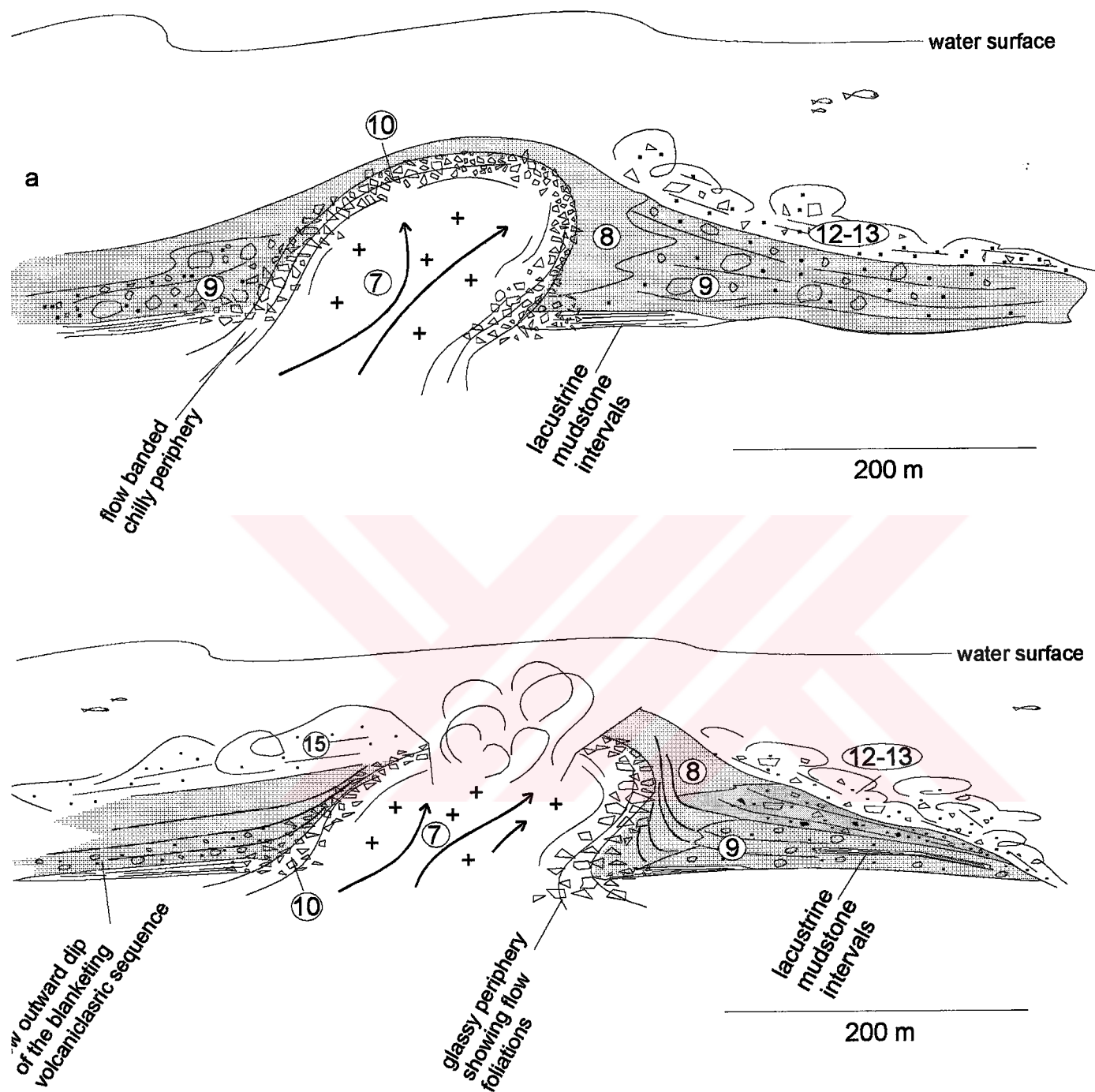


Figure 4.36 A Model for the Formation of Subaqueous Pyroclastic Sequences in Foça Region.
a. Intrusion of the Dome into the Shallow Lacustrine Environment. Coherent Lava-Water Interaction Causes the Quenching Fragmentation in Margins and Formation of Perlitic Cover Zones Surrounding the Dome. **b.** Updoming the Core and Phreatomagmatic Explosions Generate the Subaqueous Debris Flows and Ignimbrites. Numbers, Used for Each Facies, Correspond with the Numbered Facies Descriptions in the Text.

and the water column also caused the formation of massive perlites covering the rhyolite dome (Figure 4.36a). The semicircular form and gradual changes from the massive rhyolite dome to massive perlites and also thin brecciated and intensely altered facies indicate close affinity of their formations and that hydration of the rhyolite body caused the formation of the massive perlitic cover. Within the surrounding massive perlite facies, felsic magma cooled quickly and an envelope of glassy textured massive rhyolite formed. Additional input of magma and rapid cooling of newly intruded rhyolitic magma because of the already developed glassy boundary zone, caused onion-like glassy envelopes around the core of the dome and a banded internal structure at the periphery. These steeply dipping flow bands were caused by rapid cooling of the magma at the periphery of the dome. Here, the term “flow banding” in our usage implies both the viscous flow of magma which is characterized by plastically folded rhyolitic magma, and the bedding-like planar structures resulting from the successive cooling of magma at the periphery.

As extrusion continued, the central part of the dome grew higher than the periphery and resulted in the deposition of blankets of phreatically erupted pyroclastic debris deposits. The large-scale dome-like map patterns of figure 3 are the direct affect of piling up of volcanoclastic materials around these topographically positive areas. As the core of the massive rhyolite dome was pushed farther up, the surrounding blanketing volcanoclastic sequences tilted vertically, or in places overturned (Figure 4.36b). In case of the Eski Foça dome, the extrusion of the rhyolitic magma took place from several centers and a composite dome were formed. The upper parts of the dome phreatically erupted several times and vapour-rich hyaloclastites with pumice fragments were formed. This hot, vapour-rich pyroclastic material inhibit first cooking inside and the subaqueously erupted welded ignimbrites were formed. Because of the relatively slow cooling and the high water content, interaction between the water column and the ongoing subaqueous pyroclastic flows caused the perlitization within the welded parts and the brecciated perlite intervals were formed which were originally composed of water-rich fine particles. Cas et al. (1990) discusses the function of external water in such eruptions that of a catalyst triggering explosive disruption of magma already in an incipient state of explosive disintegration due to exsolved magmatic volatiles. To the authors, water causes quenching of the thin walls of vesicles in the magma, so depressuring the gas in the vesicles which then expands violently and explodes. Some

external water would also be flashed in producing a secondary explosive thrust top ejecting pyroclasting debris. In the Foça area, external water clearly played a role to trigger quenching, and to form pumiceous pyroclastic flows.

The role of welding in subaqueous pyroclastic flow deposits has been controversial debate. On the other hand, the process is questioned because of the supposition that cold water becomes throughly mixed with shattered fragments during subaqueous eruption (Sparks et al., 1980, Stix, 1991). Kokelaar & Busby (1992), on the other hand, has suggested that the controversy over the occurrence of subaqueous welding of pyroclastic flows has arisen not because it is rare, but because of poor preservation of diagnostic microstructures and the difficulty of unequivocal demonstration of the paleoenvironment of deposition. In this case, however, the clear evidents of the subaqueous welding which will be mentioned in following paragaphs, are observed.

The presence of some pumice fragments in the Foça volcanoclastic sequence and phreatomagmatic explosive activities suggest a very shallow water depth which may be 1 m or less and conversion of subaerial conditions from time to time as pyroclastic debris accumulated and piled up. Fisher & Schminke (1984) and Cas & Wright (1987) suggested at most a few hundred meters depth of water for the formation of subaqueous pumices and phreatomagmatic explosive activity. In the Foça area, the evidences of the shallow subaqueous welding of pyroclastic pumice flows such as lacustrine mudstone interlayers (Figure 4.36a, b) and secondarily quartz-infilled gas bubbles adjacent to flow foliated fine matrix are found even in the uppermost parts of the pyroclastic sequence (Figure 4.31).

A critical factor in subaqueous welding is whether compaction is due to hot-state welding or post or syndiagenetic burial compaction. (Branney & Sparks, 1990) showed that syndiagenetically burial compaction produces the flattened clasts that normally do not show a viscous attenuated microscopic vesicular texture and individual shards are commonly not preserved. That is why Kokelaar & Busby (1992) noted that the resultant streaky-textured rocks are not equivocal in respect to discriminating welding from compaction. Allen (1988) suggests the pumice and glass shard clasts that have been pseudomorphically replaced by microcrystalline quartz and feldspar aggregates by devitrification are the best preserved

welding fabrics. In the study area, flattened magmatic gas bubbles (vesicles) in pumice fragments and glass shards that are replaced by microcrystalline quartz (Figs. 4.29, 30) are common components in the pyroclastic sequence and indicate hot-state welding in subaqueously emplaced ignimbrites. Siliceous nodules, filled by microcrystalline quartz, in flow foliated fine pumiceous matrix are observed in the uppermost parts of this welded ignimbrite unit (Fig. 4. 31). Wright & Coward (1977) noted similar nodules in Pitts Head tuff that indicate the shallow marine emplacement of ignimbrites and these nodules originally were gas bubbles which were filled by quartz in later stages of welding. The pumice fragments and gas bubbles filled by recrystallized granoblastic quartz, indicate the subaqueous emplacement as also noted by Cas et al.(1990) and Kokelaar & Busby (1992).

The high particle concentrations in the rhyolite pumice and lithic fragment bearing volcanoclastic facies (facies 4) are consistent with pyroclastic flow emplacement rather than surge deposits. In the lower parts of the subaqueous welded ignimbrite facies (facies 15) flattened pumice fragments and flow banding in matrix indicate the intense welding. In the uppermost parts of the deposits, on the other hand, these structures become less significant which indicates the poorly-developed welding as indicated by the presence of crude columnar jointing (Fig. 2. 39). In Foça Peninsula, the evidence of the shallow subaqueous welding of pyroclastic pumice flows includes lacustrine mudstone interlayers and secondarily quartz-infilled gas bubbles adjacent to flow foliated fine matrix (Fig. 4. 36a, b). These features are found even in the uppermost parts of the pyroclastic sequence (Fig. 2. 39a, b) and indicate that the volcanism was mostly developed in subaqueous environment. The porphyritic texture in the central parts of the massive rhyolite dome indicates crystallization during the final stages of the emplacement under relatively slow cooling conditions which finally plugged the dome structures.

CHAPTER FIVE

TECTONIC CONTROLS on the NEOGENE FOÇA VOLCANISM: A DISCUSSION

In western Anatolia, stratigraphy and chemical affinities of the magmatic associations and relations of these associations with the neotectonic regime have been discussed since 1960's. (Arpat & Bingöl, 1969; Ketin, 1970; Şengör & Dewey, 1980; Şengör and Yılmaz, 1981; Şengör, 1982; Fytikas et al., 1984; Şengör, Satır and Akkök, 1984; Yılmaz, 1989, 1990; Seyitoğlu and Scott, 1991, 1992; Yılmaz, Genç, Gürer, Bozcu, Yılmaz, Karacık, Altunkaynak and Yılmaz, 2000 and Yılmaz, 2000).

In all these studies three main ideas have been outlined:

1. The magmatic activity has been developed under a N-S directed extensional tectonic regime starting from the Late Oligocene and being continuous since then (Seyitoğlu and Scott, 1991, 1992),

2. The magmatism was generated in relation with the north-dipping subduction of the east Mediterranean ocean floor along the Hellenic trench (Fytikas et al., 1984; Pe-Piper and Piper, 1989; Gülen, 1990) and

3. The magmatic activity evolved in different episodes and the magmatism was formed in different tectonic settings (Şengör and Yılmaz, 1981; Ercan et al., 1984, Ercan et al., 1995; Yılmaz, 1989,1990; Yılmaz et al., 1994; Savaşçın and Gülen, 1990; Güleç, 1991; Yılmaz, 1997, 2000).

In the first proposition, under a N-S extensional tectonic regime which is caused by the spreading and thinning of the previously thickened crust, the western Anatolia has been extending since the Early Miocene. During the first Early Miocene stage of the deformation, the western Anatolian volcanism was generated by partial melting in the lower parts of the excessively thickened western Anatolian crust.

Fytikas et al.(1979 and 1984), on the other hand, proposed that the chemical characteristics of the volcanic rocks, in the Aegen Region, have a steady change in time. According to the authors, the widespread, early phase of the volcanism has a calc-alkaline nature and during the 12-7 ma interval this first stage passes into scattered high-K andesitic to shosonitic, calc-alkaline suite and are all replaced by the alkaline volcanism from Late Miocene to Quaternary. These authors pointed out that the calc-alkaline volcanics show chemical and petrographical characteristics of the orogenic-type, active continental margin and K_2O / SiO_2 ratio increases depending on the increasing the dip of subducting slab. Fytikas et al.(1979 and 1984) suggested further that, the Oligocene-Miocene calc-alkaline volcanism in the Aegean Region was generated by the north-dipping subduction along the Hellenic Arc and the relatively younger alkaline volcanism in the westen Anatolia were formed by the extension which is caused by sauthwestward escape of the Anatolian Block along the North Anatolian Fault.

In recent years the third view has been noted in many studies in which it was stated that during the first episode, the magma was generated under a N-S compressional regime during the Late Oligocene-Middle Miocene time, and during the following stages, the magma was formed under a N-S extensional regime (Şengör and Yılmaz, 1981; Ercan et al., 1984, 1985, 1995; Yılmaz, 1990; Altunkaynak and Yılmaz, 1998; Genç, 1998). Yılmaz, (1990) also noted that the compressional episode generated the calc-alkaline, hybrid magmatism and the later extensional regime gave way to the alkaline magmatism. Yılmaz, (1989, 1990, 1997 and 2000), Genç, (1998), Karacık and Yılmaz, (1998) and Yılmaz et al., (2000) are agree that the first stage formed because of the thickening of the continental crust, resulted from the continuing compression. In these studies, it was stated that the first calc-alkaline volcanism was irrelevant from any true subduction but resulted from an excessively thickened crust. Yılmaz, (2000), claimed that the N-S compressional regime caused the NNE-SSW trending oblique faults in western Anatolia which controls both formation of the Early Miocene lacustrine sedimentary basins and accompanying

calc-alkaline volcanism. According to the writer, volcanic vents, from which calc-alkaline magma was erupted, are found along these NNE-SSW trending compression-related oblique faults.

Yılmaz (1989) noted also that, the compressional regime was replaced by an extensional regime and alkaline volcanism in the Pliocene time. In the latest studies of Yılmaz (2000) and Yılmaz et al. (2000), the beginning and dying ages of the volcanic stages have been subjected a small change, and it was indicated that, the calc-alkaline volcanism died out in Middle Miocene and the younger alkaline volcanism started in the Late Miocene time. According to the writer, the Middle to Late Miocene time span, in the area, was the time of compressional deformation and formation of folds and some thrust faults.

Geochemically, the Helvacı and Çaltılı andesites and the Dumanlıdağ dykes are all andesite-trachyandesite in composition and calc-alkaline in nature. The major element contents show significant differences between the Helvacı andesites and Çaltılı andesites. However, trace element contents of all these three units have nearly the same trends indicating the similar tectonic setting (Ch.3). The comparison of the average major and trace element compositions of the Helvacı and Çaltılı andesites and the Dumanlıdağ dykes with some typical orogenic andesites from different tectonic settings, roughly show a continental margin origin for the Yuntdağ volcanics which supports the model, proposed by Yılmaz (1989). In addition to that, the calc-alkaline and post orogenic nature of the rhyolites (Ch. 3) which are genetically related with the andesitic suite, also supports the model of Yılmaz (1989). However, although a rough NNE-SSW trend of the calc-alkaline andesites and rhyolites, is observed in large-scale geological maps, aerial photos and landscape materials, there is no unequivocal field data, observed in the study area, and detailed geological maps indicating that the volcanic vents and products of this volcanism follow these NNE-SSW faults.

In the Foça Peninsula, open folds of the widespread tuffaceous sequence of the Foça volcanic complex, are characteristic (Fig. 2.17, Plate 1). In addition to these folds, there are rare, meso-scale high to low angle reverse faults supporting the idea of a compressional tectonic regime. However, under a tensional tectonic condition, sedimentary successions overlying normal faults would take an appearance of drape folds. If in some localized areas displacements along normal faults increase, gravity bending of a upthrown side of a high-

angle fault attain an appearance of a reverse fault, phenomenon common around block-faulted terranes. Plastic deformation during the pyroclastic flows, might be another possibility to explain such rare and meso-scale reverse faults.

In the Aliğa-Foça Area, the calc-alkaline volcanic suite laterally pass into the Neogene lacustrine deposits. The lacustrine limestone lenses interlayer with mudstones and even with massive lavas (Ch. 2). In addition to that, in the upper parts of the Foça volcanic complex, the alkaline lavas interdigitate the calc-alkaline pyroclastics. The alkaline volcanics were stated in the earlier literature as Late Miocene to Recent in age (Savaşçın, 1978; Fytikas et al., 1980; Güleç, 1991; Innocenti et al., 1982; Savaşçın, 1982; Fytikas et al., 1984; Seyitoğlu and Scott, 1991, Yılmaz, 1989, 1990; Ercan et al., 1995; Altunkaynak and Yılmaz, 1998; Genç, 1998; Yılmaz, 2000; Yılmaz et al., 2000). The major and trace element composition of the Foça alkaline volcanics show a close similarity with the alkaline continental rift volcanics and within plate volcanics and are in harmony with the previous studies, mentioned above. All these stratigraphic relations and chemical properties of these units indicate that the compression-related calc-alkaline suite and the extension-related sedimentary and alkaline volcanic sequences formed progressively and the volcanism continued during the Late Miocene, and probably at the beginning of the Pliocene in western Anatolia..

CHAPTER SIX

CONCLUSIONS

In the Aliğa-Foça region, three main rock associations crop out. These are 1. **The Yuntdağ volcanics**, 2. **The Foça volcanic complex** and 3. **The Aliğa limestones**. The Yuntdağ volcanics consist of four different volcanic units. The Helvacı andesites are composed of thick lava flows of andesite, trachyandesite and dacite. In the uppermost parts, this intermediate succession is darker in colour and finer in texture, and passes into the flow foliated Çaltılı andesites. The coarse grained volcanoclastic debris of the Haykıran blocky pyroclastic unit interdigitates with these coherent lava flows in different stratigraphic levels. In the central vents from which the Yuntdağ volcanism extruded, the andesitic to dacitic dykes and subvolcanic stock of the Dumanlıdağ unit, are observed.

Geochemically, the Helvacı and Çaltılı andesites and the Dumanlıdağ dykes are all andesite-trachyandesite in composition and they are calc-alkaline. The comparisons of the average major and trace element compositions of the Helvacı and Çaltılı andesites and the Dumanlıdağ dykes with some typical orogenic andesites from different settings, roughly show a continental margin origin for the Yuntdağ volcanics. The major element contents of the Helvacı andesites and Çaltılı andesites show some minor differences. However, their trace element contents are similar and show smooth trend suggesting genetically related origins.

The Yuntdağ volcanics are overlain by the Foça volcanic complex. The Foça volcanic complex consists of three main rock associations. These are 1. **The Foça rhyolites**, 2. **The Foça volcanoclastics** and 3. **The Foça alkaline volcanics**. In the Foça volcanoclastics three subunits are distinguished as 1. **Pyroclastic flows**, 2. **Hyaloclastic breccias** and 3. **Perlites**.

The geochemical characteristics of the massive rhyolites in the Foça volcanic complex show a distinctive rhyolite composition and a calc-alkaline chemical affinity. Trace element composition of the unit characterizes post-orogenic tectonic setting for massive rhyolite domes. The Foça alkaline volcanics, on the other hand, are alkaline basalt, trachyandesite and phonolite in composition and have alkaline chemical affinity. The major and trace element composition of the Foça alkaline volcanics shows a close similarity with the alkaline continental rift volcanics and within plate volcanics.

The youngest unit, observed in the Aliğa-Foça region, is the Aliğa limestones consisting of yellow-white limestones, clayey limestones and claystones. In the upper parts of the Foça volcanic complex, the Aliğa limestones interdigitate with the Foça volcanoclastics and overlie them concordantly.

In the Aliğa-Foça region two distinct central vents are distinguished from which the thick Yuntdağ volcanism, extruded. These central vents are 1. **The Dumanlıdağ caldera** and 2. **The Yuntdağ caldera**. The Dumanlıdağ caldera is an approximate diameter of 5 km. In this caldera the typical radial dykes and high-angle faults bounding the caldera, are clearly observed.

The Yuntdağ caldera is located in the northernmost part of the study area, between Yuntdağ and Siyekli villages with an approximate diameter of 5 km. In the Yuntdağ caldera, the boundary faults and subvolcanic equivalents of the volcanic products are not well-exposed and deep alteration and erosion exposing approximately circular central depression area is seen. Surrounding the caldera, thick andesite lavas of the Helvacı unit with horizontal or low-angle flow foliations, crop out.

In the Foça Peninsula, the Foça volcanic complex is characterized, by the massive rhyolite domes or stubby lava flows and pyroclastic sequences surrounding the massive rhyolite bodies. Around Eski Foça town, small rhyolite domes and dykes form a composite dome structure and in this area relations between the massive rhyolite bodies and the accompanying volcanoclastic sequence are well exposed. At this location, the massive rhyolite domes are surrounded by in situ brecciated hyaloclastic breccias and reassembled hyaloclastic breccias. Close to the massive domes, the relatively coarse grained rhyolite

pumice and lithic breccia flow deposits form another dominant lithology. Massive perlite interlayers are found in this coarse grained sequence. Outward, the pyroclastic sequence becomes fine grained and slightly welded ignimbrites form the upper parts of the pyroclastic sequence. Fine laminated lacustrine mudstones interdigitate with the volcanoclastic sequences. In the upper parts, pyroclastic material were piled up and subaerial condition predominated which is characterized by the lithic breccia-rich channel fill deposits.

In the Foça Region, the calc-alkaline andesitic lavas of the Yuntdağ volcanism, calc-alkaline rhyolites of the Foça volcanic complex and alkaline lava flows are stratigraphically and chemically gradational to each other. Andesite lavas of the Helvacı and Çaltılı andesite units are clearly high-K, basic andesites, and upward they pass into the calc-alkaline Foça rhyolites and Foça volcanoclastic sequences. The Foça alkaline lavas laterally pass into these rhyolitic volcanoclastic sequence and even the lacustrine limestones. This kind of a stratigraphic and chemical gradation show that there is no a prominent gap between these two chemically different volcanic suites hence the tectonic regimes given rise these volcanic products.

REFERENCES

- Akartuna, I., (1958). Türkiye' de Magmatik Faaliyet. TJK Bult., v: 2, Ankara
- Akyürek, B. and Soysal, Y., (1978). Geology of the Kırkagac-Soma (Manisa-Savastepe-Korum-Ayvalık (Balıkesir)-Bergama (Izmir) Region. MTA Report: (unpublished).
- Altunkaynak, Ş. and Yılmaz, Y., (1998). The Mount Kozak Magmatic Complex, Western Anatolia. Journal of Volcanology and Geothermal Research, v. 85, 211-231
- Allen, R.L., (1988). False pyroclastic textures in altered silicic lavas with implications for volcanic-associated mineralization. Econ. Geol. 83, 1424-1446
- Altunkaynak, Ş. and Yılmaz, Y., (2000). Geology and active tectonic of Foça Area, Western Anatolia. Batı Anadolu' nun Depremselliği Sempozyumu, Bildiriler, 160-165
- Altuntaş, S., (1997). Çaltılıdere Volkaniklerinin Litolojik, Petrografik ve Jeokimyasal Özellikleri. DEÜ. Müh. Fak. Jeoloji Müh. Böl. B.t.rme Tez., 42 s. (Unpublished).
- Arpat, E., and Bingöl, E., (1969). Ege Bölgesi Graben Sisteminin Gelişimi Üzerine Düşünceler. MTA Dergisi, no. 73, p. 1-9
- Becker-Platen, J.D., Besang, C., Harre, W., Kreuzer, H. and Müller, P., (1971). Kalium-Argon alter des Afyon Vulkanismus (Anatolien) und die Datierung der Miozan-Pliozangrenze. Ber. Archiv BGR Hannover (unpublished)(in Yılmaz, Y., (1989). Comparison of Young Volcania Associations of Western and Eastern Anatolia Formed

- Under a Compressional Regime: a Review. Journal of Volcanology and Geothermal Research, v. 44, p. 69-87.
- Benda, L., Innocenti, F., Mazzuoli, R., Radicati, F. and Steffens, P., (1974). Stratigraphic and Radiometric Data of the Neogene in Northwest Turkey, Zeitschrift de Deutschen Geologischen Gesellschaft, 125, 183-193
- Bellon, P.H., Jarrige, J.J and Sorel, E.D., (1979). Les Activités Magmatiques égéennes de l'Oligocène à nos jours et leurs cadres géodynamiques. Données nouvelles et synthèse. Revue de Geologie Dynamique et de Geographie Physique, 21, 41-55.
- Besang, C., Eckhardt, F.J., Harre, W., Kreuzer, H. and Müller, P., (1977). Radiometrische Altersbestimmungen an Neogenen Eruptiv Gesteinen der Türkei. Geol. Jahrb., B. 25, 3-36
- Bingöl, E., (1977). Muratdağı Jeolojisi ve Ana Kayaç Birimlerinin Petrolojisi (Geology and Petrography of Muratdağı Region). Bulletin of Geological Society of Turkey, 20, 13-67.
- Borsi, S., Ferrara, G., Innocenti, F. and Mazzuoli, R. (1972). Geochronology and Petrology of Recent Volcanics in the Eastern Aegean Sea (West Anatolian and Lesvos Island). Bull. of Volcanol., 36, 473-496
- Branney, M.J. and Sparks, R.S.J., (1990). Fiamme formed by diagenesis and burial-compaction in soils and subaqueous sediments. J. Geol. Soc. London., 147, 919-922
- Cas, R., A., F. and Wright, J., W., (1987). Volcanic successions: modern and ancient, a geological approach to processes, products and successions. Allen and Unwin, London.
- Cas, R., A., F., Allen, R., L., Bull, S., W., Clifford, B., A. and Wright, J., V., (1990). Subaqueous, rhyolitic dome-top cones: a model based on the Devonian Bunga Beds, southwestern Australia and a modern analogue. Bull. Volcanol. 52, 159-174

- Cox, K.G., Bell, J.D. and Pankhurst, R.J., (1979). The Interpretation of Igneous Rocks. George Allen and Unwin Ltd. London, 450 p.
- Debon, F. and Le Fort, P., (1983). A Chemical-Mineralogical Classification of Common Plutonic Rocks and Associations. Trans.R. Soc. Edinburgh. Earth Sci., 73, 135-149
- Dora, O.Ö., (1964). Geologisch-lagerstättenkundliche Untersuchungen im Yasmanlar-Gebirge nördlich vom Karşıyaka (Westanatolien). Maden Tetkik ve Arama Enstütüsü yayınları, no: 116.
- Emre, T., (1996). Gediz Grabeni' nin Jeolojisi ve Tektoniği. Turkish Journal of Earth Sciences. 5, 171-185.
- Ercan, T. (1979). Batı Anadolu, Trakya ve Ege Adalarındaki Senozoyik Volkanizması. Jeoloji Mühendisliği, Eylül, 1979
- Ercan, T. (1987). Ege Bölgesindeki Senozoyik Volkanitlerinde Yapılan Radyometrik Yaş Belirlemeleri. Jeomorfoloji Dergisi Sayı. 15, 83-90.
- Ercan, T., Türkecan, A., Akyürek, B., Günay, E., Çevikbaş, A., Ateş, M., Can, B., Erkan, M., Özkirişçi, C., (1984). Dikili-Bergama-Çandarlı (Batı Anadolu) Yöresinin Jeolojisi ve magmatik Kayaların Petrolojisi. Jeoloji Mühendisliği, 20, 47-60
- Ercan, T., Satır M., Kreuzer, Türkecan, A., Günay, E., Çevikbaş, A., Ateş, M., Can, B.(1985). Batı Anadolu Senozoyik Volkanitlerine Ait Yeni Kimyasal, İzotopik ve Radyometrik Verilerin Yorumu. Türkiye Jeoloji Kurumu Bülteni, c.28,121-136
- Ercan, T., Türkecan, A., Karabıyıköğlu, M., Şaroğlu, F., Sevin, D., (1995). A review of tertiary and Quaternary Volcanism in Wsetern Anatolia. In: International Earth Sci. Colloquium on the Aegean Region (IESCA), İzmir, Güllük, Turkey, Program, Abstracts, 3.

- Ewart, A., (1982). "The Mineralogy and Petrology of Tertiary-Recent Orogenic Volcanic Rocks: With Special Reference to the Andesitic-Basaltic Compositional Range. In Andesites: Orogenic Andesites and Related Rocks. R.S. Thorpe (ed.), 26-87, Chicester, Wiley
- Farrand, W.H. and Singer, R.B., (1992). Alteration of hydrovolcanic basaltic ash: observations with visible and near-infrared spectrometry. J. Geophys. Res., 97, 17393-17408
- Fischer, R., V., (1984). Submarine volcanoclastic rocks. (In Kokelaar and Howels, 1984) In Cas and Wright, 1987.
- Fischer, R., V., and Schmincke, H., U., (1984). Pyroclastic Rocks. Berlin, Springer-Verlag.
- Foden, J.D., (1983). The Petrology of the Calc-Alkaline Lavas of Rindjani Volcano, East Sunda Arc: A Model for Island-Arc Petrogenesis. J. Petrol., 24, 98-130.
- Fytikas, M., Giuliani, O., Innocenti, F., Marinelli, G. and Mazzuoli, R., (1976). Geochronological Data on Recent Magmatism of the Aegean Sea. Tectonophysics, 31, 29-34
- Fytikas, M., Giuliani, O., Innocenti, F., Manetti, P., Mazzuoli, R., Peccerillo, A. and Villari, L., (1979). Neogene Volcanism of the Northern and Central Aegean Region. Ann. Geol. Pays. Hell. 30, 106-129
- Fytikas, M., Innocenti, F., Manetti, P., Mazzuoli, R., Peccerillo, A. and Villari, L., (1984). Tertiary to Quaternary evolution of volcanism in the Aegean Region. In: J.E. Dixon and A.H.F. Robertson (eds.), The Geological Evolution of the Mediterranean. Geol. Soc. Spec. Publ. , 17, 687-699.
- Genc, Ş.C., (1998). Evolution of the Bayramiç Magmatic Complex, Northwestern Anatolia. Journal of Volcanology and Geothermal Research. 85, 233-249

Gill, J.B., (1981). Orogenic Andesites and Plate Tectonics. Berlin: Springer-Verlag, 358 pp

Güleç, N., (1991). Crust-Mantle Interaction in Western Turkey: Implications from Sr and Nd isotope Geochemistry of Tertiary and Quaternary Volcanics. geol. Mag. , 23, 417, 435

Gülen, L., (1990). Isotopic Characterization of Aegean Magmatism and Geodynamic Evolution of the Aegean Subduction. In: Savaşçın, M.Y. and Eronat, A.H. (Eds.). International Earth Sci. Colloquium on the Aegean Region 8IESCA, İzmir, Turkey. Proceedings, II, 143-166.

Heiken, G.H and Wohletz, K., (1985). Volcanic ash. University of California Press, Berkeley, 246 pp.

Innocenti, F., Kolios, N., Manetti, P., Rita, F. and Villari, L., (1982). Acid and Basic Late Neogene Volcanism in Central Aegean Sea: Its Nature and Geotectonic Significance. Bulletin Volcanologique, 45, 87-97.

Innocenti, F., Manetti, P., Mazzuoli, R., Peccerillo, A. and Poli, G., (1985). REE Distribution in Tertiary and Quaternary Volcanic Rocks from Central and Western Anatolia. In: İzdar, E. and Nakoman, E. (Eds.), Sixth Colloquium on Geology of the Aegean Region. Piri reis Int. Conf. Series, Publ. no: 2, 289-301

Irvine, T.N. and Baragar, W.R.A., (1971). A Guide to the Chemical Classification of the Common Volcanic Rocks. Canadian Journal of Earth Science, 8, 523-548

Jacobsson, S.P and Moore, J.G., (1980). Unique hole shows how volcano grew. Geotimes, April 1980, 14-16.

Karacık, Z., Yılmaz, Y., (1998). Geology of the Ignimbrites and the Associated Volcano-Plutonic Complex of the Ezine Area, Northwestern Anatolia. Journal of Volcanology and Geothermal Research. 85, 251-264.

- Kaya, O., (1979). Ortadoğu Ege çöküntüsünün (neojen) Stratigrafisi ve Tektoniği. Türkiye Jeoloji Kurumu Bülteni, c. 22, 35-58
- Kaya, O., (1981). Miocene Reference Sections for the Coastal Parts of Western Anatolia. Newsl. Stratigr., 10 (3), 164-191
- Kaya, O., Savaşçın, Y. (1981). Petrologic Significance of the Miocene Volcanic Rocks in Menemen, West Anatolia. Aegean Earth Sciences, v.1, 45-58
- Ketin, İ., (1970). Batı Anadolu Neojen Havzalarının Sismotektonik Durumu. Gediz Depremi Simpozyumu, tebliğler, Tartışmalar. İnşaat Müh. Od. , s. 8-16
- Kokelaar, P. and Busby, C., (1992). Subaqueous explosive eruption and welding of pyroclastic deposits. Science, 257, 196-201.
- Krushensky, R.D., (1976). Neogene Calc-Alkaline Extrusive and Intrusive Rocks of the Karalar-Yeşiller Area. Bulletin Volcanologique, 39, 336-360.
- Lopez-Escobar, L., Frey, F.A. and Vergera, M., (1976). Andesites from Central-South Chile: Trace Element Abundances and Petrogenesis. In. Proc. Symp. Andean Antarctic. Volcanol. Probl., IAVCEI, pp725-761
- McKenzie, D. and Yılmaz, Y., (1991). Deformation and volcanism in Western Turkey and the Aegean. Bulletin of the Technical Univ. of Istanbul, 44, 345-373.

- Öğdüm, F., (1983). menemen Dumanlıdağ Volkan Konisi ve Kaşderasının jeomorfolofisi-Evrimi. Jeomorfoloji Dergisi, 11, 45-52.
- Pearce, J.A., Harris, N.B.W. and Tindle, A.G., (1984). Trace Element Discrimination Diagrams for the Tectonic Interpretation of Granitic Rocks. Jour. Petrology, v.25, 956-983
- Peccerillo, A., and Taylor, S.R., (1976). Geochemistry of Eocene Calc-Alkaline Rocks From the Kastamonu Area, Northern Turkey. Contrib. Mineral. Petrol. 58, 63-81
- Pe-Piper, G.G. and Piper, D.J.W., (1989). Spatial and temporal variations in Late Conozoic back-arc volcanic rocks, Aegean Sea Region, Tectnophysics, 196, 113-134.
- Selley, R.C., (1978). Ancient sedimentary environments, 2nd edition, London: Chapman and Hall
- Savaşçın, M.Y., (1978). Foça-Urla Neojen Volkanitlerinin Mineralojik, Jeokimyasal İncelenmesi ve Kökensel Yorumu: Doçentlik Tezi, Ege Üniv., Yerbilimleri Fak. Unpublished, 65 pp
- Savaşçın, M.Y., (1982). Batı Anadolu Neojen Magmatizmasının Yapısal ve Petrografik Özellikleri. TBAG Project no: 392, unpublished
- Savaşçın, M.Y. and Gülen, N., (1990). Relationship between magmatic and tectonic

- Seyitođlu, G., Scott, B.C., (1992). Late Cenozoic Volcanic Evolution of the Northeastern Aegean Region. Journal of Volcanology and Geothermal Research, 54, 157-176
- Seyitođlu, G., Scott, B.C., (1992). The Age of the Büyük Menderes Graben (West Turkey) and Its Tectonic İmplications. Geol. Mag. v. 129, p. 239-242.
- Seyitođlu, G., Scott, B.C. (1994). Late Cenozoic Basin Development in West Turkey : Gördes Basin : Tectonics and Sedimentation. Geol. Mag. v. 131, pp. 631-637.
- Seyitođlu, G., Benda, L. and Scott, B.C., (1994). Neogene palynological and isotopic data from Gördes Basin, west Turkey, Newsletters on Stratigraphy, 31, 133-142
- Seyitođlu, G., Scott, B.C., Rundle, C.C. (1992). Timing of Cenozoic Extensional Tectonics in West Turkey. Journal of the Geological Society, v. 149, pp. 533-538.
- Sparks, R.S.J., Sigurdsson, H. and Carey, S.N., (1980). The entrance of pyroclastic flows into the sea, II. Theoretical considiretions on subaqueous emplacement and welding. J. Volcanol. Geotherm. Res., 7, 97-105.
- Stix, J., (1991). Subaqueous, intermediate to silicic-composition explosive volcanism: a review. Earth Science Review, 31, 1-21
- Şengör, A., M., C., (1982). Ege' nin Neotektonik Evrimini Yöneten Etmenler. Batı Anadolu' nun Genç Tektoniđi ve Volkanizması Paneli. Türkiye Jeoloji Kurultayı, pp. 59-71
- Şengör, A., M., C. and Dewey, J., F., (1980). Post-Oligocene Tectonic Evolution of the Aegean and Neighbouring Regions: Relations to the North Anatolian Transform Fault. Sixth Colloquium on Geology of the Aegean Region. Piri Reis International Contribution Series, Publ. no: 2
- Şengör, A., M., C., and Yılmaz, Y., (1981). Tethyan Evolution of Turkey: A plate tectonic Approach. Tectonophysics, 75, 181-241

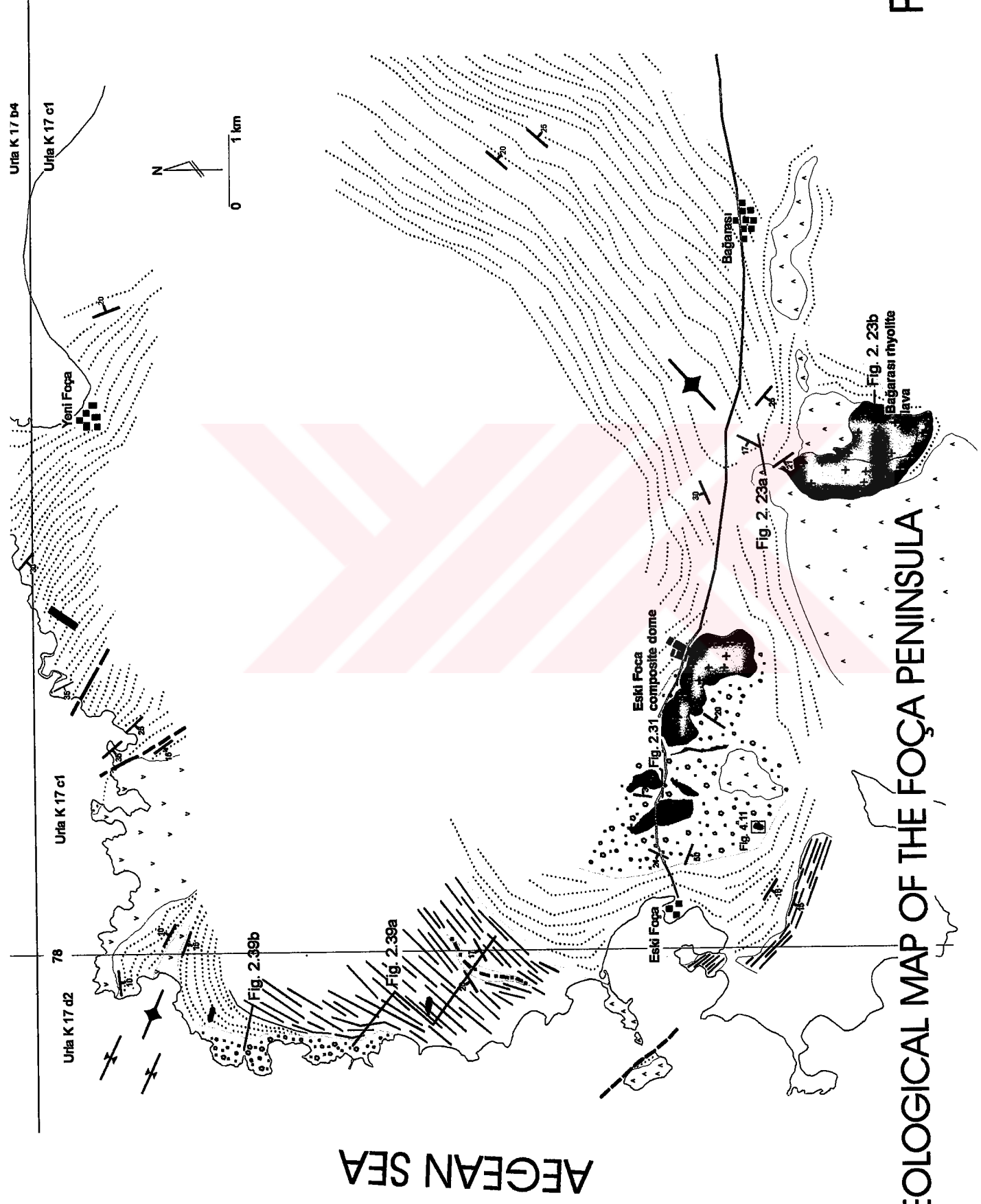
- Şengör, A., M., C., Satır, M., and Akkök, R., (1984). Timing of Tectonic Events in the Menderes Massif, Western Turkey: Implications for Tectonic Evolution and Evidence for Pan-African Basement in Turkey. tectonics, 3, 693-707
- Şengör, A.M.C., Görür, N. and Şaroğlu, F., (1985). Strike-Slip deformation, Basin Formation and Sedimentation: Strike-Slip Faulting and Related Basin Formation in Zones of Tectonic Escape: Turkey as a Case Study. In Biddle, K.T. & Christie-Blick, N. (eds.) Strike-Slip Faulting and Basin Formation. Society of Economic Paleontologists and Mineralogists. Special Publication. 37, 227-264.
- Şengör, A.M.C., Cin, A., Rowley, D.B. and Nie, S.-Y., (1993). Space-time patterns of magmatism along the tethysides: a preliminary study. Journal of Geology, 101, 51-84
- Ünker, C., (1984). Yamanlar Volkanitinin Jeolojisi. Yamanlar Köyü (Karşıyaka). Deü, Müh. Fak. Jeoloji Mühendisliği Bölümü, Bitirme Ödevi (unpublished)
- Yılmaz, Y. (1989). An Approach to the Origin of Young Volcanic Rocs of Western Turkey. Tectonic Evolution of the Tethyan Region, 159-189
- Yılmaz, Y. (1990). Comparison of Young Volcania Associations of Western and Eastern Anatolia Formed Under a Compressional Regime: a Review. Journal of Volcanology and Geothermal Research, v. 44, p. 69-87.
- Yılmaz, Y., (1997). Geology of Western Anatolia. Active Tectonics of Northwestern Anatolia-The Marmara Poly-Project. A Multidisciplinary Approach by Space-Geodesy, Geology, Hydrogeology, Geothermics and Seismology. 31-53
- Yılmaz, Y., (2000). Active tectonics of the Aegean Region. Batı Anadolu' nun Depremselliği Sempozyumu. Bildiriler. 3-14
- Yılmaz, Y., Altunkaynak, Ş., Karacık, Z., Gündoğdu, N., Temel A., (1994). Development of Neo-Tectonic Related Magmatic Activities in Western Anatolia. Int. Volcanol. Congr. Ankara, Abstracts, p. 13.

Yılmaz, Y., Genç, Ş.C., Gürer, F., Bozcu, M., Yılmaz, K., Karacık, Z., Altunkaynak, Ş., Elmas, A., (2000). When did the western Anatolian grabens begin to develop? From Bozkurt E., Winchester, J.A., Piper, J.D. (eds.) *Tectonics and Magmatism in Turkey and the Surrounding Area*. Geological Society, London, Special Publications, 173, 353-384.

Walker, G.P.L., (1971). Grainsize characteristics of pyroclastic deposits. J. Geol. 79, 696-714.

Winchester, J.A. and Floyd, P.A., (1977). Geochemical Discrimination Products Using Immobile Elements. Chem. Geol., 20, 325-343.

Wright, J.V. and Coward, M.P., (1977). Rootless vents in welded ash-flow tuffs from Northern Snowdonia, North Wales. Geol. Mag. 114, 133-140.



AEGEAN SEA

GEOLOGICAL MAP OF THE FOÇA PENINSULA

GEOLOGICAL MAP OF THE GEREN VILLAGE - YENI FOÇA AREA

Urta K 17 c2

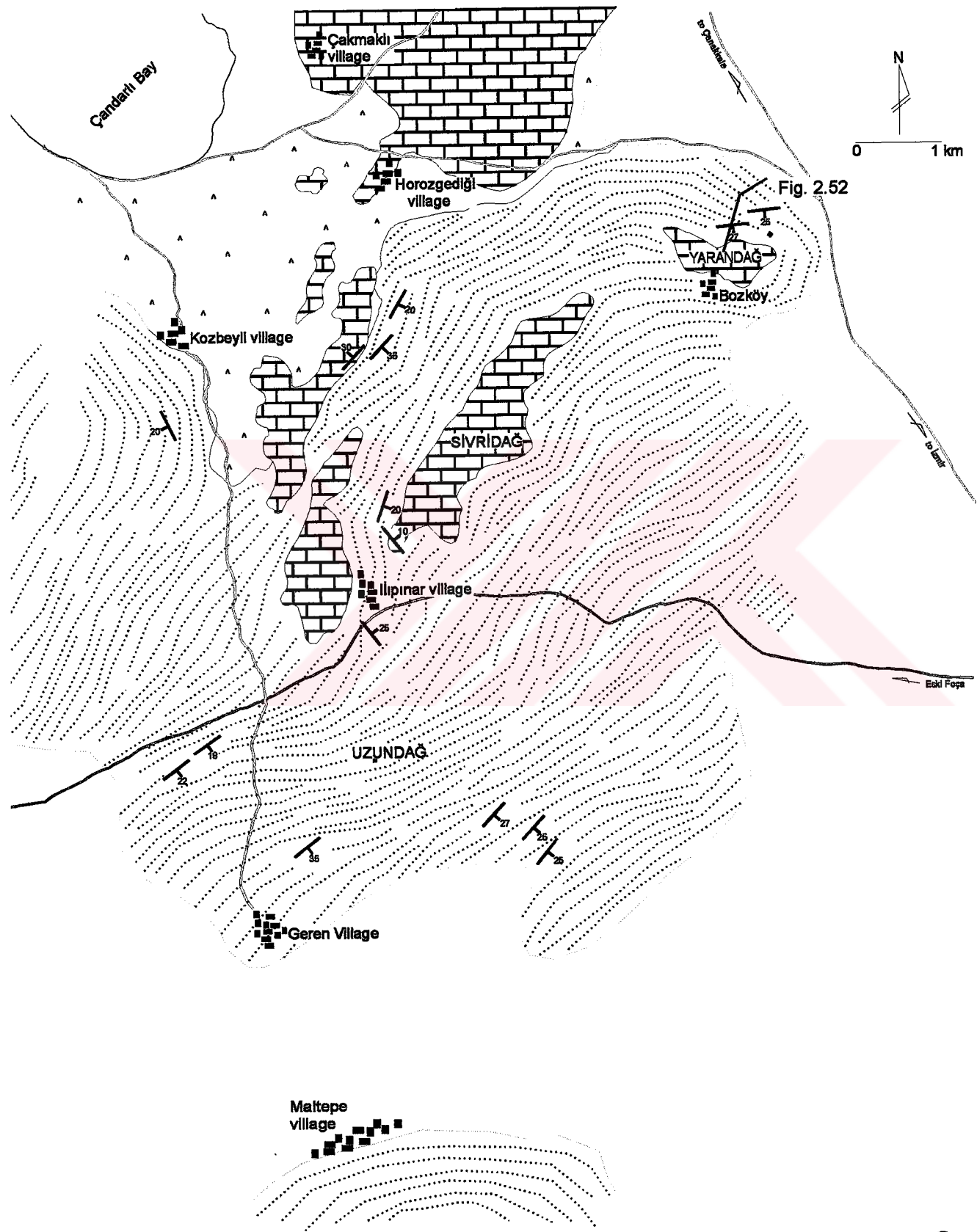
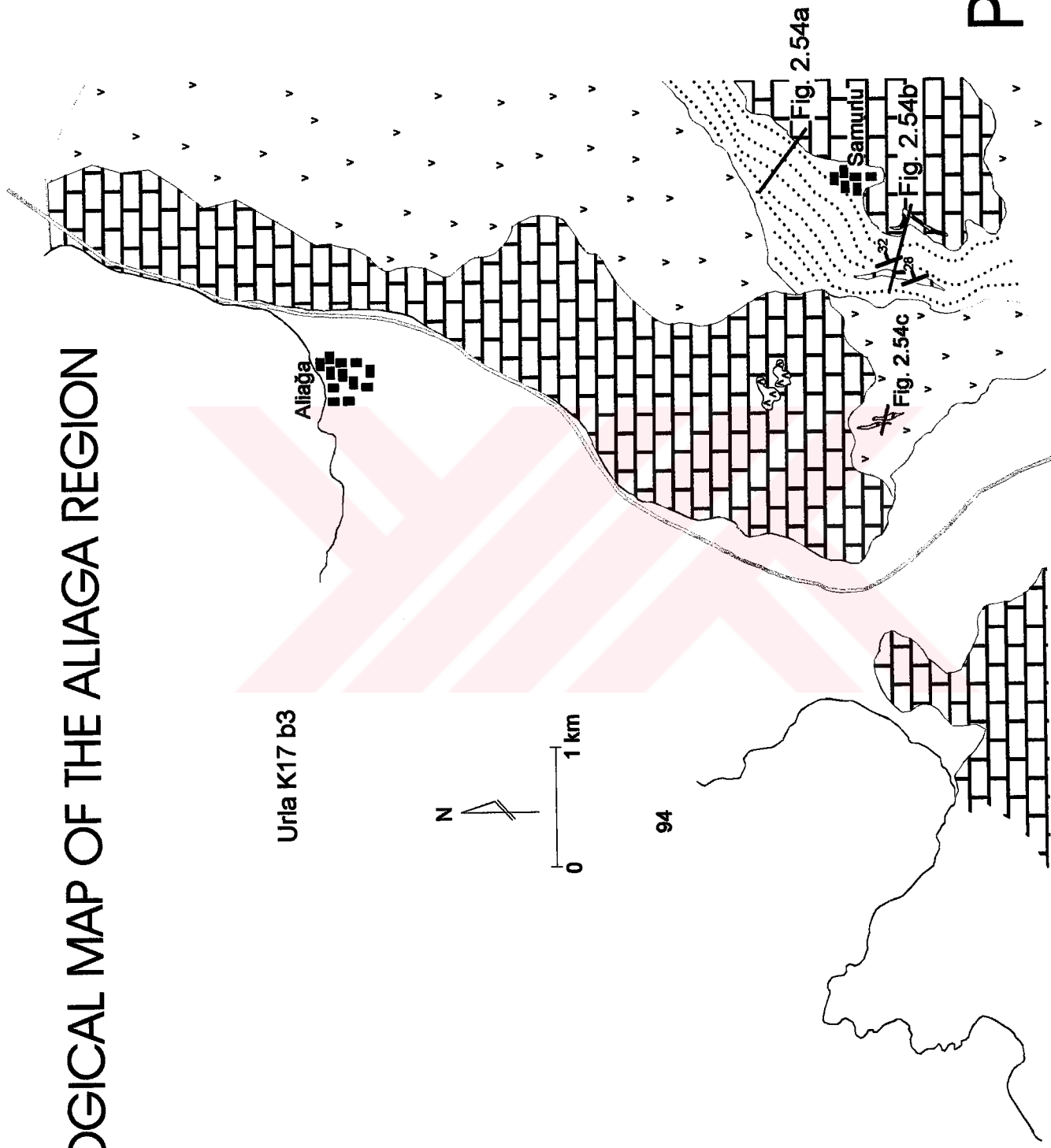


PLATE 2

GEOLOGICAL MAP OF THE ALIAGA REGION



Urla K17 b3

N

0 1 km

94

PLATE 3

GEOLOGICAL MAP OF THE ALTILIDERE - YENISAKRAN AREA

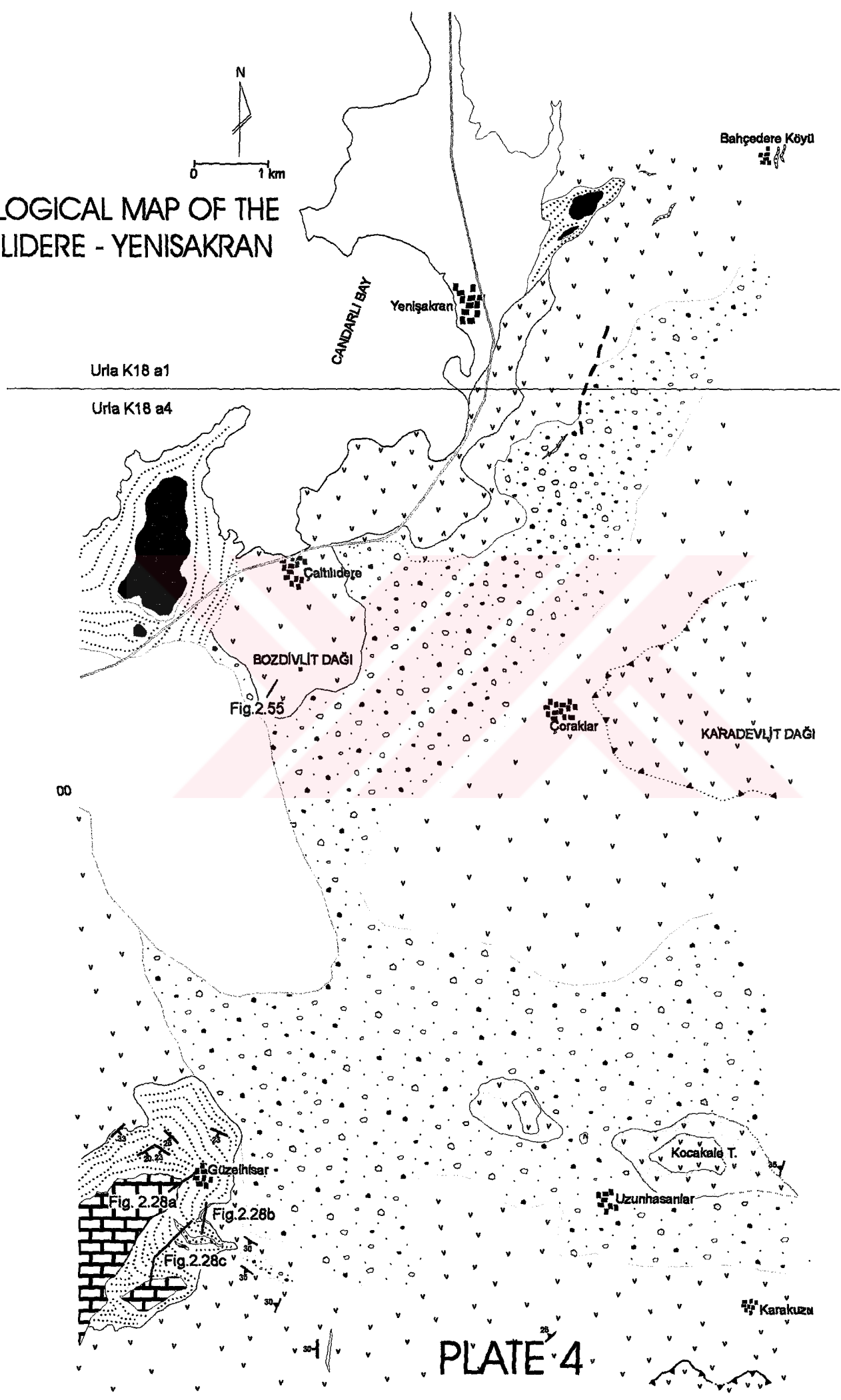
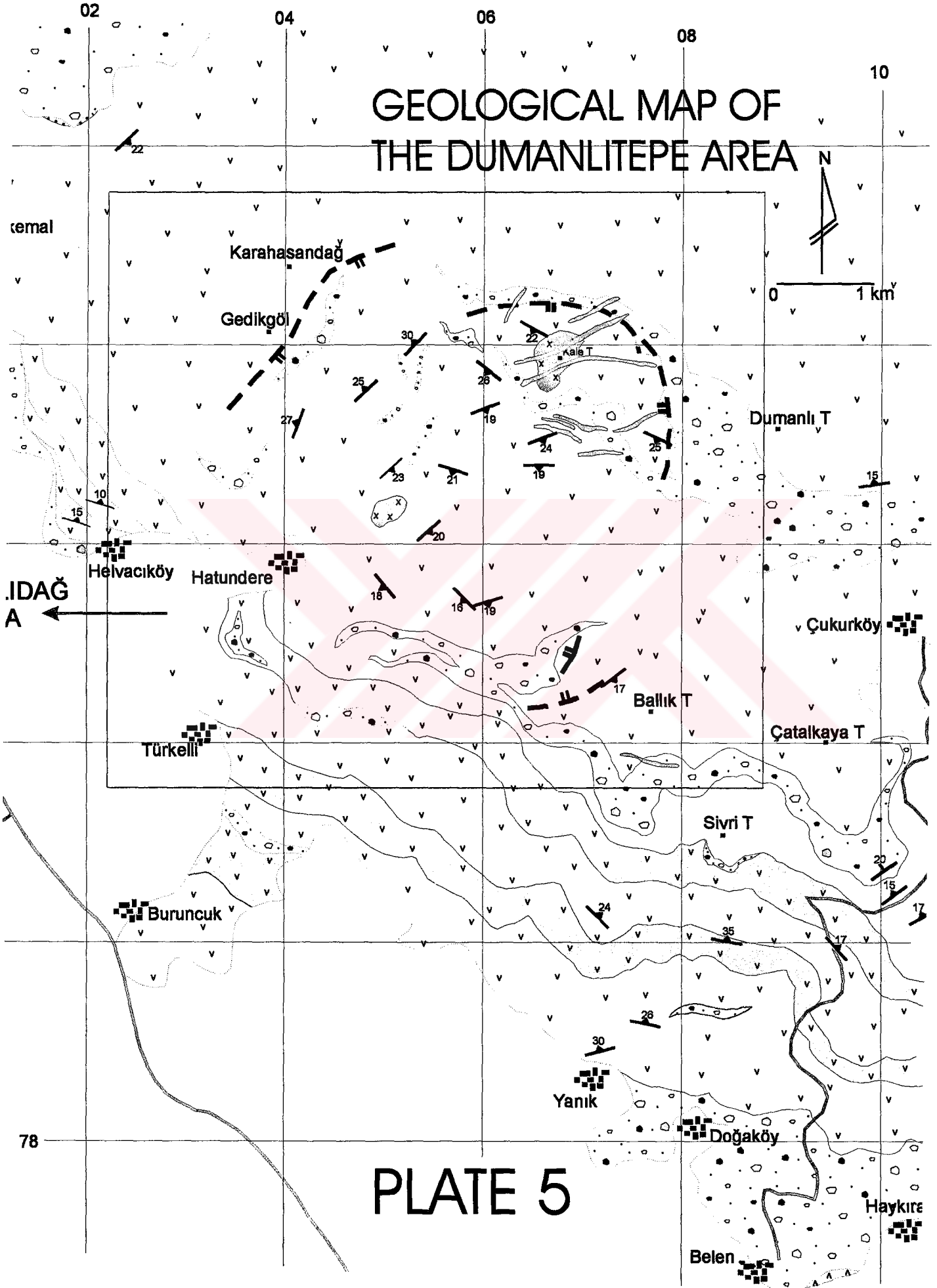
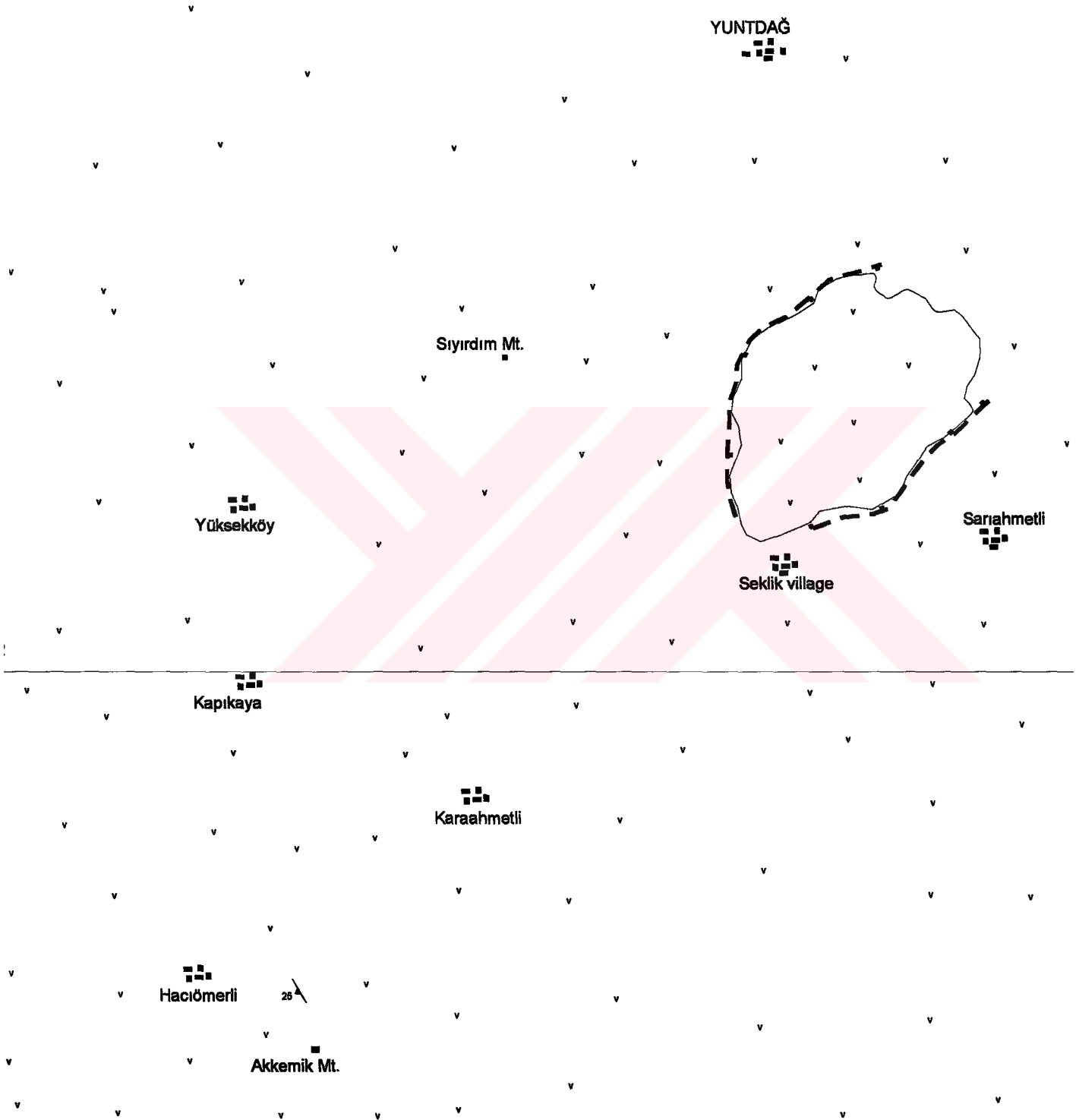


PLATE 4

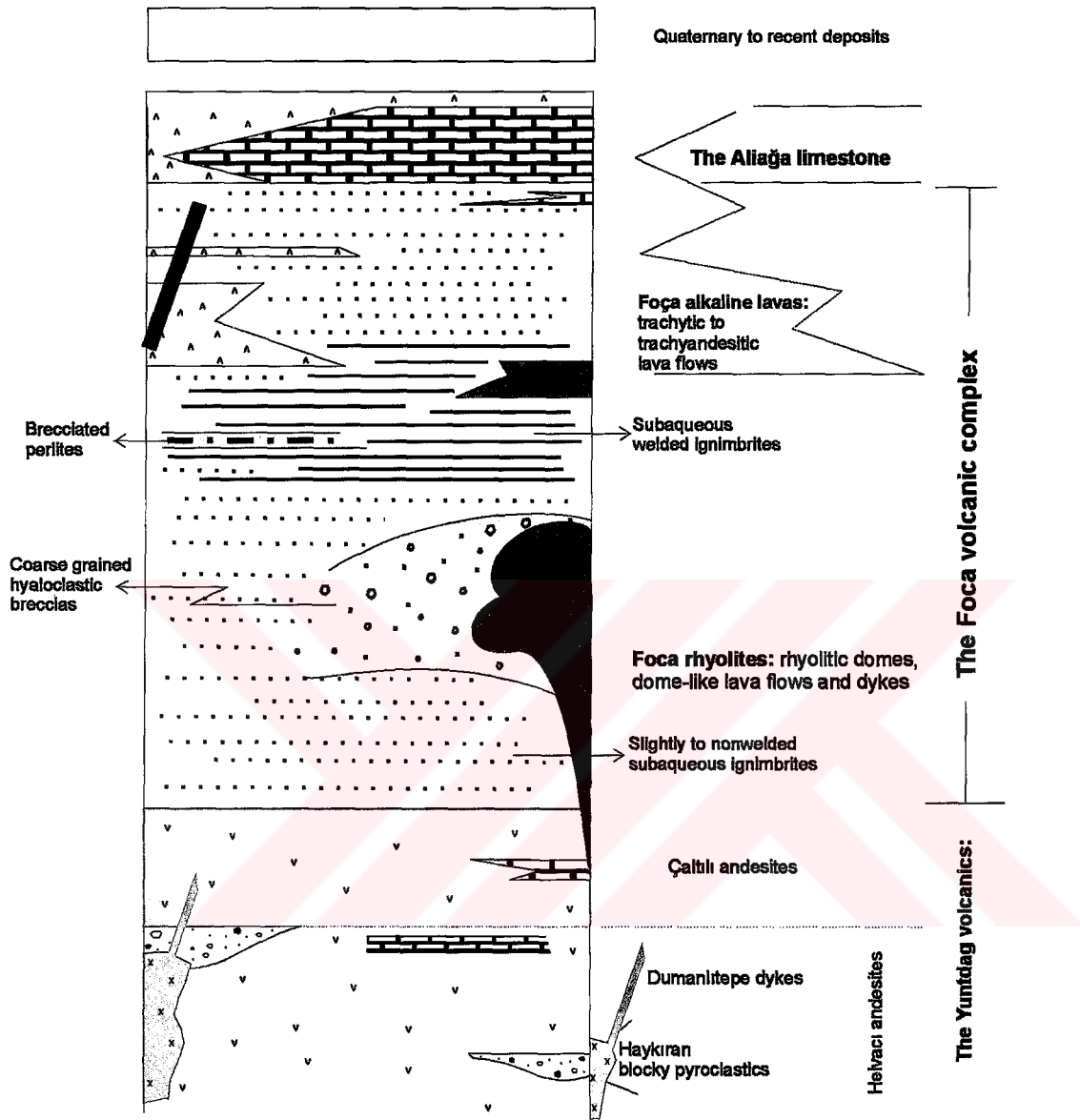
GEOLOGICAL MAP OF THE DUMANLITEPE AREA



ZOOLOGICAL MAP OF THE YUNTDAG AREA



EXPLANATIONS



- Geological boundaries
- Faults
- Section lines
- Fold axis
- Strik and dips
- 10 --- Flow foliations
- 24 --- Hills
- Urban areas